Lamar University

BEAUMONT, TEXAS

TECHNICAL REPORT

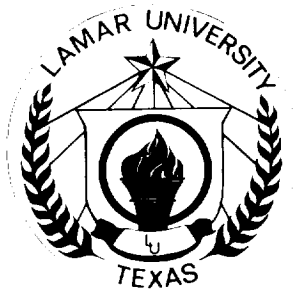

COLLEGE OF ENGINEERING

Advanced Support Systems Development and Supporting Technologies for Controlled Ecological Life Support Systems (CELSS)

FINAL REPORT
NASA Grants NAG9-620 and NAG9-640

August 31, 1994

Lamar University
College of Engineering
Beaumont, Texas

William E. Simon, Ph.D., P.E., Principal Investigator
Ku-Yen Li, Ph.D., P.E., Research Associate
Carl L. Yaws, Ph.D., P.E., Research Associate
Harry T. Mei, Ph.D., P.E., Research Associate
Vinh D. Nguyen, Ph.D., Research Associate
Hsing-Wei Chu, Ph.D., Research Associate

CONTENTS

I. FOREWORD

This report documents the results of work accomplished under two related grants, as follows:

NAG9-620	Advanced Closed Life Support System Technology Development for Space Applications
NAG9-640	Regenerative Life Support Systems Technology Development

The period of performance for these grants was September 1992- August 1994.

Since the content and activities of these two grants were closely related, work was carried on as one combined effort. Consequently, by agreement with the JSC technical monitor of these grants, Mr. Michael Hoy, this report documents the results of both programs.

The primary task was the development of a methyl acetate reactor which was subsequently used to perform a subscale kinetic investigation supporting JSC efforts to design and optimize a full-scale metabolic simulator for extended-duration testing of life support systems. The simulator is being developed by JSC to be used in its planned closed ecological life support system (CELSS) test program. Lead Engineer for this task at Lamar University was Dr. K.-Y. Li (Chemical Engineering). Dr. Carl L. Yaws (Chemical Engineering) served as Research Assistant.

Other tasks of an analytical nature were agreed to with JSC and conducted in support of the overall effort. The tasks are:

1. Heating, Ventilation and Air Conditioning (HVAC) Analysis of Variable Pressure Growth Chamber (VPGC) - Lead Engineer: Dr. H. T. Mei (Mechanical Engineering); Research Associate: Dr. William E. Simon (Mechanical Engineering)

2. Design of Experiments for the Statistical Analysis of Plant Crops - Lead Engineer: Dr. H.-W. Chu (Industrial Engineering); Research Associates: Dr. K.-Y. Li (Chemical Engineering) and Dr. V.D. Nguyen (Mechanical Engineering)

3. Resource Recovery for Closed Life Support Systems - Lead Engineer: Dr. K.-Y. Li (Chemical Engineering); Research Associate: Dr. Carl L.Yaws (Chemical Engineering)

4. Data Acquisition Software Development for Automation of Environmental Growth Chamber - Lead Engineer: Dr. V. D. Nguyen (Mechanical Engineering)

Lamar University Principal Investigator for the two grants was Dr. William E. Simon.

The hardware development task for the kinetic reactor, and the four analytical tasks, have all been completed. Interim reports were submitted to JSC as the work progressed, through presentations at meetings either at Lamar or at JSC. Accompanying the presentations were periodic status reports on 10/1/92, 1/5/93, 3/24/93, 4/2/93, and 7/16/93. These reports are documented in detail under separate cover and were submitted to JSC at the time of the meetings. These periodic meetings served as a vehicle to provide JSC with the latest results available at each meeting milestone, insuring that results were passed on as they became available. Following the last formal quarterly meeting in July 1993, a no-cost grant extension was requested, and granted, to continue testing and analysis. Another status meeting was held in December 1993, after which informal meetings were then conducted during the final eight months of the grant period. This final report includes results obtained through the extended period of performance.

II. SUBSCALE CATALYTIC REACTOR HARDWARE DEVELOPMENT

II.1 INTRODUCTION

One of the most challenging problems associated with long-duration manned space flight is found in the development of Controlled Ecological Life Support Systems (CELSS). This includes the technologies of air revitalization, water recovery, waste processing and food production, and the integration of these systems into an optimal closed life support system for future space missions [Elikan, 1966; Schwartzkopf, 1992]. While early studies addressed some of these technology areas on an individual basis, little effort was put forth to develop an integrated, closed-cycle ecological space life support system. Since JSC has been designated by the Agency as the Systems Integration Research Center, the JSC Crew and Thermal Systems Division (CTSD) has converted the 20 feet man-rated vacuum chamber in Building 7A to a full-up Systems Integrated Research Facility (SIRF), with the long-term goal of conducting a fully integrated reduced-pressure (10.2 psia) test with 4 humans and all required closed-cycle life support equipment to sustain the crew for one year in an isolated condition.

To achieve this goal, subsystem development work began with the construction of experimental waste-processing and plant growth facilities at JSC, as well as contractor development of various subsystems. To facilitate efficient development and testing of these systems, expensive man-in-the-loop testing of early development subsystems must be avoided. To accomplish this, a human metabolic simulator (called a "canned man") is desired to simulate the presence of humans in a closed environment. Such a metabolic simulator has been conceptually designed by JSC engineers and their support contractors. This conceptual design, in summary, is based on the catalytic oxidation of methyl acetate. The simulator design provides proper carbon dioxide, humidity, and metabolic heat load to a test-bed environment [Henninger, 1993].

To supplement the JSC activity, a metabolic simulator project was initiated at Lamar University-Beaumont in 1992 to study, fabricate and test a simulator. An extensive literature survey indicated that the experimental kinetic data for the methyl acetate oxidation reaction were very limited and that data pertaining to the design temperature of the reactor was non-existent. After several meetings with NASA personnel, it was decided to initiate a sub-scale kinetic investigation to obtain the needed kinetic data for the catalytic oxidation of methyl acetate, and the activities of this grant were modified accordingly to provide this data. The information obtained from this sub-scale testing will be used to support and enhance the design and optimization of a full-scale simulator [Lange, 1992].

The specifications for a "canned-man" are listed in Table II-1 [Lange, 1991]. For foods or fuels composed solely of carbon, hydrogen and oxygen, the end products of metabolic oxidation and complete combustion are identical, although the reaction mechanisms are very different. This suggests that a combustor might be used as a basis for a metabolic simulator. Based on this idea, the combustion reaction for a general fuel, $C_kH_mO_n$, can be written as follows:

$$C_kH_mO_n + O_2 \longrightarrow CO_2 + H_2O$$

The effective respiratory quotient is then given by

$$R_{resp} = \frac{CO_{2production}}{O_{2consumption}} = \frac{k}{k + \frac{m}{4} - \frac{n}{2}} \qquad (1)$$

Among those proposed fuels, methyl acetate seems to be the best selection because it has an effective respiratory quotient of 0.86, which is very close to the assumed metabolic value (0.87) and meets the primary considerations.

In addition to the choice of methyl acetate as the fuel, the choice of a combustor is also very important. Combustion of a flammable substance can be accomplished with or without a flame [Spivey, 1987]. Basically, flame combustion occurs within a relatively narrow range of fuel concentration and at higher temperature. Flameless combustion can be accomplished with or without a catalyst. Because catalytic combustion occurs at a much lower temperature, it is preferred over flame combustion for this application due to a lower production of NO_x at lower reaction temperatures. Meanwhile, supported platinum and palladium catalysts have been found to be more effective for oxidation of a number of fuels [Kesselring, 1986; Becker, 1989]. Additionally, catalysts are available in both monolithic and pelletized form, and the monolithic honeycomb structure, made from ceramics or metals, has the advantage of lower pressure drop per unit surface area.

Based on the above considerations, a catalytic fixed-bed reactor was designed, fabricated and tested at Lamar University during the first year to study the methyl acetate oxidation process . Two types of pelletized 0.5% Pt/Al_2O_3 catalysts, one porous and one non-porous, were selected for the kinetic study to determine the reaction rate equation needed for the design and scale-up of a "canned-man" simulator. A nonlinear regression curve-fitting scheme was utilized for analysis of the kinetic data.

A Taguchi method of experimental design was suggested by NASA personnel, and it was used in this project to determine both the effect and the cross-effect of the controlled variables such as temperature, retention time and concentration. This experimental design method is useful in analyzing a system with several uncertainties, since it offers maximum information with minimum experiment sets [Ross, 1988].

The results of this task are reported below; however additional detail can be found in a graduate thesis on this subject [Li, 1993].

II.2 EXPERIMENT

II.2.1 Experimental Setup

The experimental setup is shown in Figure II-1. Air is supplied by an air cylinder. One air stream is bubbled through a methyl acetate storage tank submerged in an isothermal bath for temperature regulation. This air stream containing methyl acetate vapor is then mixed with another air stream from the air cylinder through a static mixer. The concentration of methyl acetate in the air is controlled by varying the flow rates of the two air streams while the total air flow rate is kept constant. The mixed air stream containing methyl acetate vapor flows through a preheater before entering the catalytic reactor, which is controlled at a predetermined reaction temperature.

The catalytic reactor was initially fabricated using half-inch diameter by one-foot stainless steel tubing. The diameter of the reactor was later increased to one inch to allow for greater throughput. The reactor is packed with 10 grams of 1% platinum-on-alumina (Pt/Al_2O_3) 1/16 inch catalyst pellets (porous case), and 1/8 inch catalyst pellets (non-porous case).

The methyl acetate, oxygen, and carbon dioxide quantities in the inlet and outlet streams of the catalytic reactor are analyzed by a gas chromatograph (GC) Varian 3400 through an automatic sampling valve system, as shown in Figure II-1. Details of the preheater and reactor, as well as the gas sampling system, are shown in Figure II-2. Each of the components in Figure II-1 is described in the following sections.

II.2.1.1 Feed Gas Regulator System

Gas cylinders of helium, hydrogen and breathing air were obtained from the Big Three Gas Company. For the gas chromatograph, helium was used as a carrier gas and the mixture of hydrogen and breathing air served as fuel for the flame ionization detector (FID). Breathing air was also used as process air.

The effluent pressure of each gas cylinder was controlled by two-stage gas regulators manufactured by the Victor Equipment Company. Between the gas cylinder and the regulator, an in-line stainless-steel wire filter was installed to prevent impurities from contaminating downstream equipment.

II.2.1.2 Methyl Acetate Tank

Liquid Methyl Acetate (MA) was stored in a tank fabricated of schedule 80 stainless steel 8-inch pipe with 5 1/4 -inch NPT threads on its top. The tank was made by the Triplex Corporation of Nederland, Texas. This methyl acetate tank has 3 tubes connected to the top, one for a pressure gauge, one for the air inlet, and one for the air and methyl acetate outflow. The air inlet is connected to a 1/4 inch pipe directed toward the bottom of the tank to pick up methyl acetate by bubbling air through the liquid MA.

II.2.1.3 Water Bath

Immersed in a 10 liter isothermal water bath, the water temperature was controlled within ±0.5 °C to reduce fluctuations of methyl acetate vapor pressure and downstream concentration.

II.2.1.4 Electronic Mass Flow Meter

A mass flow meter (MAS-3010-A) with analog output and a MAS-50000 DC 12-volt Cobold power supply were used for flow rate detection. To accommodate all expected gases including corrosives, wetted surfaces were of 316 stainless steel. The analog output scheme increases the flexibility of the experimental apparatus for future applications.

II.2.1.5 Float-Type Flow Meter

Five float-type flow meters with different maximum flow rates ranging from 0.036 to 8.695 l/min (STP), were used to adjust the concentration of methyl acetate and monitor the flow rate to the GC device from sampling ports on the reactor. A Teflon flow meter, including Teflon frame, fittings and valves, was specially installed to handle the vaporized methyl acetate emerging from the MA tank.

II.2.1.6 In-Line Static Pipe Mixer

A G-04669-18 In-Line Mixer from Cole Parmer, consisting of a series of fixed stainless steel right- and left-hand elements to provide efficient mixing with minimum pressure drop, was installed in the methyl acetate vapor stream. This stream was then combined with breathing air to insure complete mixing.

II.2.1.7 Thermocouples

K-type thermocouples with heavy duty transition joints, 1/16 inch inconel sheaths, ungrounded junctions, and various lengths were procured from the Omega Corporation. The ungrounded junction was used to prevent electrical noise, at the expense of a small decrease in response time. The K-type thermocouple, with its high temperature limit (approximately 1400° F (760°C)), is suitable for the temperature range of this reaction.

II.2.1.8 Preheater

As stated above, detailed diagrams of the preheater and reactor are shown in Figure II-2. A 1/2 inch OD by 6 inch-long stainless steel tube filled with 3mm-diameter glass beads was used as a preheater. The preheater is housed in the center of the tube furnace to produce efficient and uniform heating over a short distance. The high-purity glass beads were obtained from the Kimble Company, and the stainless steel was purchased from the Rawson Corporation.

II.2.1.9 Reactor

The fixed-bed reactor is made of 1-inch OD stainless steel tube cut to 3-inch lengths. At the both ends of the catalyst region, two pieces of stainless steel wire mesh were used to support the 1/8 inch pellet catalyst bed. Welded onto the one-inch stainless steel unions are two sampling ports made of 1/8 inch-to-1/16 inch tube end reducers. Upstream of the catalyst bed, glass beads were packed to an axial length of approximately 1/3 inch to serve as a distributor to eliminate non-uniform flow rate distribution.

II.2.1.10 Tube Furnace

Two tube furnaces, Lindberg Model 55035 with model 847 digital controllers, were purchased and installed. The furnaces, with a maximum operating temperature of 1100° C, have a 12 inch heated length, 1-inch vestibule ID and a convenient LED digital indication of the furnace set point and chamber temperature. The exposed thermocouple inside the furnace chamber was disconnected, and another thermocouple of the same type was inserted adjacent to the catalyst bed and wired to the temperature controller for accurate reaction temperature control. CAUTION: For future operation, care must be taken to avoid any electrical short while reconfiguring this equipment. The criticality of the setting of the operating parameters on the front panel of the controllers is discussed in a later section of this report.

II.2.1.11 Heating Tape

Heavy insulated heating tapes (catalog numbers 11-463-50A and 11-403-50B) suitable for direct contact with metal were procured from the Fisher Scientific Company. Fibrox fibrous glass insulation covering the standard heating tape offered a heating capability to 483 °C. As a safety precaution, these heating tapes should be used only with power regulators or input controllers to limit the temperature to the recommended maximum. In this experiment, the heating tape was connected to a solid relay, with electrical power output governed by the digital controller within the furnace.

II.2.1.12 Valves

Two types of valves (ball and needle) were used. The needle valves, 4Z-V4LR-SS CPI valves with 1/4 inch tubing connectors, were obtained from Parker and used when complete closure was important or accurate adjustment was desired, such as for flow-rate control. On the other hand, the ball valve was used wherever quick opening and closing capability is required. The Lawson Corporation of Beaumont, Texas provided the Whitney 40 series ball valves with 1/16 inch tubing connectors, which were used for effluent analysis.

II.2.1.13 Pressure Gauge

For pressure measurement, 4-1/2-inch dial-diameter pressure gauges and 2-1/2-inch vacuum-pressure gauges were installed in the desired locations. These gauges (G-68800-40 and G-68800-48), with 1/4-inch NPT bottom connections, were procured from Cole-Parmer.

II.2.1.14 On-Line Sampling System

A diagram of the on-line sampling system is shown in Figure II-3. To obtain gas samples both upstream and downstream of the catalyst bed, two pretreated, highly purified 1/16 inch stainless steel tubes were attached to the unions at the inlet and outlet ends of each reactor. These tubes were connected to the 1st automatic valve housed on the Varian Star 3400 Gas Chromatograph. By switching the 1st valve, a gas sample from either before or after the reaction could be sent to the sample loop (250μl) installed on the 2nd automatic valve. The gas inside the sample loop was then flushed by the carrier gas (He) and sent to the separation column at a later time, i.e., at the injection command to switch the second valve. Each valve is driven by a pneumatic actuator installed vertically above the valve. A flow meter between the 1st automatic valve and the sampling port on the reactor was installed to monitor the process fluid sample.

II.2.1.15 Vacuum System

The vacuum system consists of a Barnant vacuum pump (Model 400-1901) and an air tank (Speedaire Model 4F694). This diaphragm-operated pump was designed for pressure, suction and gas circulating applications. Three-foot lengths of plastic tubing at both ends of the pump were used for noise abatement.

II.2.1.16 Gas Chromatograph

The analytical instrument of this experiment was the Varian Star 3400 gas chromatograph (GC) equipped with a Flame Ionization Detector (FID), a Thermal Conductivity Detector (TCD), two 1041 universal injectors, and a plotter.

The FID was used to detect hydrocarbons where high sensitivity was required. In the FID, the eluate coming from the CTR column was combined with the hydrogen fuel and air to form a combustible mixture. When ignited, this mixture results in a flame which provides sufficient energy to ionize most organic and some inorganic sample components in the eluate. Upon striking the collector electrode, the positive ions formed by the flame produce an electrical current, which is amplified and recorded. The current flowing through the circuit is proportional to the number of ions striking the collector, which in turn is proportional to the concentration of ionizable sample components entering the flame. Thus, the detector's response increases with increasing numbers of carbon atoms in the component molecule.

The TCD was used to monitor the heat transfer rate from an electrically heated wire by the column eluate. Passing the eluate through one filament and the carrier gas through the other filament, the relative resistance of the two heated filaments was continuously monitored using a Wheatstone bridge. With the signal produced by the difference in resistance, the detector's output changed in response to the type and amount of the gas through the filament.

II.2.1.17 Column

The CTR column installed in the GC was Alltech's configuration of concentric columns, which offers many advantages for certain types of difficult analysis. A CTR column is essentially a column within a column. This permits two different packings to be used simultaneously for one analysis. This configuration is useful in permitting the separation of oxygen, nitrogen, carbon monoxide, carbon dioxide and methane in one analysis at room temperature. Usually this analysis is accomplished by performing either two separate runs on the sample of interest, or using a switching valve and polarity change during the analysis. The reason for this difficulty is that carbon dioxide is irreversibly adsorbed on the molecular sieves to separate oxygen and nitrogen.

II.2.1.18 Microliter Syringe

For the calibration of methyl acetate, Hamilton 7000 series microliter syringes with a one-μl capacity were purchased from Fisher. The included guide assembly was used on syringes with small-diameter plunger wires to minimize damage due to excessive force. Additionally, the Chaney adapter ensured a reproducibility within 1% when injections of identical volumes were required.

II.2.1.19 Data Acquisition System

A 386 DX 40 MHz computer was used for signal analysis from the TCD and the FID. The Star Workstation software from Varian provided a convenient way of handling a large amount of experimental data and implementing GC remote control. Two data acquisition boards were installed in the computer, one for the Star Workstation and the other for digital/analog signal conversion.

II.2.1.20 Catalyst

Aldrich provided a 0.5% platinum content catalyst (Catalog Number 20601-6) for laboratory use in the form of 1/8 inch ×1/8-inch nonporous platinum-coated alumina pellets. A second type of catalyst investigated in this project consisted of a 1/16-inch porous cylinder from Englehard.

II.2.2 Experimental Procedure

II.2.2.1 Catalyst Preparation

The 1/8 inch x 1/8 inch pellet catalyst was first weighed with an analytical balance (0.1 mg accuracy) before being placed into the reactor. The amount of catalyst normally used was in the range of 0.5 - 5.0 grams. To support the catalyst in the reactor, two pieces of stainless steel wire mesh were fixed at both ends of the catalyst bed. The reactor was leak-checked at 30 psig before beginning operation.

Prior to the reaction exposure, the catalyst was pretreated by calcining it in flowing air. The calcination process was conducted by drying the catalyst at 125 °C in air flowing at 1.0 liter/min for 2 hours. The catalyst temperature was then raised gradually to 425 °C and maintained for 16 hours. Following calcination, the catalyst temperature was decreased to 250 °C and hydrogen was forced through it to reduce any oxidized surface. Precautions were taken during the hydrogen flow procedure to preclude possible sparking and subsequent ignition.

II.2.2.2 Column precondition

To precondition the GC column, one end of the column was connected to the injection port and the other end was left open. A normal flow of carrier gas was initiated through the column (i.e., 25 cc/min for 1/8 inch CTR column). It was required that the carrier gas (He) be free of oxygen, moisture and oils, since columns of this type deteriorate rapidly even with trace quantities of oxygen in highly purified carrier gases. This preconditioning process was carried out at room temperature for 30 minutes. The column was then programmed to a desired temperature at least 25 °C lower than the upper temperature limit indicated on the column tag. Alternatively, it was conditioned at 25 °C above the maximum operating temperature used in the analysis, provided it did not exceed the upper temperature limit less 25 °C. In this study the column was conditioned at 130 °C, since the operating temperature was 105 °C.

The preconditioning process was continued for 24 hours at 130 °C. Usually, overnight conditioning was sufficient; however, in some cases, a longer period of up to 48 hours was needed. Additionally, if a column had been out of use for a while, it was reconditioned briefly by purging with pure carrier gas for 30 minutes, programming to the desired temperature, and holding that temperature for 30 minutes to 2 hours before starting analysis.

II.2.2.3 Pressure Test

A pressure test was conducted before each run, with the system pressurized to 30 psig and then allowed to stand. If the pressure remained constant for more than 30 minutes, the test was considered acceptable. Otherwise, a soap solution was used to locate the leak.

II.2.2.4 Calibration of Flow meter

A soap-bubble flow meter was used to calibrate the float-type flow meter. Calibration results are shown in Figure II-4.

II.2.2.5 Calibration Curve for Methyl Acetate

The calibration curve for methyl acetate, needed for the GC analysis, was obtained by injecting several standard samples into the injection port of the GC. Ten standard MA samples were prepared by diluting known quantities of MA into methanol solutions. The weight percent of MA standard samples were from 0.0015% to 0.00002%. For the MA concentration of 10 to 15000 ppm and the sampling loop size of 250μl, the amounts of MA injected were in the range of 1×10^{-10} to 1.5×10^{-7} gram. This range is in the linear range of the calibration curve as shown in Figure II-5. The calibration data are included in Table II-2.

II.2.2.6 Operating Procedure for Catalytic Reactor

1. The liquid level in the methyl acetate vaporization tank was checked and the temperature of the isothermal water bath was set to 25 °C.
2. Air supply pressure was set at 10 psig. For some cases, 10 psig was insufficient to produce the required flow rate. For example, when mesh 60/80 grounded Pt/Al_2O_3 porous catalyst was used, a bigger pressure drop occurred through the catalyst bed, especially under higher flow rate (above 8 l/min). Under this condition, the air pressure was set at 15 psig.
3. Methyl acetate tank pressure was set at 5 psig by adjusting the regulator located just upstream of the MA tank.
4. The needle valves upstream of the flow meter were adjusted for both air and saturated methyl acetate vapor to dilute the methyl acetate to the desired concentration. Typical values fell between 100 and 10,000 ppm. A rough estimate could be obtained through the readings on the flow meters while an accurate concentration value was obtained from GC analysis. As operational experience was gained with the test rig, it was found that fluctuations of the float inside the flow meter were caused by ruptured sealing rubber, bad tube connections, or clogged solid materials. Correctional action was taken in each case as required.
5. The reactor temperature was increased to the operating range (240 - 380 °C). It was soon learned that great care must be taken with the front panel setting of the PID parameters of the tube furnace. The setting specified by the manufacturer was not applicable in every instance, especially when the thermocouple inside the tube furnace was disconnected, and another thermocouple (the same K type) was connected to the ports on the back of the Eurotherm 847 controller. Corrective action was taken to assure that the temperature measured was the reaction temperature in the catalyst bed and not simply the furnace temperature. For different runs of this experiment, the optimum setting of those parameters was obtained by activating the "tune" function to obtain the best values of proportional band (Prop.), integral time constant (Int.t) and derivative time constant (Der.t).
6. The chart recorder was then activated to monitor temperature oscillations. An example of such an oscillation is shown in Figure II-6. Before taking samples, the temperature was maintained constant at least 10 minutes to achieve a uniform temperature across the catalyst bed.

II.2.2.7 Operating Procedure for On-Line Effluent Analysis

1. The catalytic reaction was first stabilized by bringing it to steady state.
2. The vacuum pump was then started.
3. The breathing valve connected to the vacuum tank was adjusted to keep the tank at the desired vacuum level (-1 mm Hg to -20 mm Hg), depending on the sampling requirement. For the on-line analysis, -1 mm Hg was sufficient, while -20 mm Hg was applied when the sample loop was filled with a standard gas sample from the Scotty gas cylinder in which a certain percentage of gas components (e.g., CH_4, O_2, CO_2 or N_2), was premixed by the manufacturer.
4. The sampling flow rate was checked by the flow meter connected on-line between the vacuum tank and the sampling port attached to the reactor. Typical flow rates were 20 to 30 cc/min to guarantee that the sample loop (250 μl) was entirely flushed within 20 sec by the fluid with the same concentration as that in the reactor.
5. The sample from the outlet of the reactor was taken first.
6. Immediately after the first injection, the sample from the inlet of the reactor was flushed into the sample loop. One minute later, both sampling valves were closed to isolate the gas sample inside the sample loop while waiting for the second injection.

II.2.2.8 Operating Procedure for Gas Chromatograph

1. The pressures of the He, H_2 and breathing air cylinders were checked. In accordance with the manufacturer's suggestion, pressures of the He, H_2 and breathing air were maintained at 80 psig, 40 psig and 60 psig, respectively.
2. Leak checks were performed on the 1/8 inch copper tubing connecting the GC and the gas cylinders.
3. The carrier gas (He) flow rate was set at 60 cm^3/min.
4. The Star Work Station was initiated (by typing win/s).
5. The parameters in the Method Editor were set as shown in Table II-3.
6. The parameters for both relays were set as shown in Table II-4.
7. The stability of the TCD and FID baselines was checked. When the baseline was not stable, it was necessary to wait until there were no significant fluctuations, since an unstable baseline can be caused by unstable column or detector temperature, which is an important factor in GC operation.
8. A run was initiated by the control computer through clicking on the "start" icon on the screen in the system control section.

II.3 EXPERIMENTAL RESULTS

II.3.1 Deactivation Test of Catalyst

Prior to the experiment, a test for possible catalyst deactivation was performed. The catalyst was continuously exposed for 70 hours to a dry air stream containing 3000 ppm methyl acetate at 258°C . During this time period, the conversion of methyl acetate was monitored and recorded continuously. These results are presented in Figure II-7. The drop in methyl acetate conversion at approximately 14 hours was due to a temperature change from 265°C to 258°C. Other than this, no significant change in the conversion of methyl acetate was detected during the 70 hours. This demonstrated that the catalyst did not lose its effectiveness for at least 70 hours. Thus, the catalyst used in obtaining kinetic data was exposed to the oxidation of methyl acetate for less than 70 hours. Once over 70 hours, the catalyst was replaced or regenerated with hydrogen.

II.3.2 Preliminary Test Without Catalyst

A test run was made to determine the conversion percent of methyl acetate without catalyst prior to the full-up experiment involving the kinetic measurement process. Glass beads of approximately 6.9 g were placed in the reactor as a substitute for the catalyst. Methyl acetate was then fed through the reactor at the lowest flow rate (0.6 ml/min) and the highest temperature (380 °C) during this test. An average 2.75% conversion of the methyl acetate was obtained for different concentrations of MA. This suggested that noncatalytic conversion due to thermal decomposition could be neglected in comparison to the catalytic conversion process.

II.3.3 Elimination of Interphase Mass Transfer Resistance

In order to obtain a true reaction rate, all distortion due to the effects of interphase mass transfer resistance must be eliminated. If the rate of the reaction is much greater than the heat transfer rate, then the reaction becomes mass-transfer-controlled and a false reaction rate will be measured. Consequently, an investigation was undertaken to ascertain whether or not the reaction in this experimental setup is mass-transfer-limited. In this investigation, the Mears criterion [Mears, 1971] was applied. The Mears criterion is:

$$\frac{r\, r_b\, R\, n}{k_c\, C_A} < 0.15 \qquad (2)$$

where r = reaction rate, mole/$w_{catalyst}$ sec
ρ_b = bulk density of catalyst bed, kg/m^3
R = catalysts particle radius, m
n = reaction order
C_A = bulk concentration, mol/m^3
k_c = mass transfer coefficient, m/sec

The value of the mass transfer coefficient, k_c, in a fixed-bed reactor was calculated from a semi-empirical equation [Bird et al, 1971]. The left-hand side of equation 2 is a ratio of reaction rate to mass transfer rate. If the ratio is less than 0.15, the external diffusion limitation is not significant.

It was determined through the course of experimentation that the external mass transfer resistance could be neglected during all of the kinetic measurement experiments. Under this condition, the concentration gradient between the bulk fluid and the catalyst external surface is negligible. Therefore, the measured bulk concentration is equal to the concentration on the catalyst surface, and the measured reaction rate can be used for kinetic analysis.

II.3.4 Conversion of Methyl Acetate

For a fixed-bed integral reactor, the combination of rate and design equations lead to [Froment,1979]:

$$\frac{W}{F^{\circ}_{MA}} = \int_0^x \frac{dx}{r} \qquad (3)$$

where W = catalyst weight, gram
F_{MA° = initial flow rate of reactant A, mole/sec
x = conversion of reactant A
r = rate

For a fixed amount of catalyst, W, the conversion fraction of methyl acetate, x, is a function of the flow rate, F. Therefore, a series of experimental data was acquired with the following assumptions:

1. Uniform temperature profile inside the catalyst bed within short distance (<5 cm) in both radial and axial directions
2. Plug flow pattern in the reactor
3. Negligible wall effect
4. Constant catalyst activity during the experiment.

A summary of reaction conditions is given in Table II-5. The conversion of methyl acetate as a function of retention time at different temperatures obtained by experiment is shown in Figures II-8 through II-23, with curves representing the predicted values using the Langmuir-Hinshelwood model. The problem of estimating the kinetic parameters through the use of nonlinear curve fitting is addressed in the next section.

II.4 DATA ANALYSIS

II.4.1 Analytical Model Formulation

An analytical model of the reaction process was developed, based on two primary assumptions. First, the concentration of oxygen was assumed to be constant, since the consumption of oxygen (maximum 0.75% based on inlet MA=2000 ppm) was not significant compared with the oxygen concentration in air. Second, it was assumed that the small amount of water produced (0.75% maximum) in the reaction did not affect the reaction rate. With these two assumptions, the rate equation could be simplified to involve only the methyl acetate. Two rate equations were proposed, as described in Table II-6, one based on a first-order power law, the other on the Langmuir-Hinshelwood model.

The first-order power law is the simplest approach to formulating the rate equations. This approach neglects the adsorption and desorption processes occurring on the catalyst surface and provides less information on the detailed reaction mechanism than a more elaborate formula. However, when the singular objective is reactor design, the first-order power law is advantageous because of its fewer adjustable parameters. Also, such an equation can frequently be used to accurately correlate the experimental data for an industrial reactor design [Smith, 1981]. Consequently, this approach was initially taken to fit the experimental data, with the result shown in Figure II-24. It is seen from this figure that a simple first-order rate equation cannot account for variations of MA concentration such as were encountered in this experiment. The rate constant, k, for modeling purposes was treated as a combination of a surface reaction rate constant and an adsorption equilibrium constant, i.e., the rate constant takes into account the processes of adsorption, reaction and desorption.

The second approach used to correlate the experimental data, based on the Langmuir-Hinshelwood model, shown in Table II-6, employs a rate constant, k, in the numerator which is a combination of a reaction rate constant and an adsorption equilibrium constant. Moreover, the term $k_a C_{MA}$ in the denominator takes into account the inhibition due to adsorption of reactant (k_a is the adsorption equilibrium constant). Hence, with the increase of inlet methyl acetate concentration, the reaction rate decreases due to decreased active site area available at the catalyst surface. This causes a decrease in the conversion of methyl acetate. Since the Langmuir-Hinshelwood model could adequately explain the methyl acetate concentration effect shown in Figure II-25, this model was selected for the data analysis.

II.4.2 Parameter Estimation

After the rate equation was selected, a nonlinear regression was applied to obtain the necessary parameters at each temperature investigated. First, Equation 2 above was rearranged and integrated, with the result shown in Table II-6. Following this, a nonlinear regression analysis program based on

Marquardt's method was used to fit the kinetic data at each temperature [Marquardt, 1963]. This data was needed to estimate the parameters k and k_a.

A group of 12 to 20 data points was used in determining the kinetic parameters for each temperature investigated in the nonporous catalyst case. The results, shown in Table II-7, indicate that the rate constants generally increase with an increase in temperature. On the other hand, the adsorption equilibrium constant does not show explicit dependence on temperature over the temperature range investigated. This suggests that the temperature dependence of the adsorption equilibrium constant (k_a) is not as significant as that of the rate constant (k).

The temperature dependence of the two rate constants was then correlated using the Arrhenius equation:

$$k(T) = A e^{-E/RT} \qquad (4)$$

where A = pre-exponential factor or frequency factor
E = activation energy, cal/mole
R = gas constant, 1.987 cal/mol K
T = absolute temperature, K

Parameters for use in this equation were calculated, and are presented in Table II-8.

In the Arrhenius equation, the activation energy E represents the minimum energy required by the molecules before the reaction can begin. The term $e^{-E/RT}$ represents the fraction of collisions between molecules having a minimum energy E and the total number of molecules. From the results reported in Figures II-26 through II-29 and Table II-8 for both the nonporous and porous catalyst configurations, the activation energy for the rate constant was determined to be 10,786 cal/mole for the 1/16-inch porous catalyst, and 8,847 cal/mole for the 1/8-inch nonporous catalyst. It suggested from this that the energy barrier to the reaction for the porous catalyst was larger than for that of the nonporous catalyst.

II.5 THE TAGUCHI METHOD OF EXPERIMENTAL DESIGN

The Taguchi method of experimental design can be helpful in analyzing a system with several uncertainties because it offers maximum information with minimum sets of experiments [Ross, 1988]. A Taguchi orthogonal array, L_{27}, (shown in Table II-9) was constructed based on 3-level factors with interaction, viz., reaction temperature (A), methyl acetate concentration (B), and gas flow rate (C); and 3-level factors with no interaction, viz., pressure (D), carbon dioxide concentration (E), and oxygen concentration (F). The three levels for each factor are indicated in the table. The pressure factor was eliminated due to the inability to operate this reactor at reduced pressure. Experimental results, in the form of conversion percent of methyl acetate for the twenty-seven point set, are shown in Table II-9.

Based on these experimental design results, an analysis of variance was performed. The results, shown in Table II-10, indicate that the random error, designated by the letter e in the table, and the fluctuations due to E, F and BxC factors, are all small. This implies that the effects of both carbon dioxide and oxygen concentrations on the MA conversion are insignificant. This may be realized from an irreversible oxidation reaction of MA to form carbon dioxide. Therefore the concentration of carbon dioxide will not affect the conversion of MA. It is also understandable that oxygen concentration will not affect the conversion of MA, since there is a large excess of oxygen. It is convenient, therefore, to lump the fluctuations of these parameters into a combined random error factor, resulting in a simplified analysis of variance as shown in Table II-11. The calculated F values indicate that the reaction temperature (A-factor) is the most significant factor affecting the conversion of methyl acetate. The next most significant factor is the gas flow rate factor (C), followed by the methyl acetate concentration (B). The cross effect of either AxB or AxC is insignificant based on a confidence level of 95%.

II.6 ANALYTICAL MODEL PREDICTION

II.6.1 Simulations of Temperature and Conversion Distribution in Fixed-Bed Reactors

With the rate equation established for the oxidation of methyl acetate, the design (scale-up) of a reactor can next be performed. Two different operational conditions are often assumed, adiabatic and nonadiabatic (with natural convection). Both conditions require the application of mass and energy balances to develop the temperature and conversion profiles along the length of the reactor. Depending on the equations used, certain numerical methods are then applied to solve a set of differential or algebraic equations as indicated in the following section. This approach was taken for this project, with the result that helpful guidelines were developed for the design of a human metabolic simulator, which is essentially a catalytic combustor.

II.6.1.1 Adiabatic Operation

For a well insulated reactor, the adiabatic assumption is a reasonable one. The energy balance is formulated on the premise that " the energy increased (decreased) = the energy produced (consumed)," with assumptions of no axial and radial dispersion. This results in the following equation:

$$u \rho C_p \frac{dT}{dz} = r r_b (-DH) \qquad (5)$$

where u = fluid velocity, cm/sec
ρ = fluid density, g/cm^3
C_p = fluid heat capacity, cal/g K
T = temperature, K
z = reactor position, cm
r = reaction rate, mole/g_{cat} sec
ρ_b = catalyst bulk density, g_{cat} /cm^3
ΔH = heat of reaction, cal/mole

The reaction rate, r, is then found from:

$$r = \frac{F^{0}_{MA}\, dx}{dw} \qquad (6)$$

where $F_{MA}{}^0$ = reactant flow rate, mol/sec
x = conversion
w = catalyst weight, g_{cat}

The energy balance equation now becomes:

$$\frac{dT}{dx} = (-DH) \frac{F^{0}_{MA}}{F_t c_p} \qquad (7)$$

where F_t = fluid total flow rate, mole/sec

The above equation can be integrated with initial conditions at reactor inlet, x=0 and T=T_{inlet} to obtain the following equation:

$$T - T_{inlet} = (-DH) \frac{F^{0}_{MA}\, x}{F_t C_p} \qquad (8)$$

In addition to the above equation describing the correlation between T and x from the energy balance, the reactor length (i.e., the amount of catalyst) correlated to x was obtained from the mass balance. Within a short distance along the reactor, the mass balance on the reactant leads to:

$$r\,dw = F_{MA}\,dx \tag{9}$$

The above equation can be rearranged by letting $dw=\rho_b A_c\,dz$:

The above equation can be rearranged by letting $dw=\rho_b A_c\,dz$:

$$\frac{dz}{dx} = \frac{F_{MA}}{\rho_b A_c r} = \frac{F_{MA}}{\rho_b A_c \left(\frac{k C_{MA}}{1+ka\,C_{MA}}\right)} \tag{10}$$

where Ac = section area of the reactor, cm^2
k = rate constant, l/g_{cat} sec
ka = adsorption constant, l/mole
C_{MA} = concentration of MA, mol/l

Using Equation 8 to determine temperature as a function of conversion, Equation 10 was integrated to obtain the reactor length as a function of conversion. This integration is normally accomplished by Simpson's one-third rule (three points), the three-eighths rule (four points), or the five-point quadrature formula. A computer program using the five-point quadrature formula for the adiabatic simulation was used in this analysis.

The results for a methyl acetate inlet concentration of 13,000 ppm at various inlet temperatures and reactor diameters are given in what follows, subject to the assumption that the rate law is valid to 800 °K.

II.6.1.2 Nonadiabatic Operation

Under actual conditions, the reactor will not be adiabatic. Consequently, an analysis of the nonadiabatic operation considering heat loss by natural convection was conducted. For a more accurate estimate, a two-dimensional model which considers both the radial and axial variations is required. Nevertheless, a one-dimensional model is sufficient for a preliminary design. It provides a rapid procedure for estimating reactor size and the effect of variables such as reactor diameter. For example, as the tube size decreases, the ratio of the heat transfer area to the reactor volume increases faster than in adiabatic reactors. Hence, the temperature increase (for an exothermal reaction) through the bed length will be less. The approximate length of a nonadiabatic reactor can be estimated by this simplified procedure.

The equations formulated for the nonadiabatic case are basically the same as those for the adiabatic case except that the term representing heat transfer from the reactor surface is included in the energy balance equation. Equation 6 becomes:

$$\frac{dT}{dx} = \frac{(-\Delta H_r)\,F^{\circ}_{MA}}{F_t\,C_p} - \frac{U_r(2\pi)(T-T_\infty)}{F_t\,C_p}\frac{dz}{dx} \tag{11}$$

where U_r = heat transfer coefficient, cal/cm sec K
T_∞ = ambient temperature, K

To estimate the heat transfer coefficient U_r, a uniform radial temperature distribution inside the catalyst bed, with natural convection between the reactor outer surface and ambient fluid, was assumed. Thus, the heat transfer resistances considered were only from the inner edge of the tube to the outer surface and from the outer surface to the ambient air. The heat transfer coefficients, k_r (for conduction in stainless steel tube) and h_m (for free convection) were then estimated.

For Prandtl numbers (Pr) greater than 0.6, and a horizontal cylinder in an infinite fluid, a commonly used correlation is as follows [Bird, 1971, page 413]:

$$Nu_m = 0.525\ (Gr\ Pr)^{1/4} \qquad (12)$$

where Nu_m = Nusselt number, $h_m D/k$, dimensionless
Gr = Grashof number, $D^3\rho^2 g\ \beta\ \Delta T/u$, dimensionless
Pr = Prandtl number, $C_p\ \mu/k$, dimensionless

The Prandtl number representing the ambient fluid physical properties was first calculated, as well as the Grashof number (ratio of buoyant forces to viscous forces) in the free-convection flow system. Then the Nusselt number (ratio of conductive thermal resistance to convective thermal resistance) was calculated to find h_m. The values calculated for a 70 °F ambient temperature are:

Tube OD	Pr	Gr	Nu_m	h_m[1]	k_r[2]	Bi	Ur[3]
4"	0.73	3.74E7	2.73E7	1.707	26.1	0.011	0.0012
2"	0.73	4.68E6	3.41E6	2.031	26.1	0.015	0.0007

[1] Btu/hr ft^2 F
[2] Btu/hr ft F
[3] cal/cm sec K

In the above, the Biot number ($Bi = h\ l_0\ /k$) represents the ratio of conductive resistance to convective resistance. A large value of Bi indicates that conductive resistance dominates, while a small Bi number means that convection is the controlling heat transfer mode. A criterion for determining when the system is controlled by convection is:

$$Bi < 0.1 \qquad (13)$$

From the Bi values in the table, the heat transfer between the reactor and the ambient gas under free convection is obviously always driven by convection.

Equations 9 and 10, were solved to determine the temperature (T) and the reactor length (z) as a function of the conversion fraction (x). Both Euler's method and the Runge-Kutta method were used to solve the differential equations simultaneously. The fourth-order Runge-Kutta method was found to be more accurate. A computer program in Polymath using a 4th-order Runge-Kutta method was applied to solve the problem with an initial value x=0.0 to final value x=0.9999. These results are plotted in Figures II-30 through II-37.

Comparing the results of adiabatic operations and nonadiabatic operations, a significant difference can be seen in Figure II-34. Because of the neglect of heat loss in adiabatic operations, the temperature always increased along the reactor for the exothermal reaction, as indicated in Figures II-309 through II-33. However, when heat loss is considered, the temperature distribution is determined by the heat of reaction and the heat loss. If the heat loss is larger than heat of reaction, such as is the case in

Figure II-34, the temperature decreases along the length of the reactor, and the conversion of methyl acetate does not increase rapidly. When the heat generated by the reaction is larger than the heat loss (similar to adiabatic operations), the temperature rises and the conversion of methyl acetate increases.

II.7 CONCLUSIONS

The following conclusions are drawn from this investigation:

1. The 0.5% Pt/Al_2O_3 catalyst was shown to be capable of converting methyl acetate to carbon dioxide and water at a temperature as low as 350 C.

2. The rate law of the Langmuir-Hinshelwood model was found to be better than the first-order rate law in predicting the conversion of methyl acetate. The L-H model is successful in predicting the effect of methyl acetate concentration on the conversion of methyl acetate.

3. Adiabatic and nonadiabatic operations were simulated based on the Langmuir-Hinshelwood model to guide the design of a metabolic simulator. For a 4 inch OD reactor, MA=13000 ppm and inlet temperature=250 °C, the minimum reactor length was determined to be 9.2 cm for adiabatic operation and 12.3 cm for nonadiabatic operation, considering heat loss by natural convection. Model prediction indicated that the temperature increases rapidly at the end of an adiabatic reactor.

4. Results from the Taguchi experimental design method indicate that the major factors affecting the conversion of methyl acetate are temperature, flow rate and methyl acetate concentration, in order of decreasing effectiveness. Concentrations of carbon dioxide and oxygen were found to have insignificant (less than 1%) effect on the conversion of methyl acetate.

II.8 TABLES FOR SECTION II

Table II-1
Canned-Man Requirements

Process	Metabolic Rate		
	Average	Minimum	Maximum
O_2 consumption,			
mo_2 (g/min)	0.58	0.37	0.99
Vo_2 (sLpm)	0.41	0.26	0.70
CO_2 production,			
mco_2 (g/min)	0.69	0.45	1.19
Vco_2 (sLpm)	0.35	0.23	0.61
H_2O vapor production by respiration and perspiration,			
mHO_2 (g/min)	1.27	0.51	3.38
VHO_2 (sLpm)	1.58	0.63	4.21
Air ventilation,			
m_{air} (g/min)	12.1	7.8	>21
V_{air} (sLpm)	9.3	6.0	>16
Sensible heat production,			
q_{sens} (kJ/min)	5.1	4.0	5.9
Latent heat production,			
q_{lat} (kJ/min)	3.1	1.2	8.2
Total metabolic heat production,			
q_{met} (kJ/min)	8.2	5.3	14.1

Source: Lange, K. E. (1991). Summarized Work on the Analysis of a Proposed Metabolic Simulator. NASA/JSC Document.

Area Counts volt sec	MA Injected mole
2.721E+07	1.50E-07
1.268E+07	7.51E-08
2.617E+06	1.61E-08
1.322E+06	8.04E-09
7.557E+05	4.13E-09
5.048E+05	3.15E-09
3.505E+05	2.07E-09
3.717E+05	2.07E-09
2.712E+05	1.57E-09
2.429E+05	1.57E-09
1.459E+05	8.24E-10
1.454E+05	8.24E-10
6.987E+04	4.12E-10
6.801E+04	4.12E-10
3.063E+04	2.06E-10
2.994E+04	2.06E-10

Table II-2
Experimental Data for the Calibration of Methyl Acetate

Table II-3
Operating Parameters for Gas Chromatograph

TCD (Thermal Conductivity Detector)	
Temperature	150 °C
Attenuation	16
Range	0.5
Filament Temperature	250 °C
FID (Flame Ionization Detector)	
Temperature	200 °C
Attenuation	32
Range	12
Column Temperature	105 °C
Injector Temperature	105 °C
Column Hold Time	15 min
Channel A	TCD
Channel B	FID
Temperature Programming	Off

Table II-4
Settings for Sample Injection Relays

Time (min)	Relay# 1 position	Relay* 2 position
0.00	1	2
0.25	-1	-2
3.10	1	-2
3.35	-1	2
15.00	-1	2

\# Relay 1 is referred to switch 1 which is used to choose either injecting sample (position 1) or filling sample loop (position -1).

* Relay 2 is referred to switch 2 which is used to select sample from either after reaction (position 2) or before reaction (position -2) to flow down to switch 1.

Table II-5
Summary of Reaction Conditions

Catalyst	Reactor Diameter (inch)	Temperature (°C)	Concentration of MA (ppm)
Porous 1/16" 0.5% Pt/Al_2O_3 Englehard	1/2	230	2000
		385	200, 2000
Nonporous 1/8"×1/8" 0.5%Pt/Al_2O_3 Aldrich	1	220	170
		240	130, 1600
		260	300, 1000
		280	110, 1100
		300	160, 1600
		320	110, 1200
		340	130, 1300

Table II-6
Equations for Regression Analysis with Different Rate Laws

Rate Laws	Equations for Regression Analysis
$rate = k\,C_{MA}$ 1st order power law	$\frac{W}{F_{MA^o}} = \frac{-1}{k\,C_{MA^o}} \ln(1-x)$
$rate = \frac{k\,C_{MA}}{1 + k_a\,C_{MA}}$ Langmuir-Hinshelwood	$\frac{W}{F_{MA^o}} = \frac{-1}{k\,C_{MA^o}} \ln(1-x) + \frac{k_a}{k}\,x$

Table II-7
Rate Constants (k) and Adsorption Equilibrium
Constant (ka) at Various Temperatures for the Nonporous Catalyst.

Temperature (K)	k (l/g_{cat} sec)	Standard error	ka (l/mole)	Standard error
493	0.0015	1.10E-4	20371	2.54E4
513	.00516	3.24E-4	72654	2.59E4
533	.00319	8.24E-5	12216	2.97E3
553	.00617	3.36E-4	32192	1.96E4
573	.00962	1.05E-3	15791	2.31E4
593	.01284	7.77E-4	31074	1.57E4

Table II-8
Arrhenius Equations for Rate Constants and Adsorption Constants

Rate expression : $rate = \frac{k\, C_{MA}}{1 + ka\, C_{MA}}$

	Rate constant		Adsorption equilibrium constant	
Porous 1/16" Englehard	$k = 623.28\ e^{(-10786/RT)}$ l/g sec		$ka = 3.2827*10^{7}\ e^{(-5925/RT)}$ l/mole	
	A	623.28	A	$3.2827*10^{7}$
	E	10786 cal/mol	E	5925 cal/mol
	R	1.987 cal/mol k	R	1.987 cal/mol k
Nonporous 1/8"*1/8" Aldrich	$k = 18.5\ e^{(-8847.1/RT)}$ l/g sec		$ka = 1.4757*10^{5}\ e^{(-2123/RT)}$ l/mole	
	A	18.5	A	$1.4757*10^{5}$
	E	8847 cal/mol	E	2123 cal/mol
	R	1.987 cal/mol k	R	1.987 cal/mol k

Table II-9 Taguchi Experimental Design Orthogonal Array

Set	A	B	C	E	F	Conv.%
1	1*	1	1	1	1	0.09
2	1	1	2	2	2	0.03
3	1	1	3	3	3	0.05
4	1	2	1	2	3	0.088
5	1	2	2	3	1	0.09
6	1	2	3	1	2	0.05
7	1	3	1	3	2	0.04
8	1	3	2	1	3	0.06
9	1	3	3	2	1	0.04
10	2	1	1	3	2	0.57
11	2	1	2	1	3	0.33
12	2	1	3	2	1	0.24
13	2	2	1	1	1	0.47
14	2	2	2	2	2	0.3
15	2	2	3	3	3	0.27
16	2	3	1	2	3	0.25
17	2	3	2	3	1	0.25
18	2	3	3	1	2	0.15
19	3	1	1	2	3	0.93
20	3	1	2	3	1	0.83
21	3	1	3	1	2	0.81
22	3	2	1	3	2	0.89
23	3	2	2	1	3	0.84
24	3	2	3	2	1	0.76
25	3	3	1	1	1	0.87
26	3	3	2	2	2	0.75
27	3	3	3	3	3	0.61

level*	A:Temp.	B:MA con	C:flowrate	E:CO2 con.	F:O2 con.
1	250°C	100 ppm	1.5 l/min	0%	21.0%
2	320°C	500 ppm	3.0 l/min	3.0%	28.5%
3	420°C	2000 ppm	4.5 l/min	8.5%	40.4%

Table II-10
Variance Analysis for Taguchi Experimental Design Results

Factor	Degree of Freedom	Sum of Square	Mean Square	F
A	2	26197.91	13098.95	373.83
B	2	481.16	240.58	6.86
C	2	832.99	416.45	11.88
E	2	47.91	23.96	0.68
F	2	27.29	13.64	0.38
AxB	4	189.74	47.44	1.35
AxC	4	292.71	73.18	2.08
BxC	4	79.07	19.78	0.56
e	4	140.19	35.04	
Total	26	28288.97		

Table II-11
Variance Analysis for Simplified Taguchi Experimental Design Result

Factor	Degree of Freedom	Sum of Square	Mean Square	F*
A	2	26197.91	13098.95	533.78
B	2	481.16	240.58	9.80
C	2	832.99	416.45	16.97
AxB	4	189.74	47.44	1.93
AxC	4	292.71	73.18	2.98
e+E+F+BxC	12	294.46	24.54	
Total	26	28288.97		

* Confidence Level = 95% 99%
F(2,12) = 3.88 6.93
F(4,12) = 3.26 5.41

II.9 FIGURES FOR SECTION II

Figure II-1. Flow Diagram of Experimental Equipment

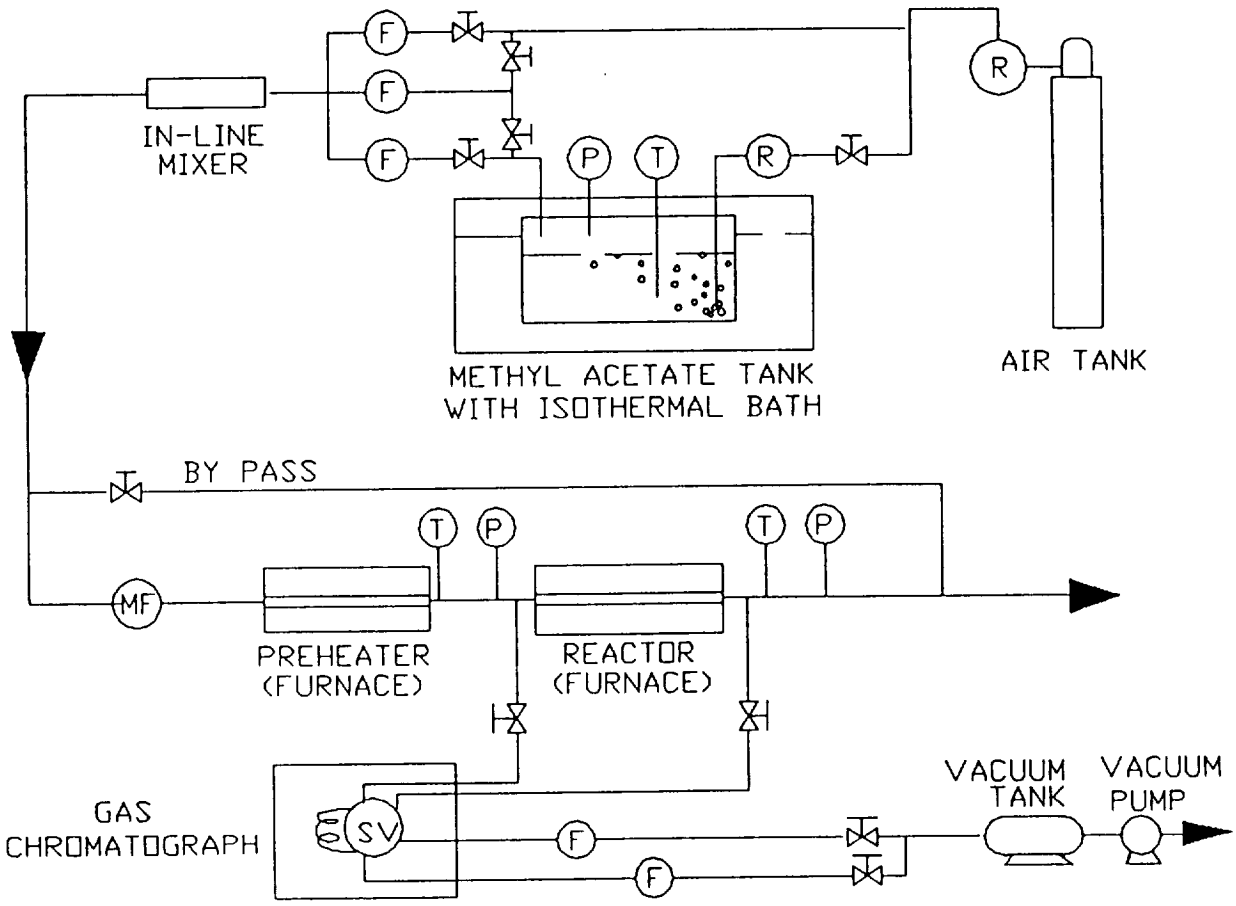

Note:
- (T) Thermo couple
- (P) Pressure Gauge
- (MF) Mass Flow Meter
- (R) Gas Pressure Regulator
- (F) Float Type Flowmeter

Figure II-2. Detailed configuration of the Preheater and Reactor

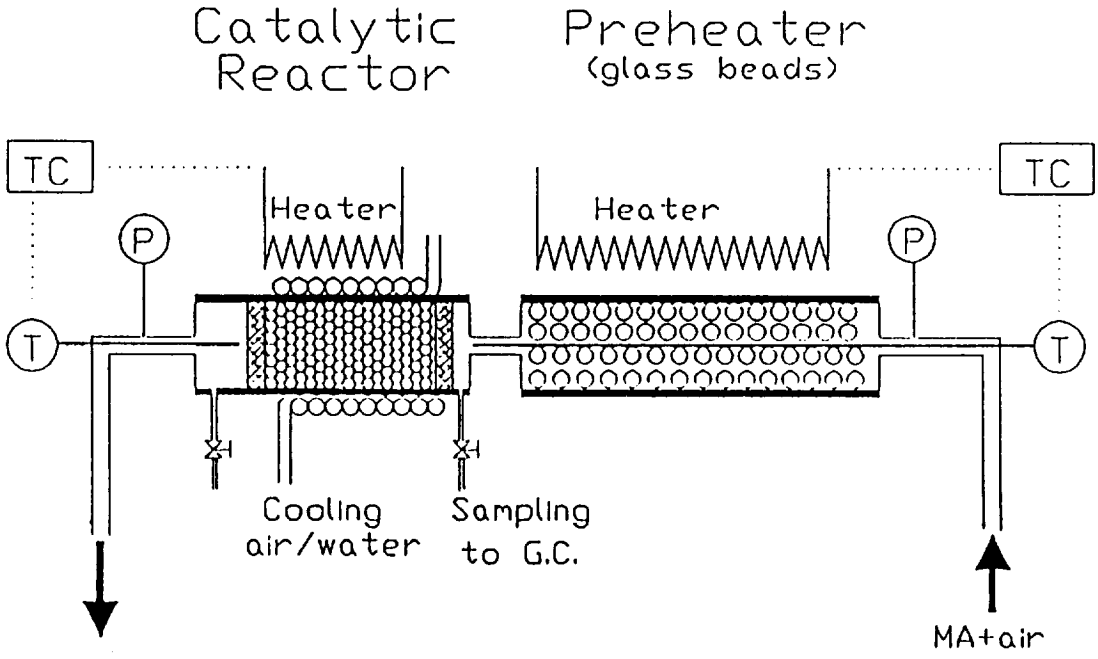

Figure II-3. Flow Diagram of On-Line Sampling System

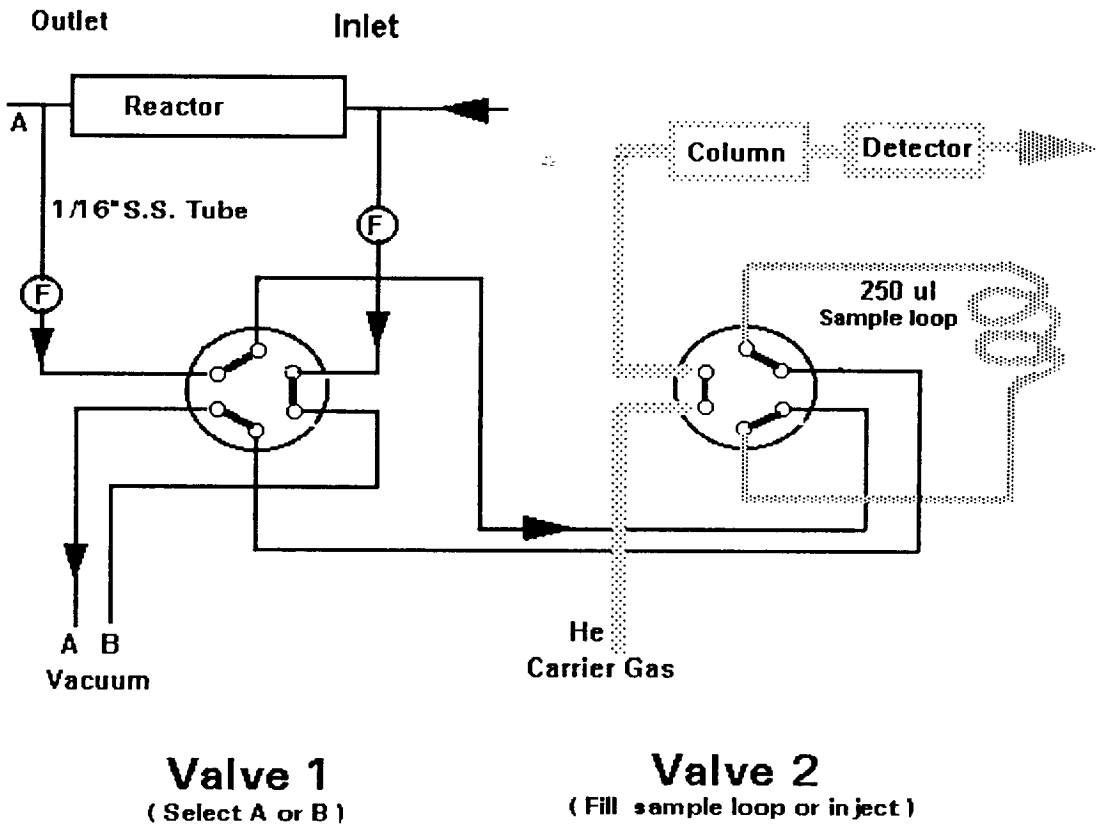

Figure II-4. Flowmeter Calibration

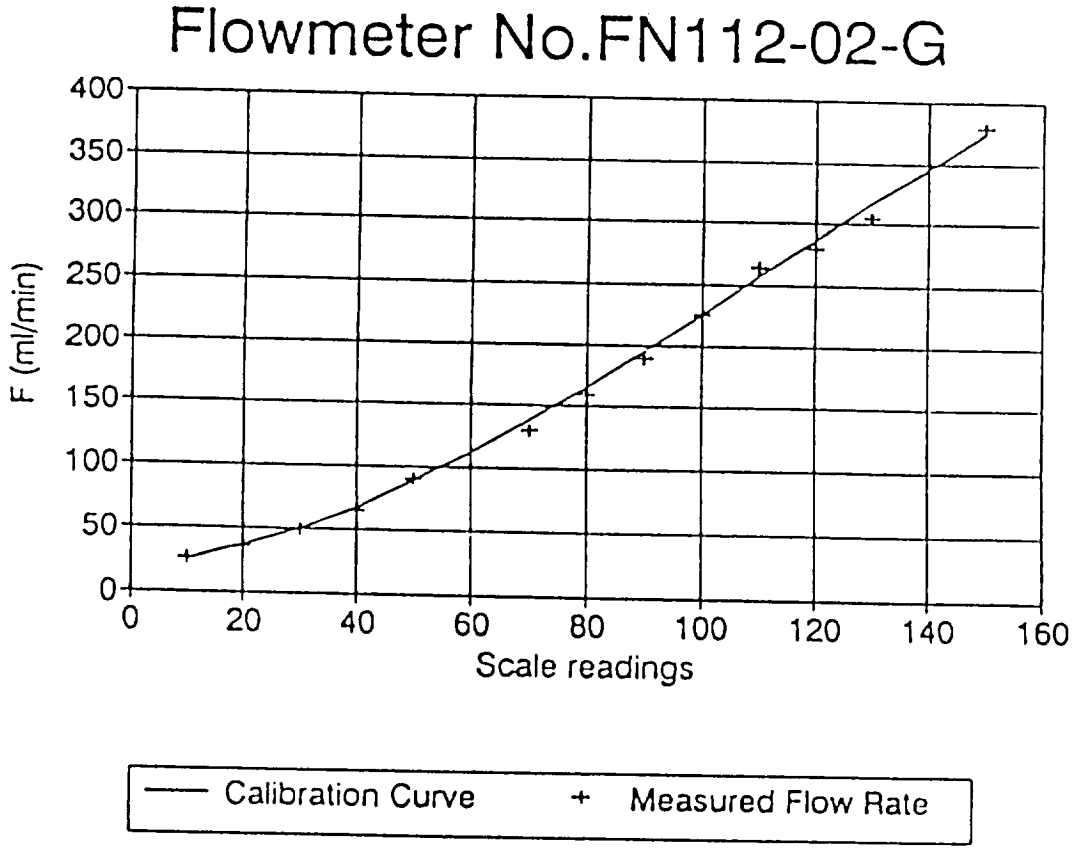

Figure II-5. Calibration Results-MA Amount vs. Area Count

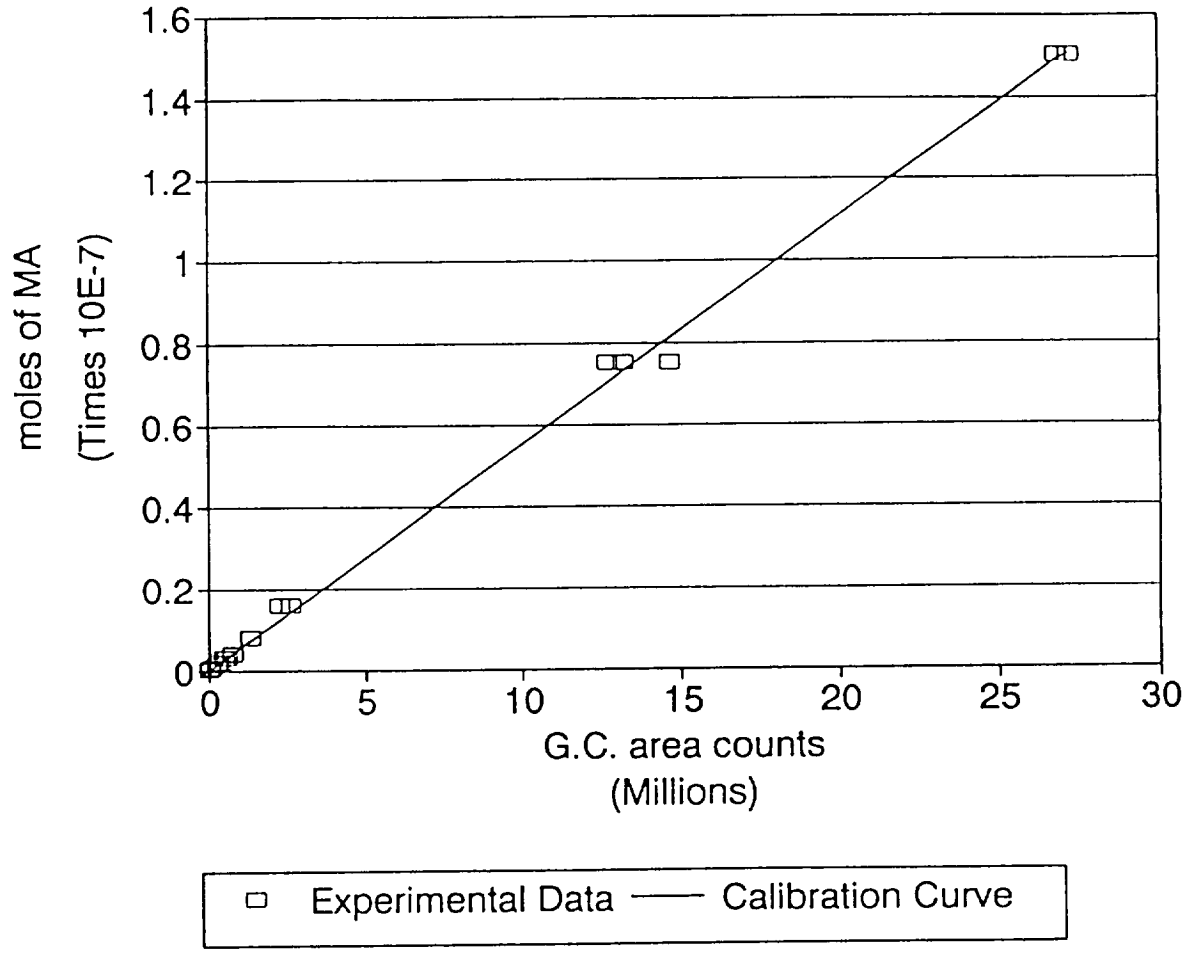

Figure II-6. Temperature Stability of the Reactor and Preheater

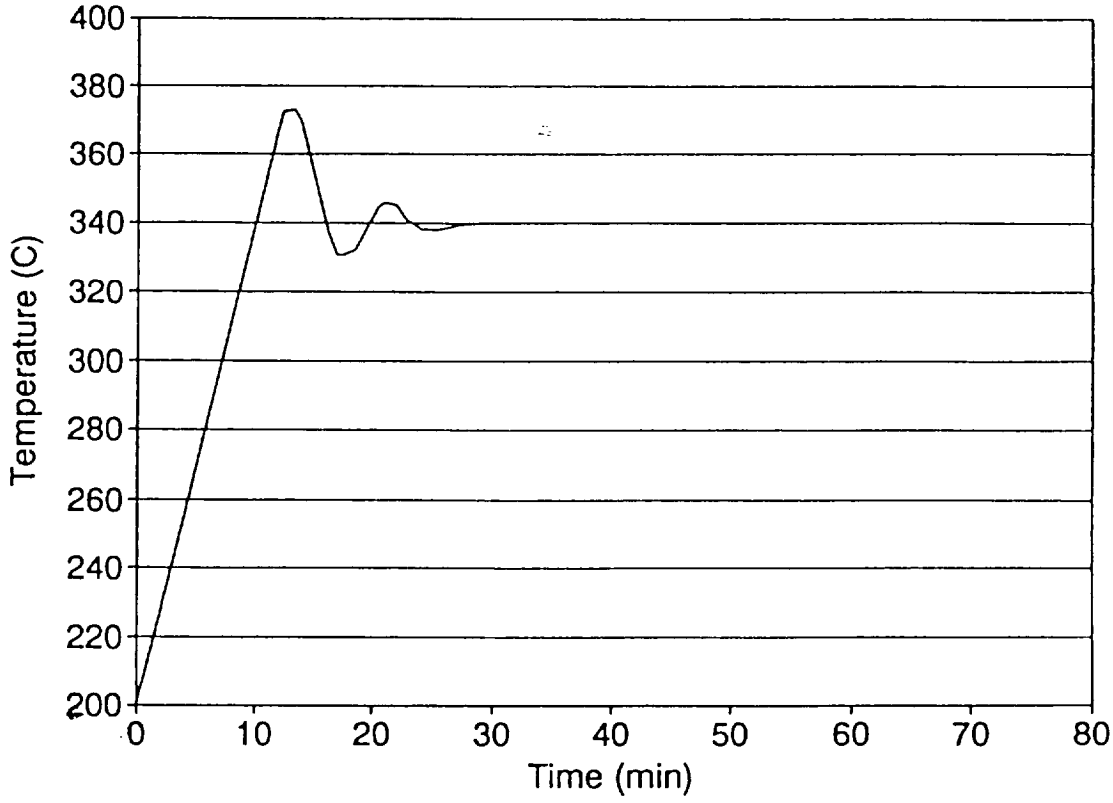

Figure II-7. The Deactivation of 1/8"×1/8" Nonporous Pt/Al_2O_3 Pellet Catalyst

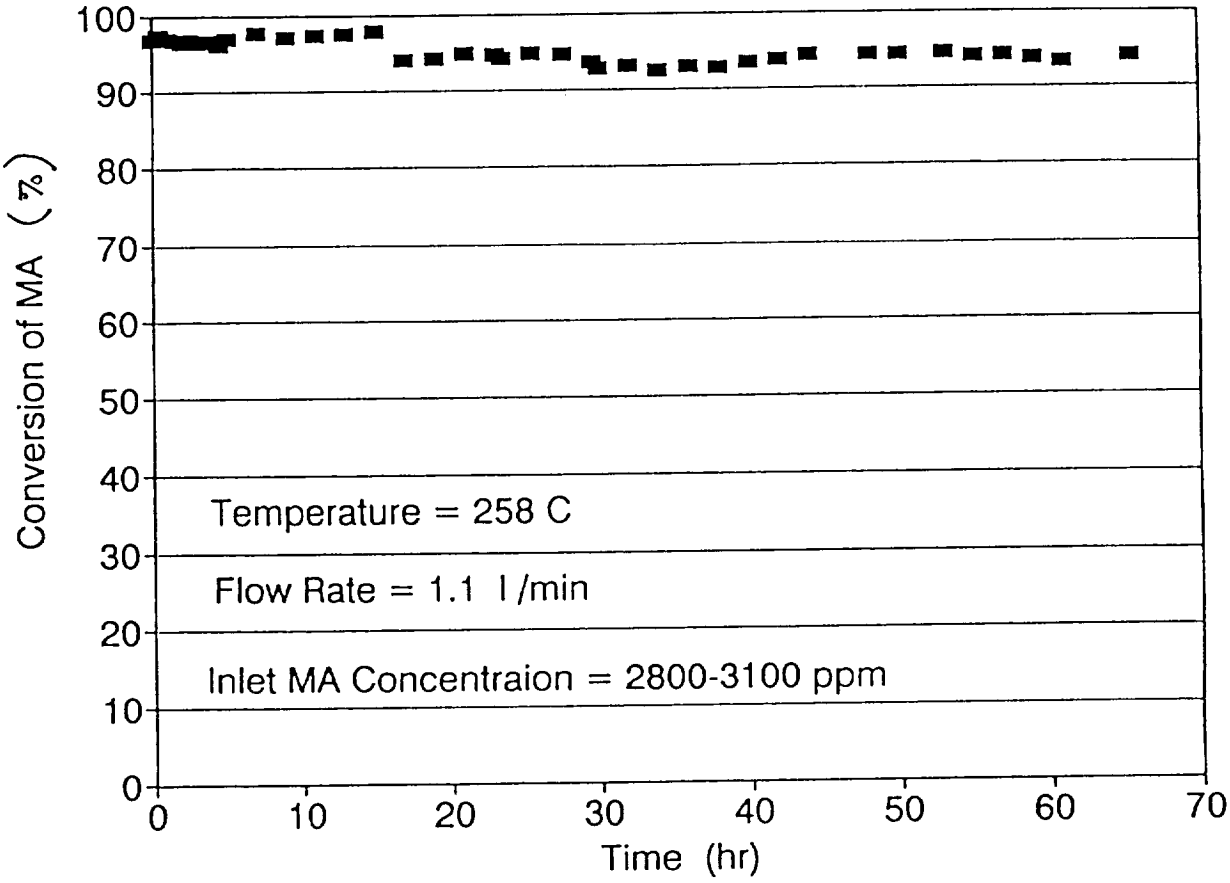

Figure II-8. Conversion vs. Residence Time at T=230°C and Inlet MA=2000 ppm for 1/16" Porous Catalyst

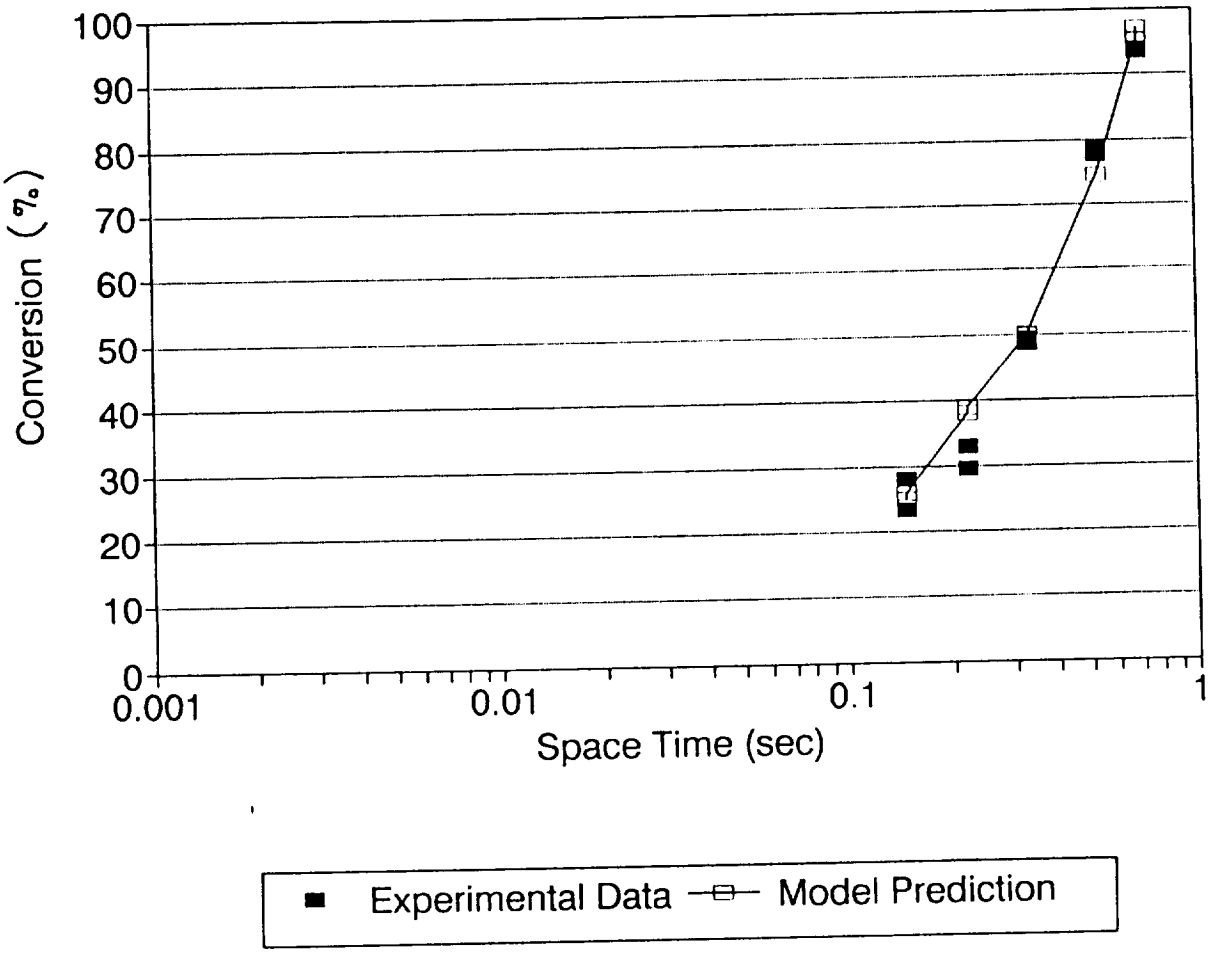

Figure II-9. Conversion vs. Residence Time at T=385°C and Inlet MA=200 ppm for 1/16" Porous Catalyst

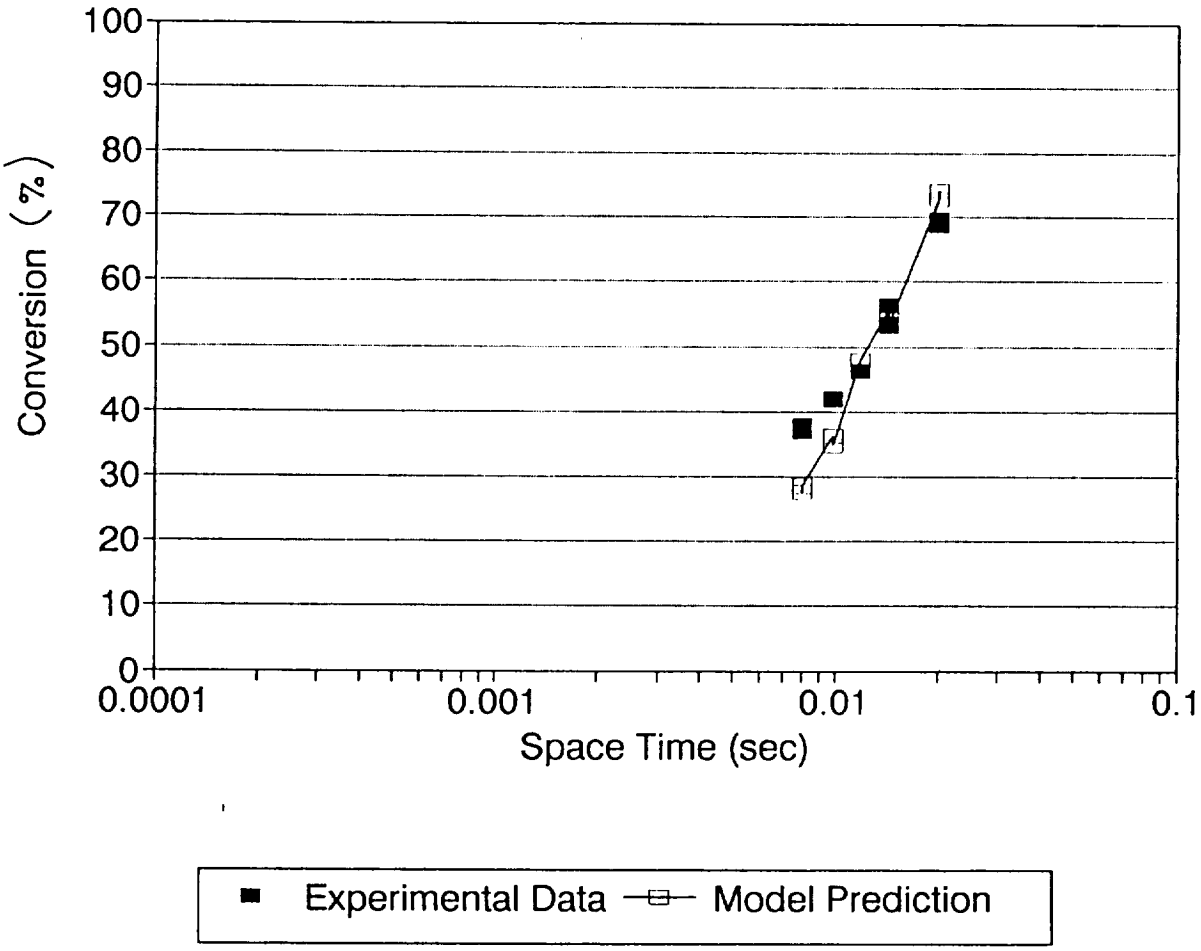

Figure II-10. Conversion vs. Residence Time at T=385°C and Inlet MA=2000 ppm for 1/16" Porous Catalyst

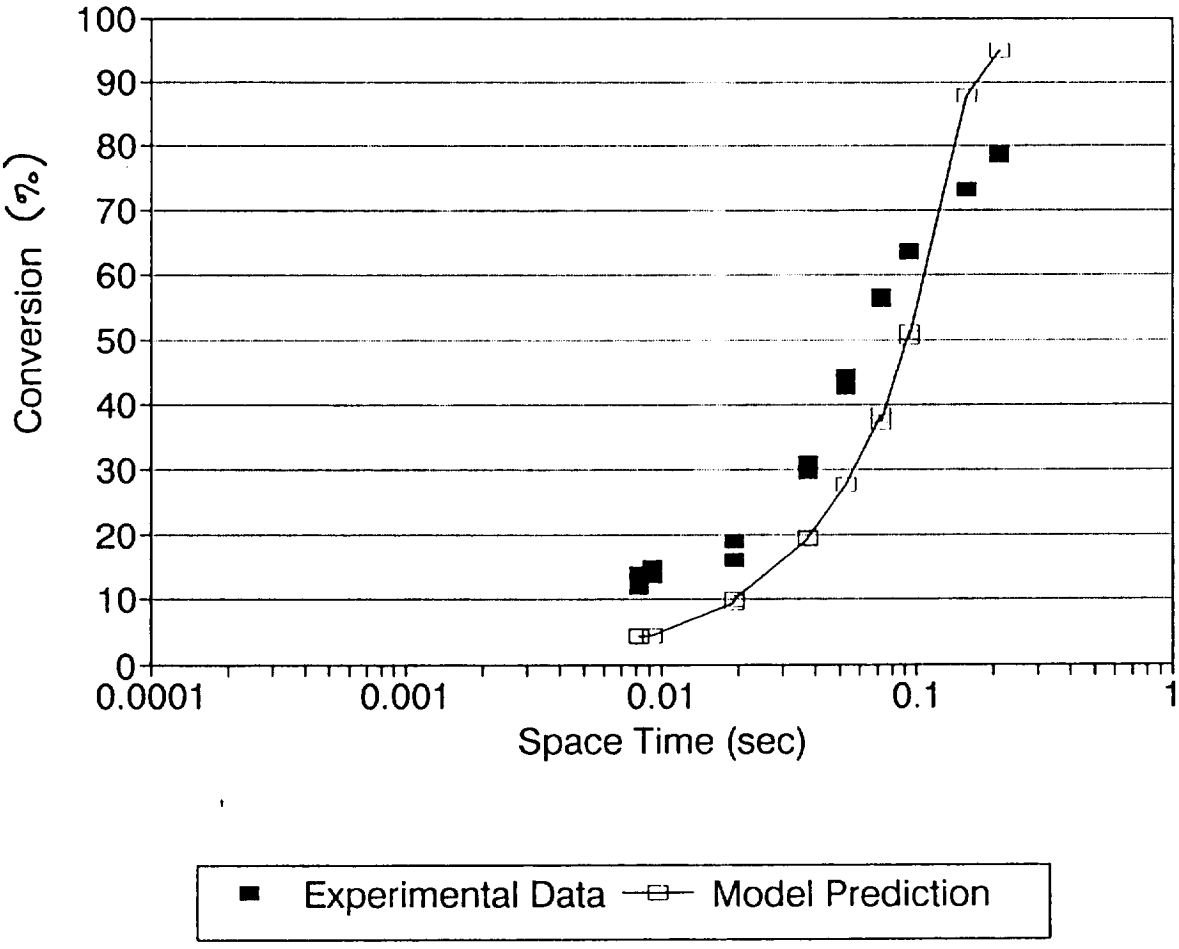

Figure II-11. Conversion vs. Residence Time at T=220°C and Inlet MA=170 ppm for 1/8"×1/8" Nonporous Catalyst

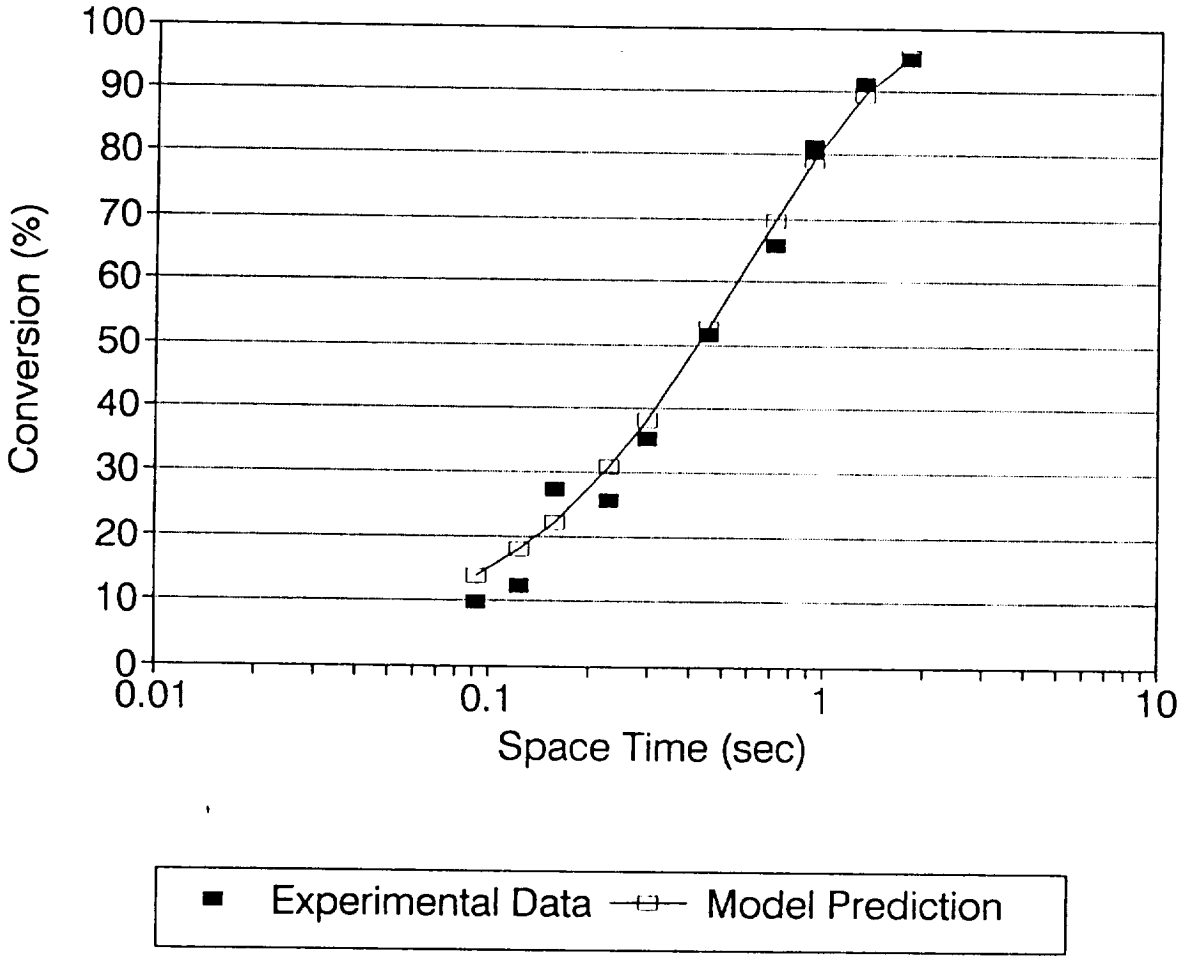

Figure II-12. Conversion vs. Residence Time at T=240°C and Inlet MA=130 ppm for 1/8"×1/8" Nonporous Catalyst

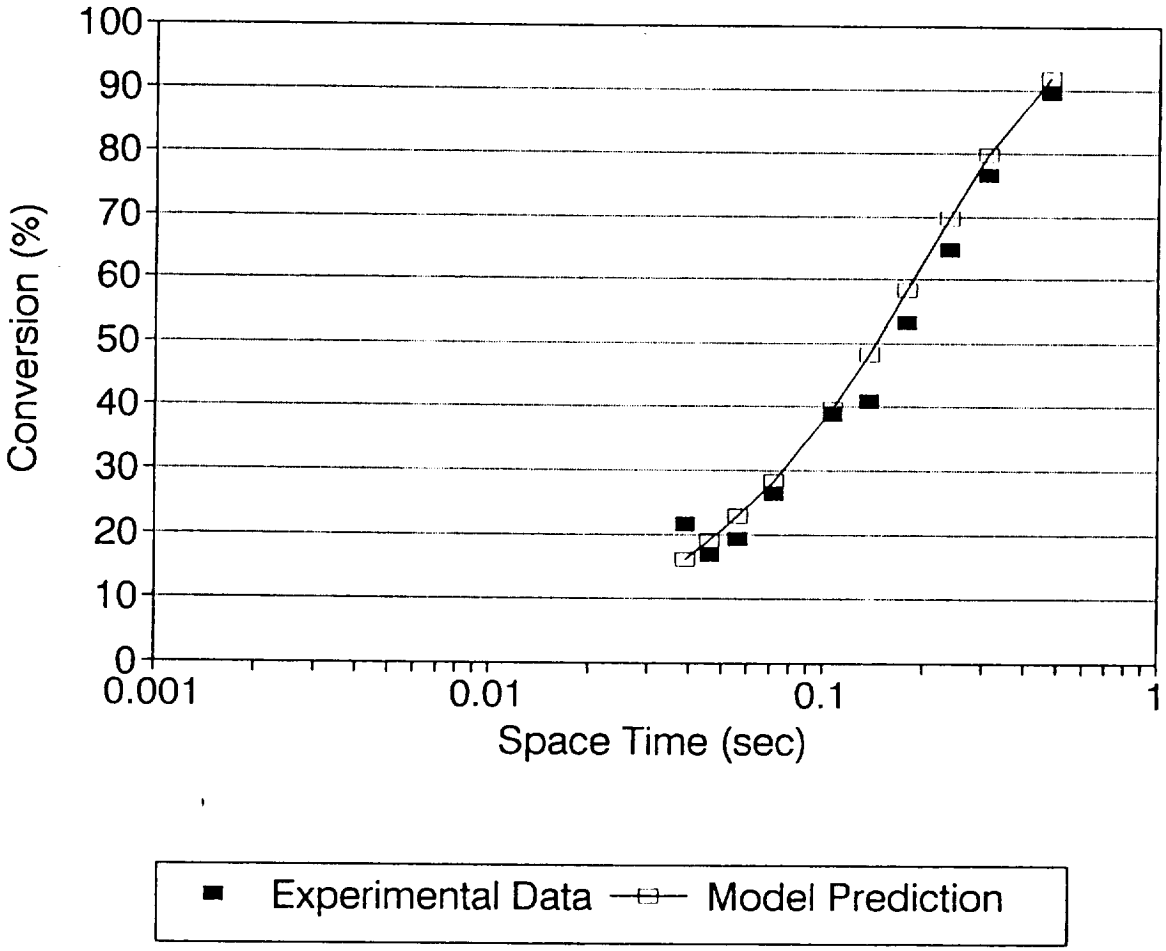

Figure II-13. Conversion vs. Residence Time at T=240°C and Inlet MA=1600 ppm for 1/8"×1/8" Nonporous Catalyst

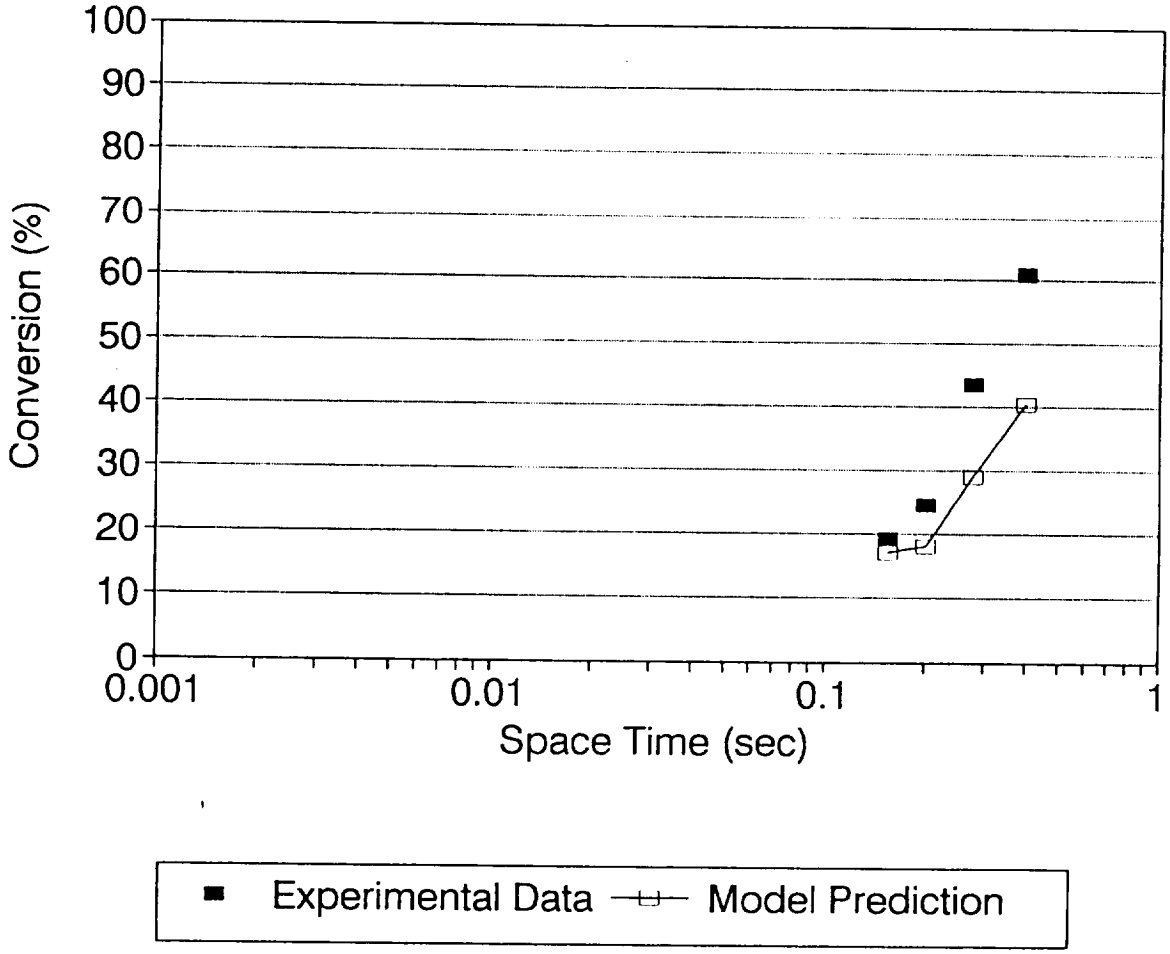

Figure II-14. Conversion vs. Residence Time at T=260°C and Inlet MA=300 ppm for 1/8"×1/8" Nonporous Catalyst

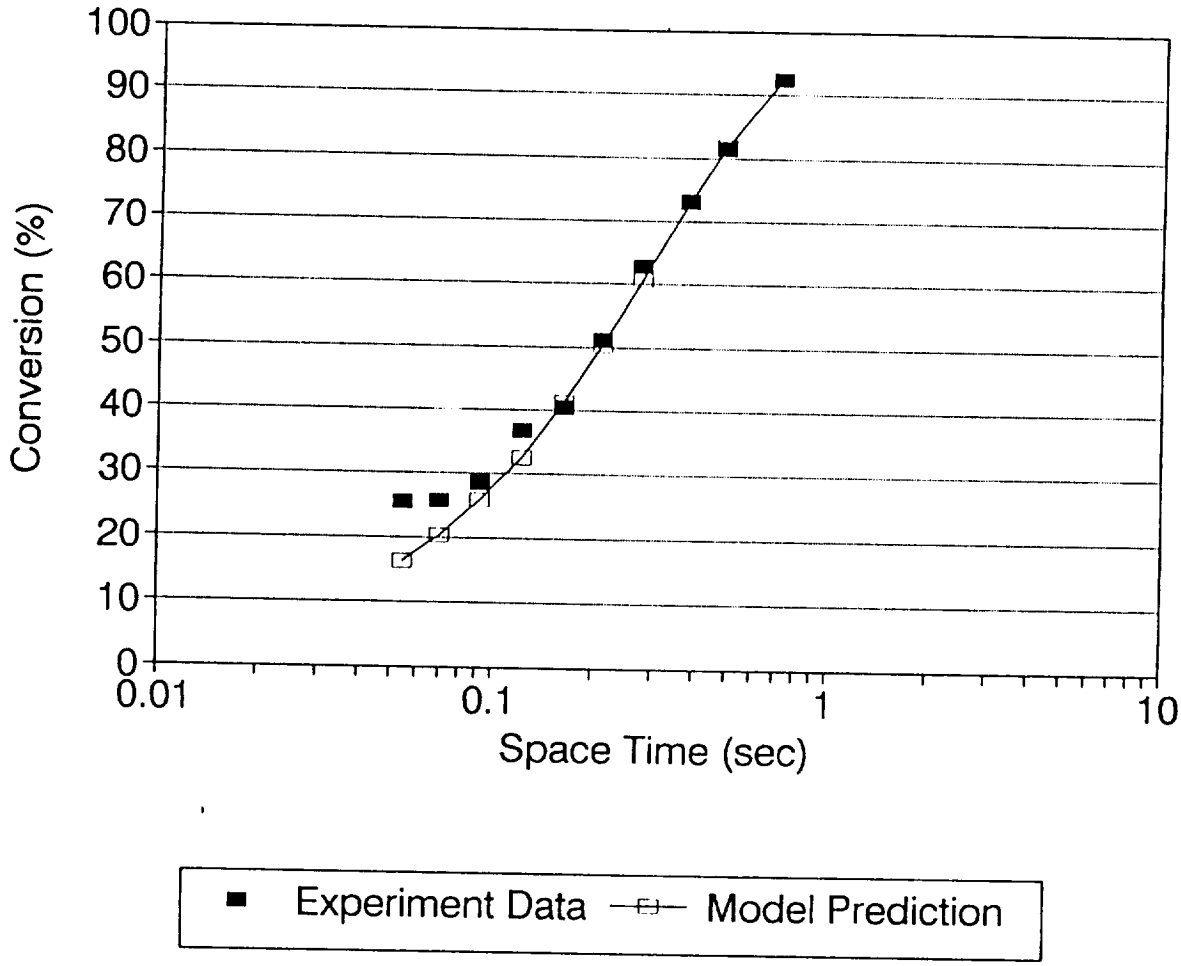

Figure II-15. Conversion vs. Residence Time at T=260°C and Inlet MA=1000 ppm for 1/8"×1/8" Nonporous Catalyst

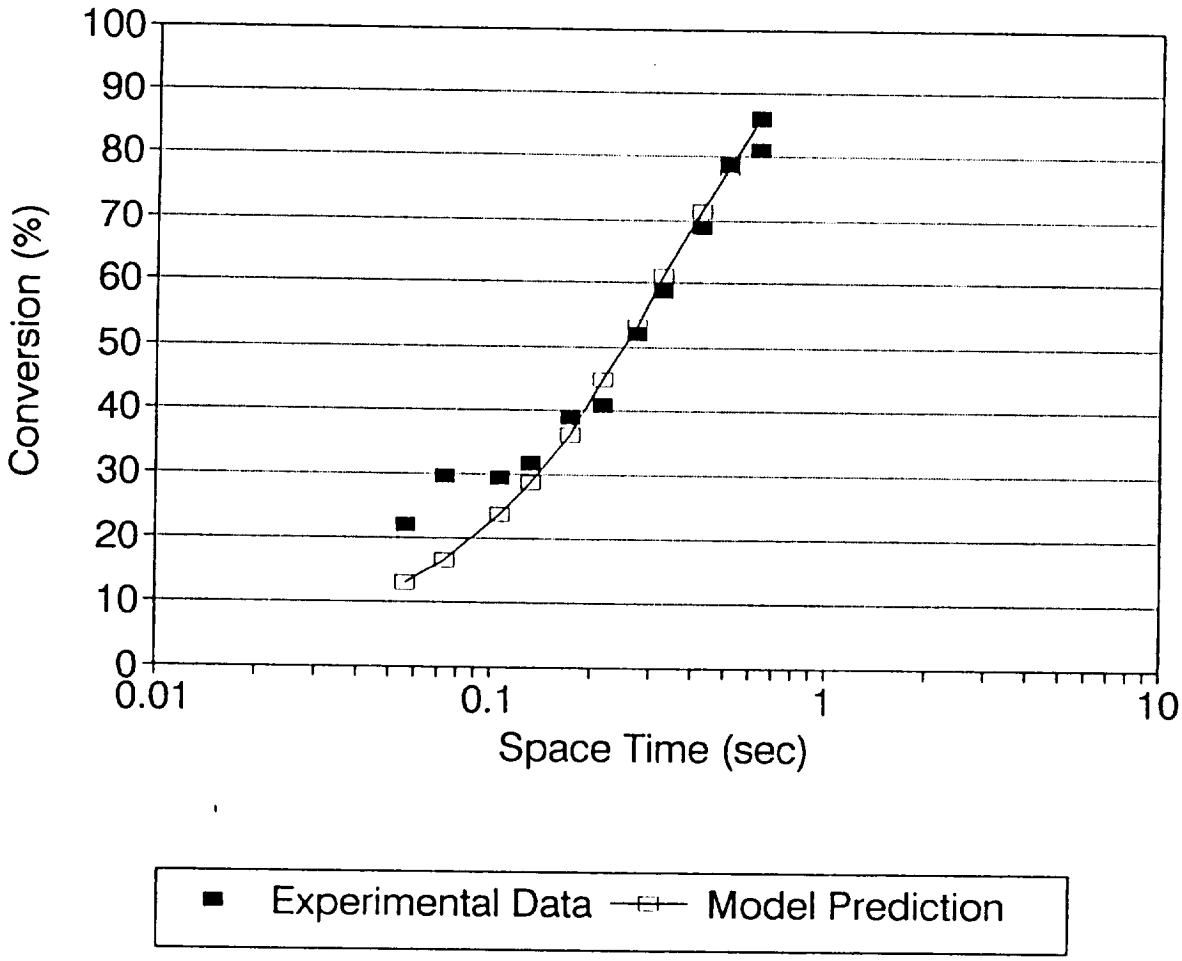

Figure II-16. Conversion vs. Residence Time at T=280°C and Inlet MA=110 ppm for 1/8"×1/8" Nonporous Catalyst

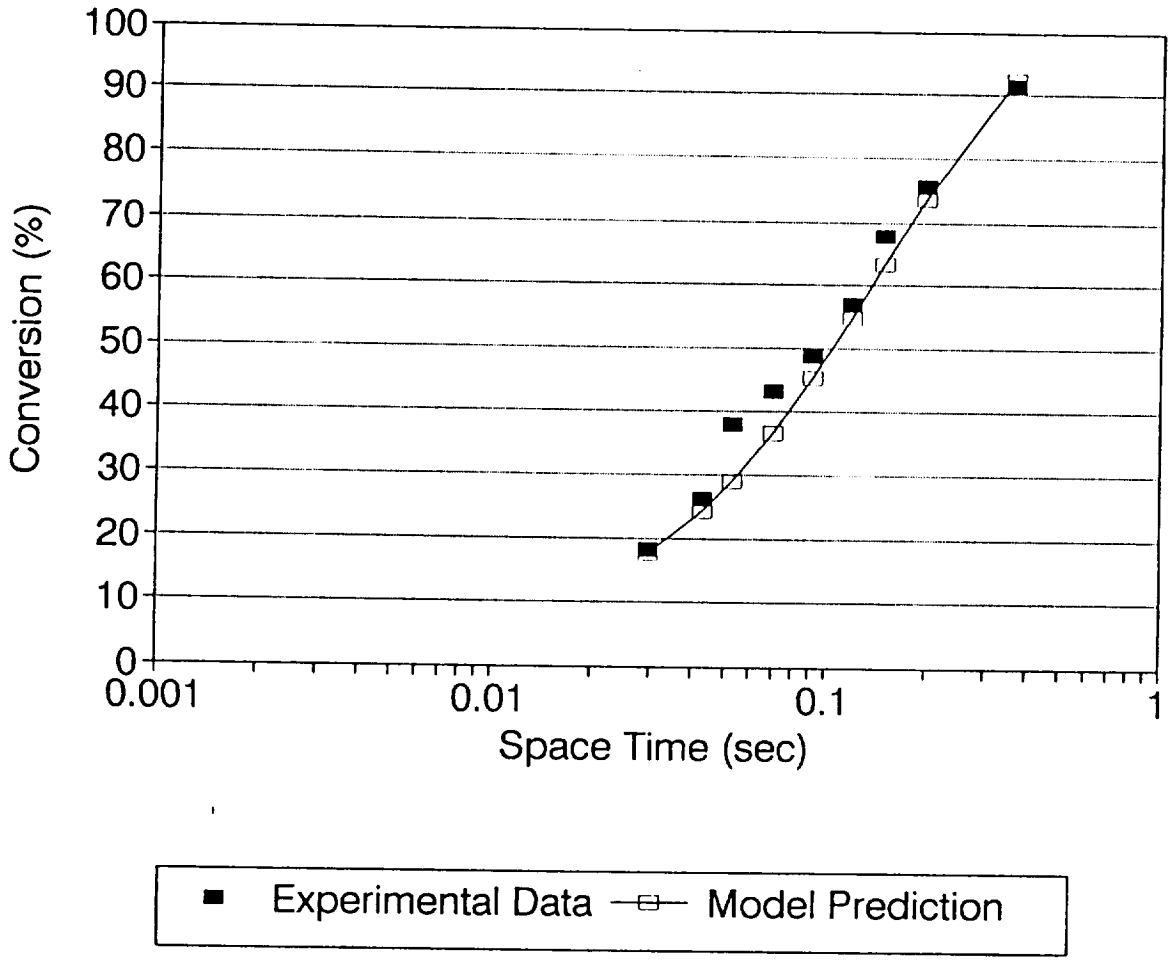

Figure II-17. Conversion vs. Residence Time at T=280°C and Inlet MA=1100 ppm for 1/8"×1/8" Nonporous Catalyst

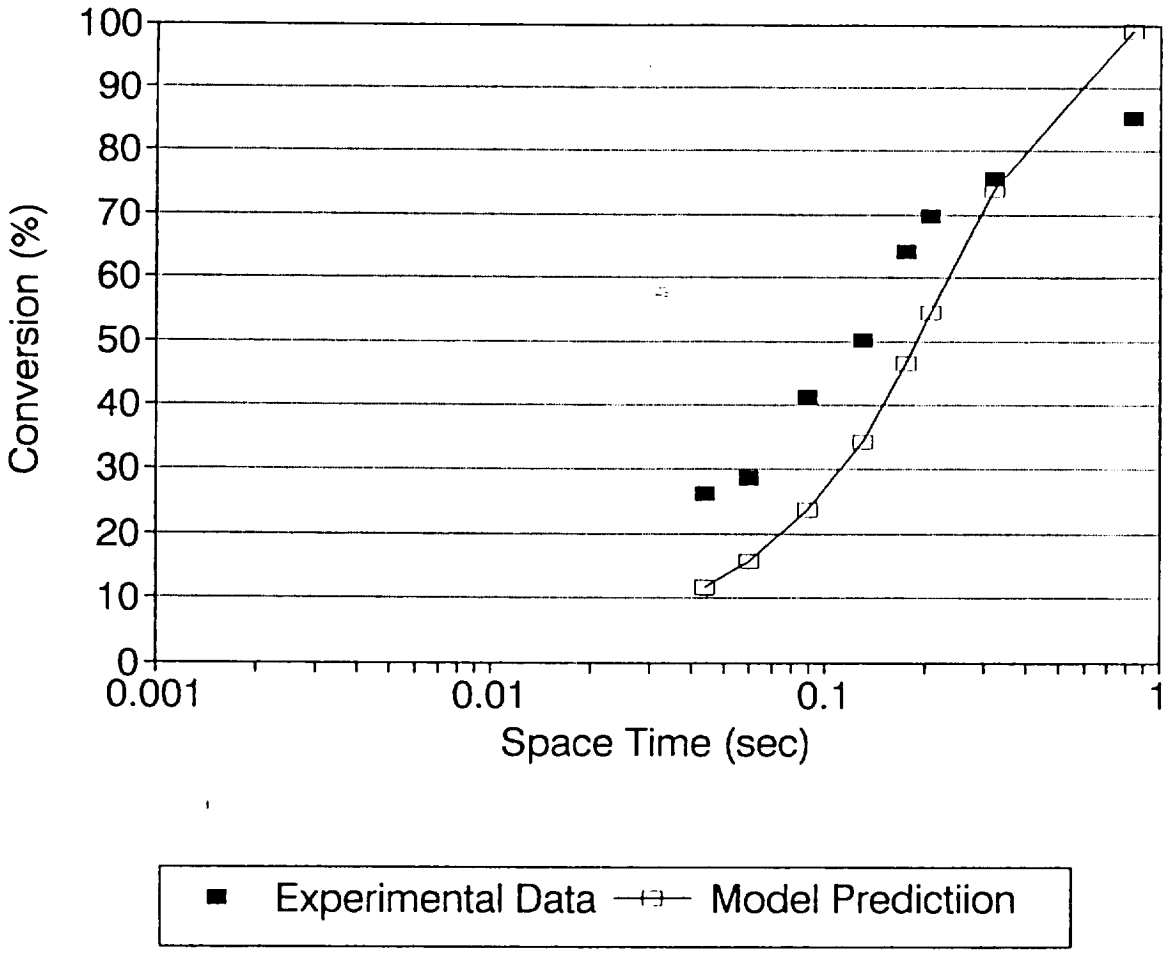

Figure II-18. Conversion vs. Residence Time at T=300°C and Inlet MA=160 ppm for 1/8"×1/8" Nonporous Catalyst

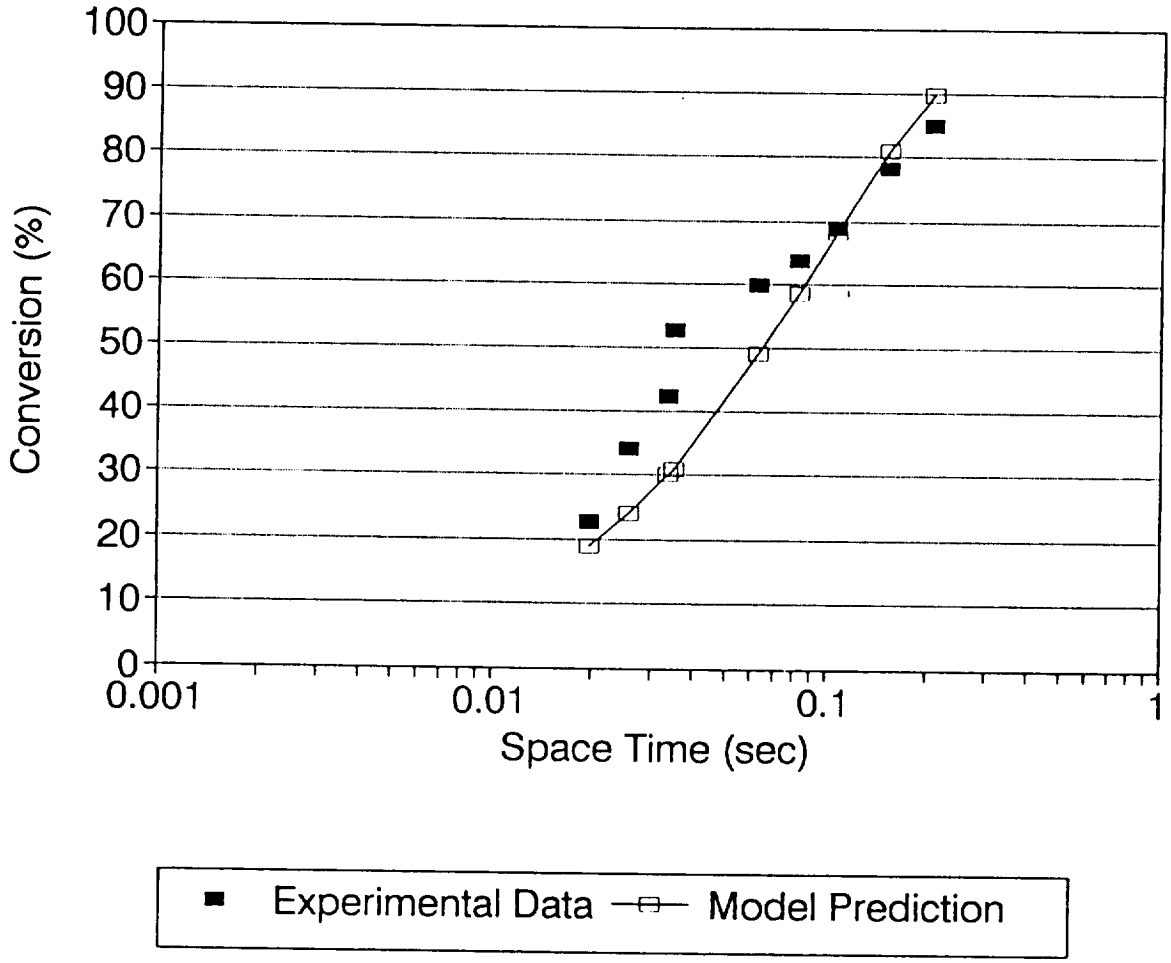

Figure II-19. Conversion vs. Residence Time at T=300°C and Inlet MA=1600 ppm for 1/8"×1/8" Nonporous Catalyst

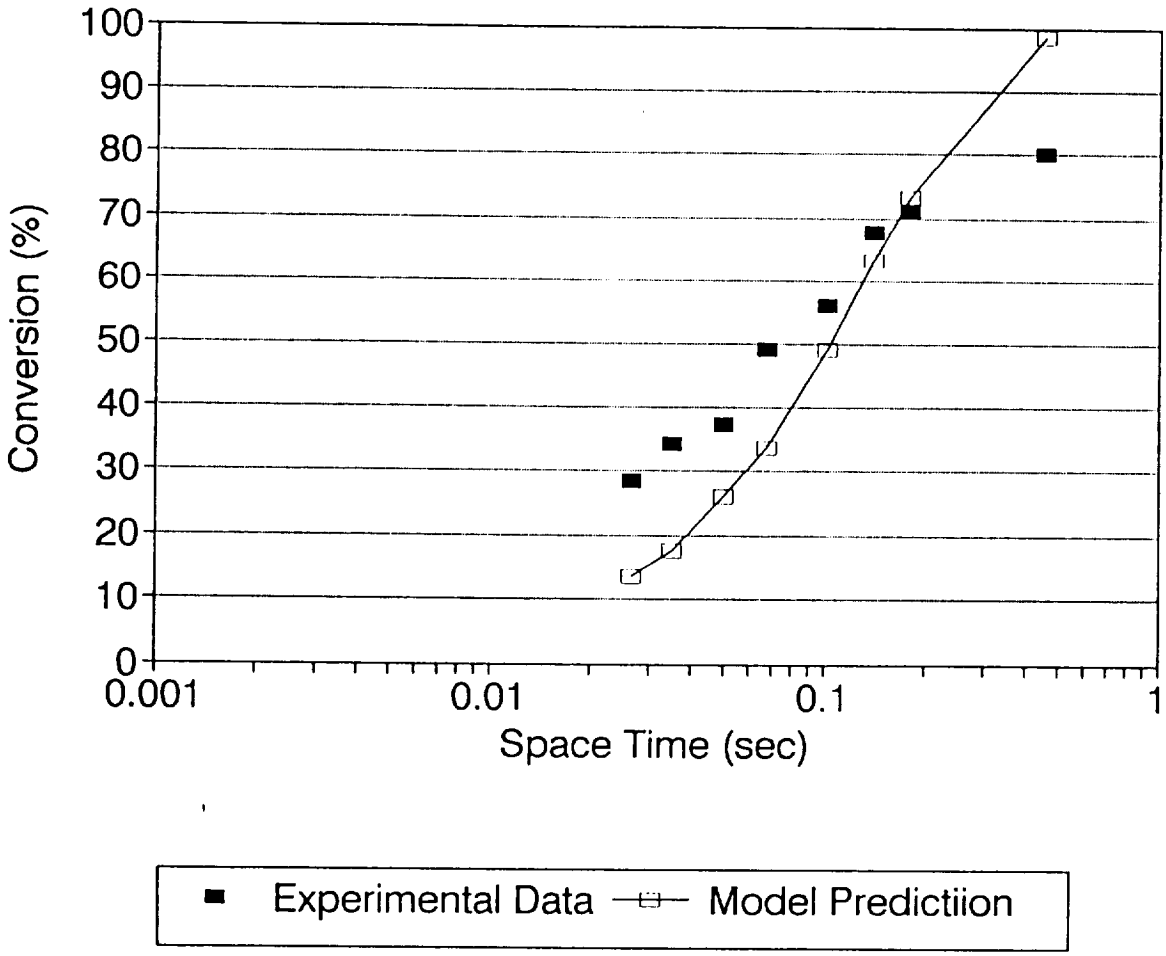

Figure II-20. Conversion vs. Residence Time at T=320°C and Inlet MA=110 ppm for 1/8"×1/8" Nonporous Catalyst

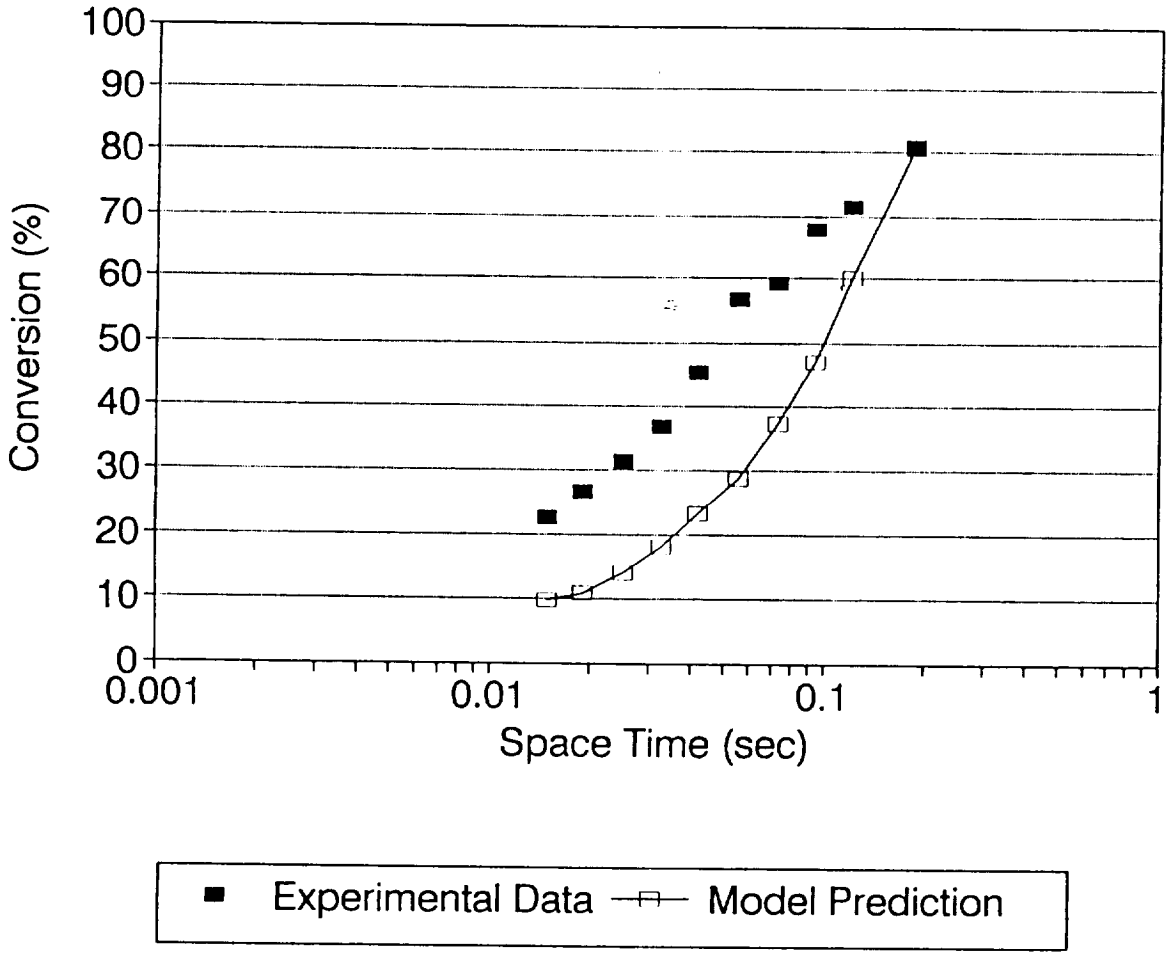

Figure II-21. Conversion vs. Residence Time at T=320°C and Inlet MA=1200 ppm for 1/8"×1/8" Nonporous Catalyst

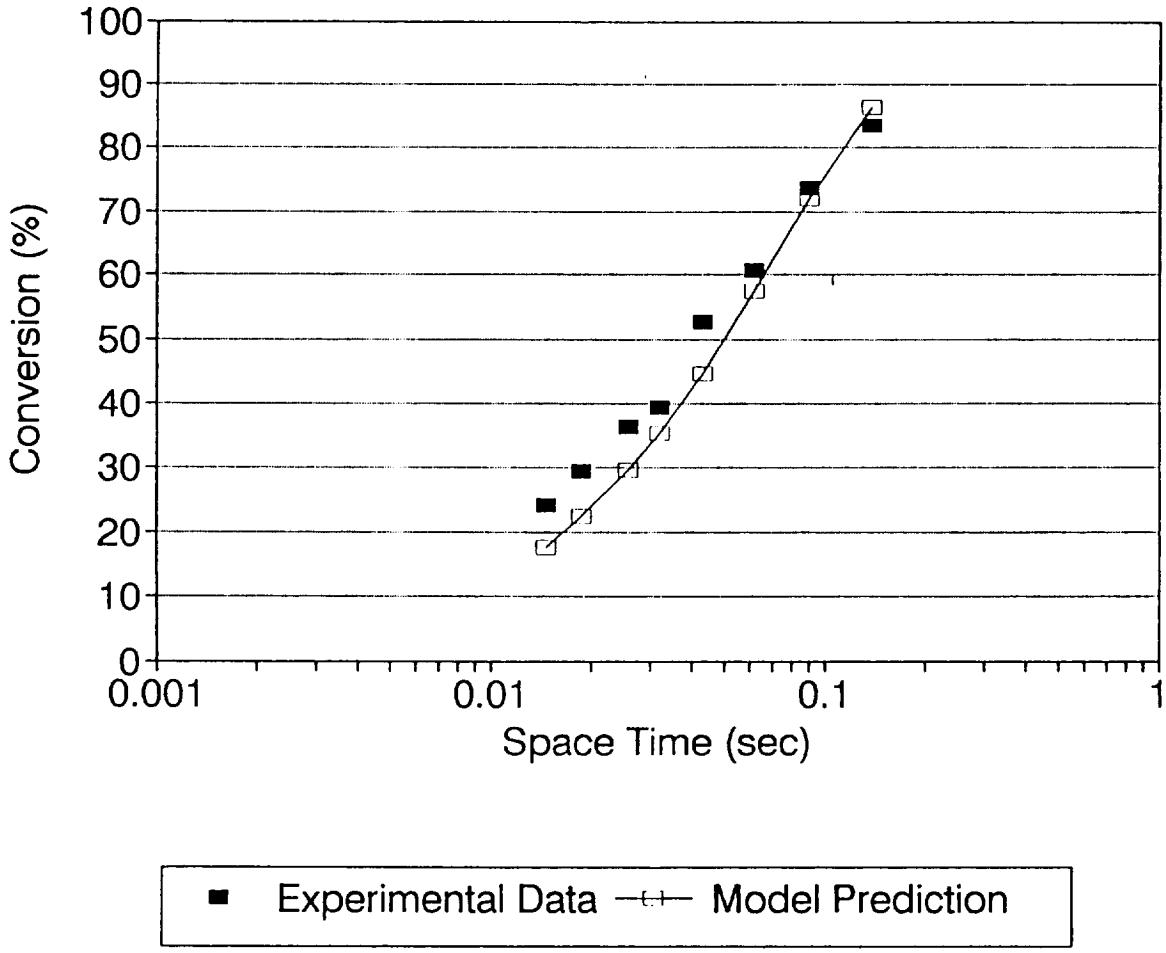

Figure II-22. Conversion vs. Residence Time at T=340°C and Inlet MA=130 ppm for 1/8"×1/8" Nonporous Catalyst

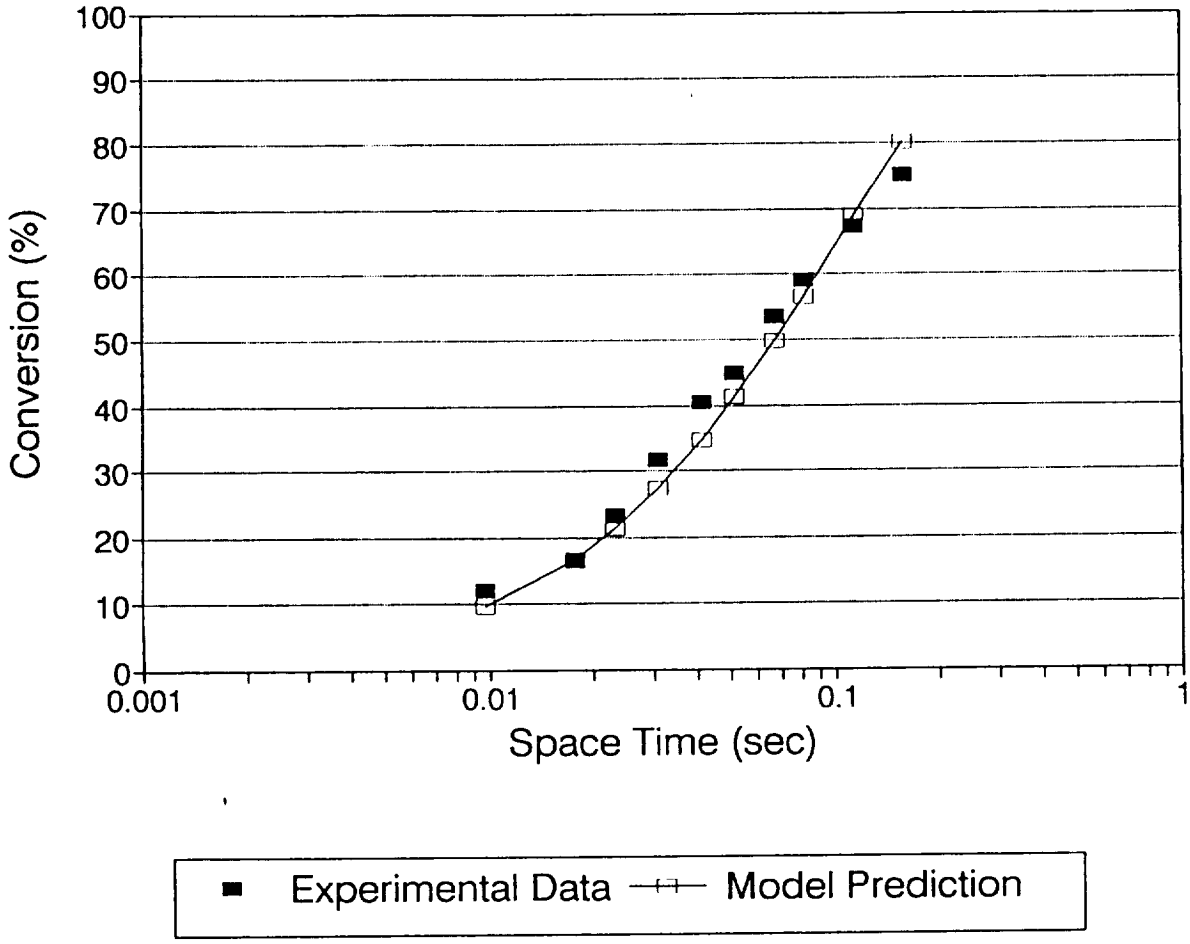

Figure II-23. Conversion vs. Residence Time at T=340°C and Inlet MA=1300 ppm for 1/8"×1/8" Nonporous Catalyst

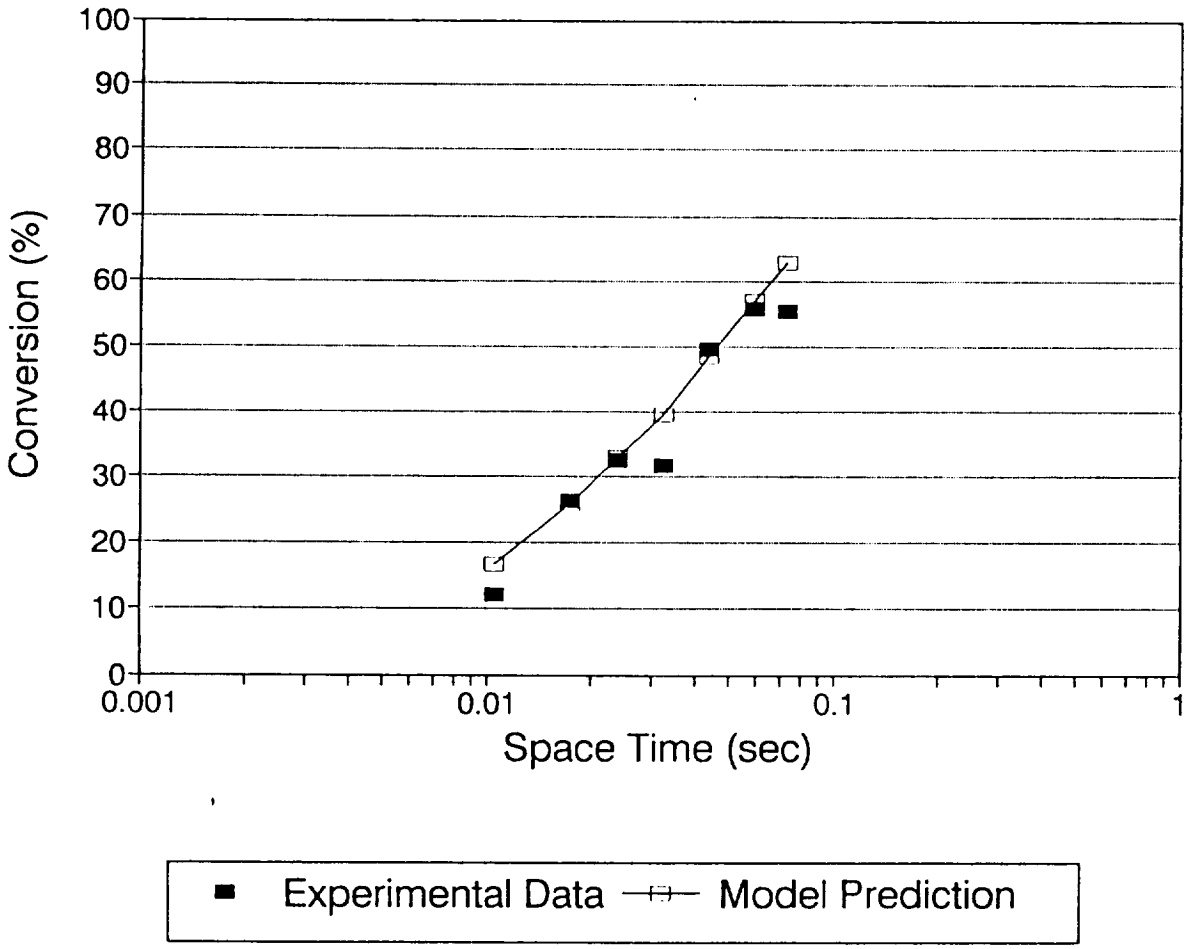

Figure II-24. Percentage Using First-Order Power Law at T=240 °C, with Inlet MA Concentrations of 130 ppm and 1600 ppm

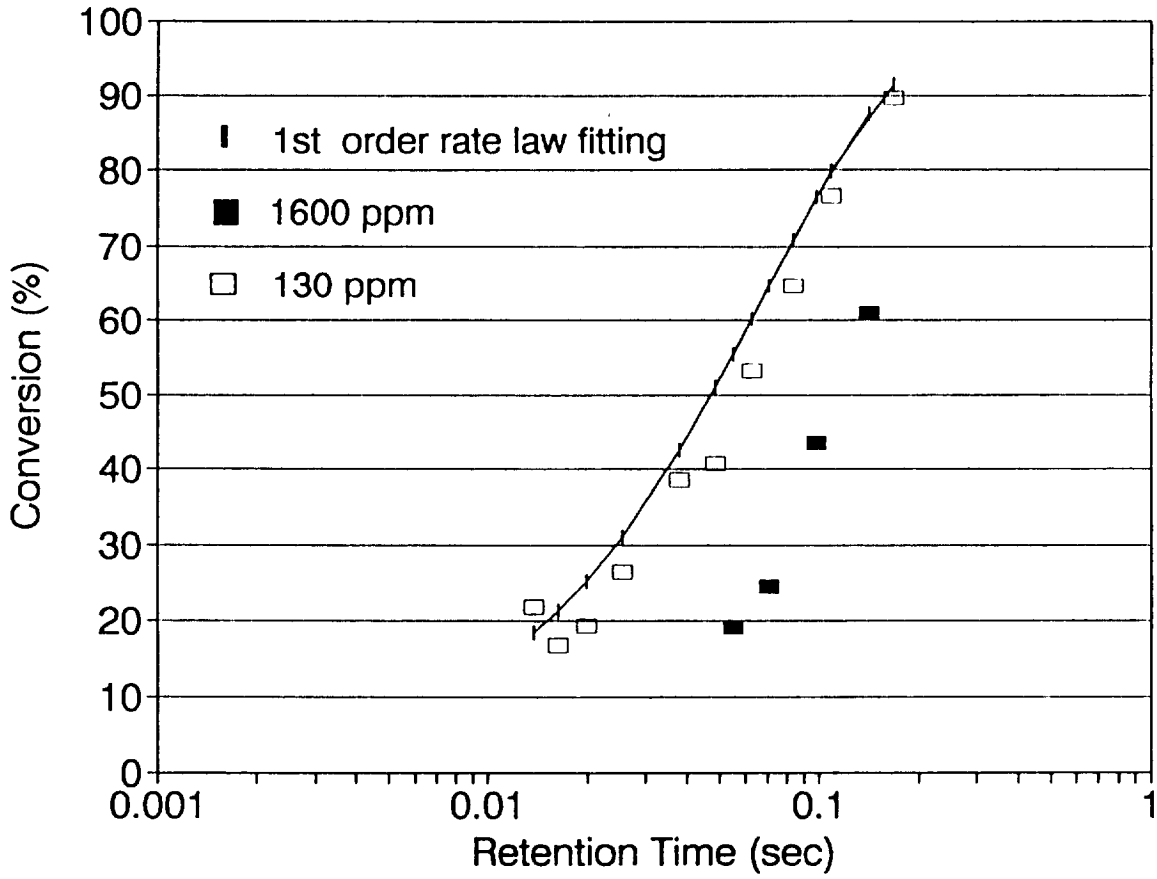

Figure II-25. Curve Fit by Langmuir-Hinshelwood Model at T=240 °C and Inlet MA=130 and 1600 ppm

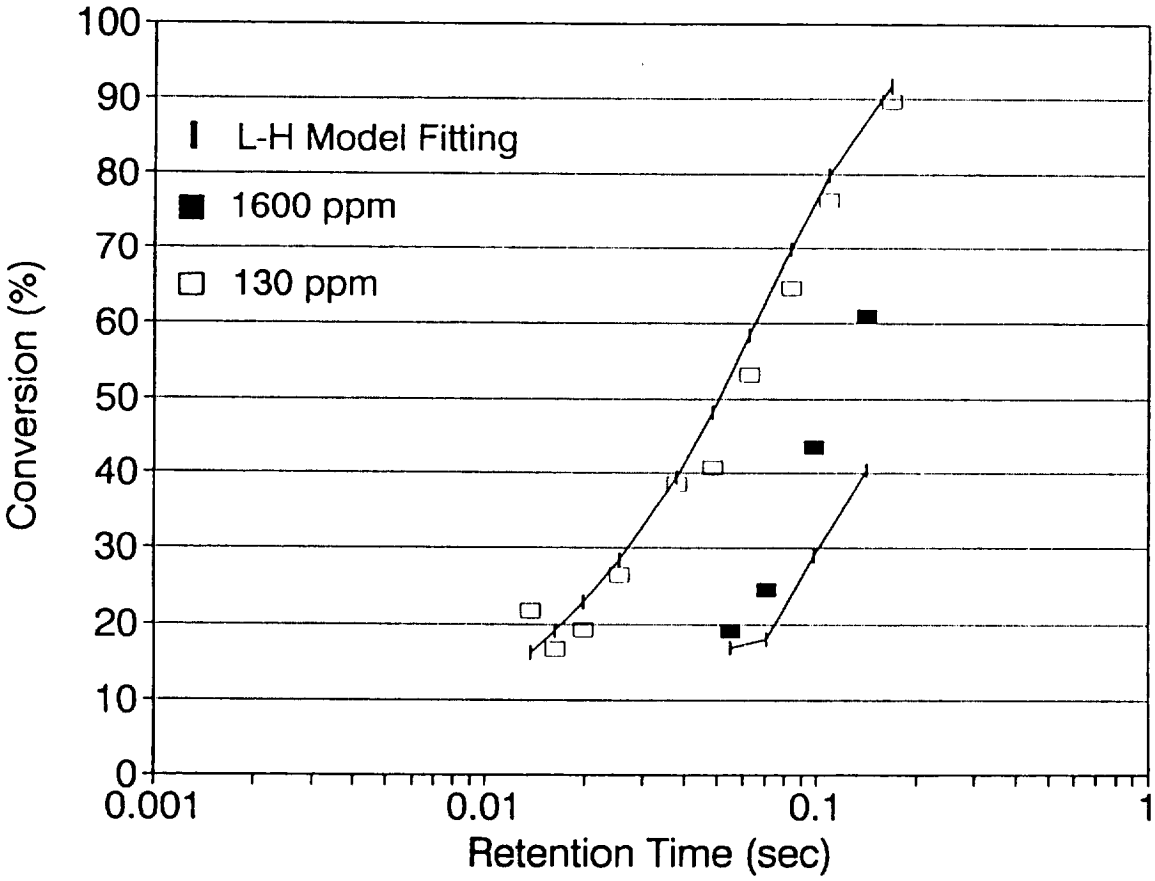

Figure II-26. Arrhenius Plot of the Rate Constant k for 1/8" Nonporous Pt/Al_2O_3 Catalyst, r^2=1.1267

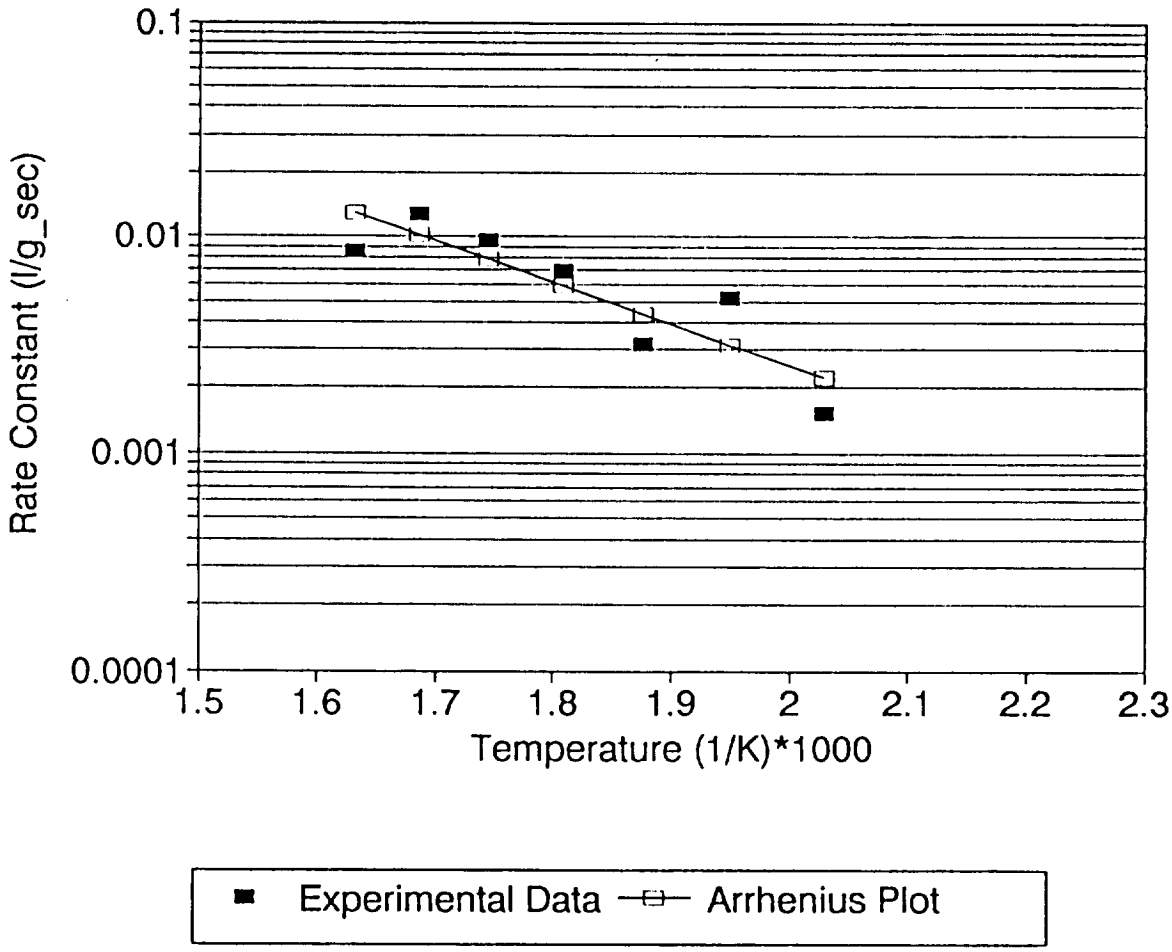

Figure II-27. Arrhenius Plot of the Rate Constant ka for 1/8" Nonporous Pt/Al_2O_3 Catalyst, r^2=1.7486

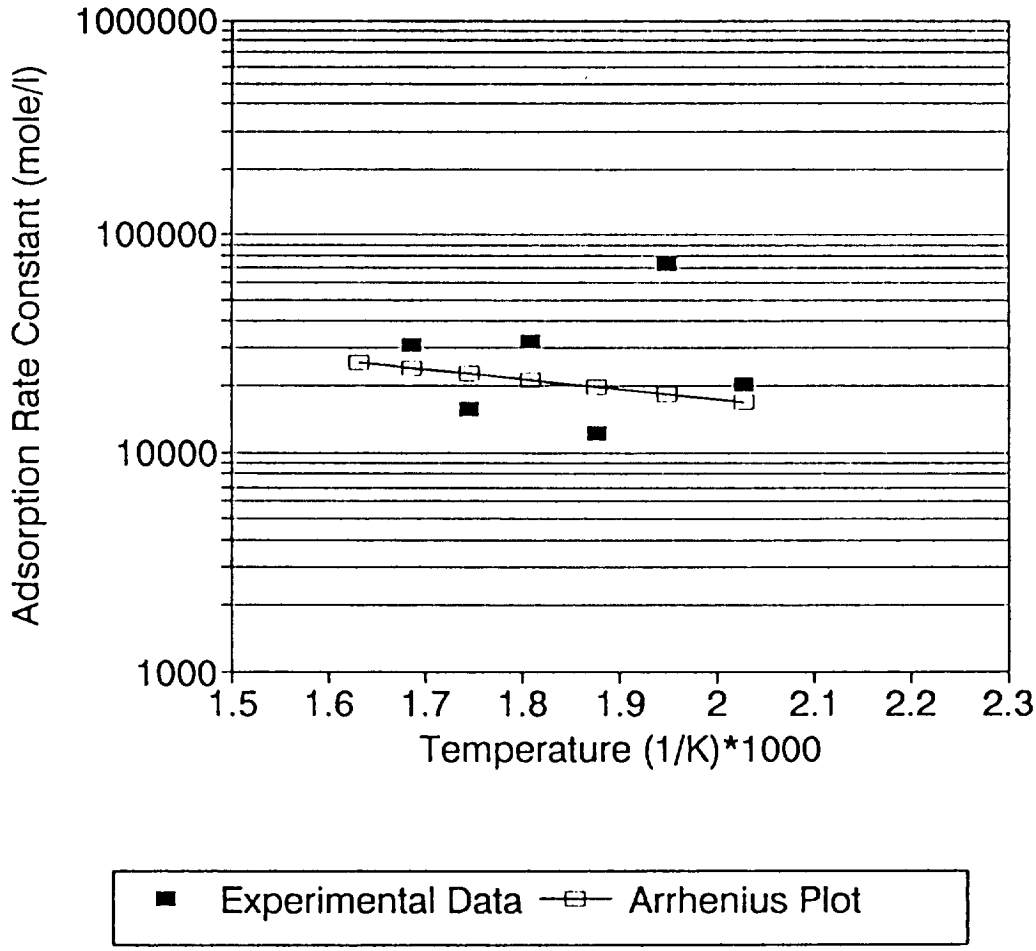

Figure II-28. Arrhenius Plot of the Rate Constant k for 1/16" Porous Pt/Al_2O_3 Catalyst

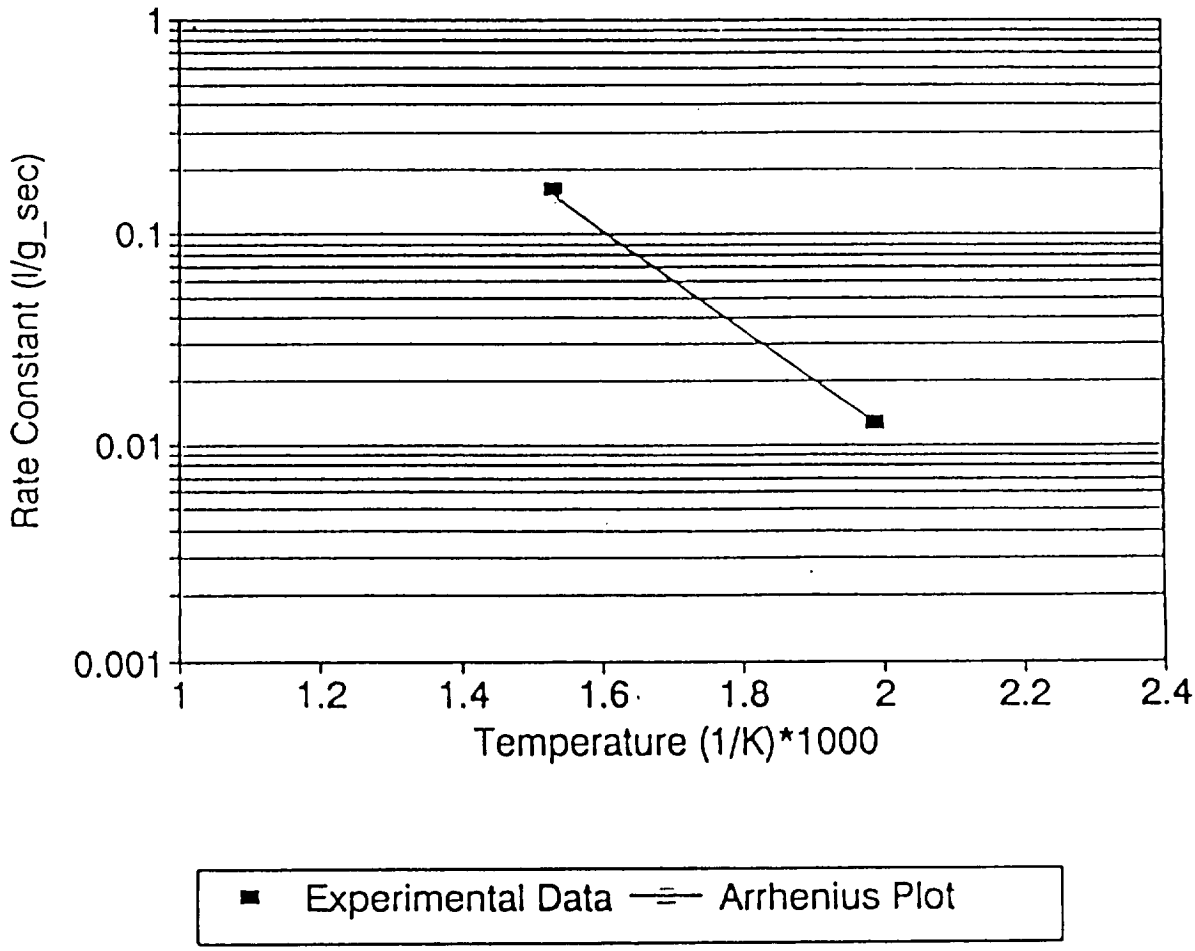

Figure II-29. Arrhenius Plot of the Rate Constant ka for 1/16" Porous Pt/Al_2O_3 Catalyst

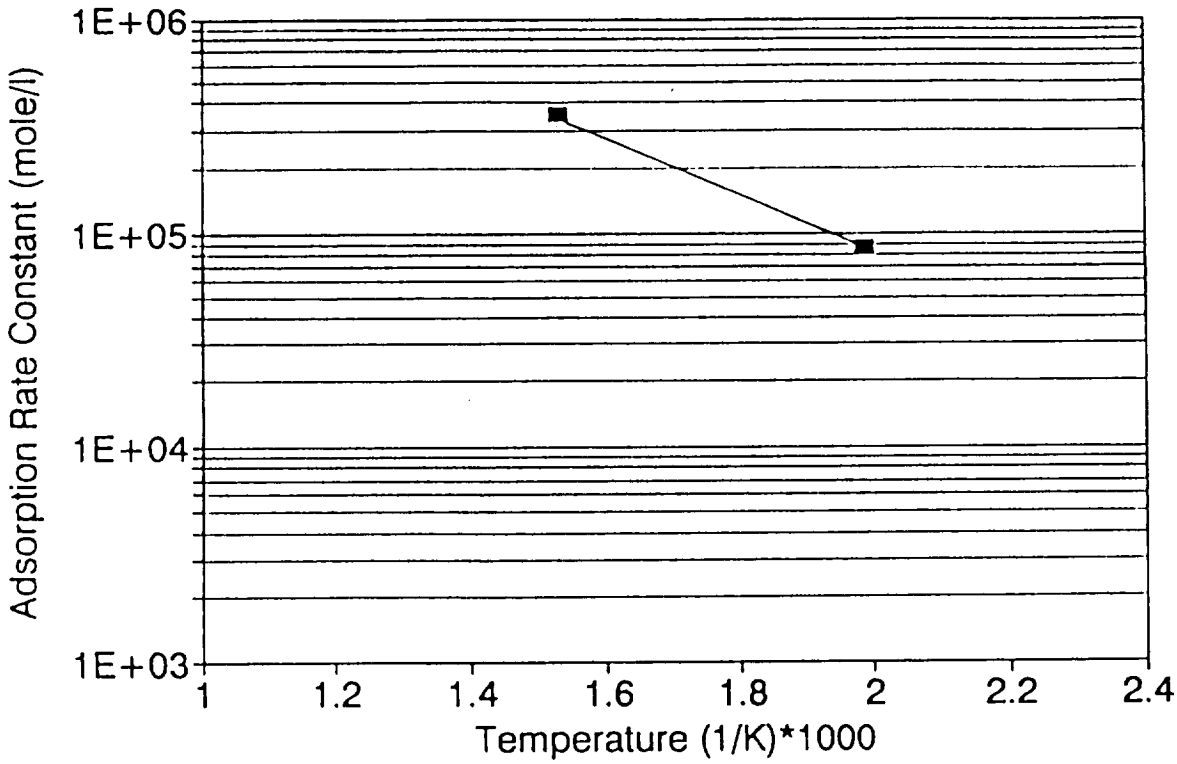

Figure II-30. Model Prediction for an Adiabatic Reactor with Inlet Temperature=250 °C, MA Concentration=13000 ppm, and Reactor OD=2"

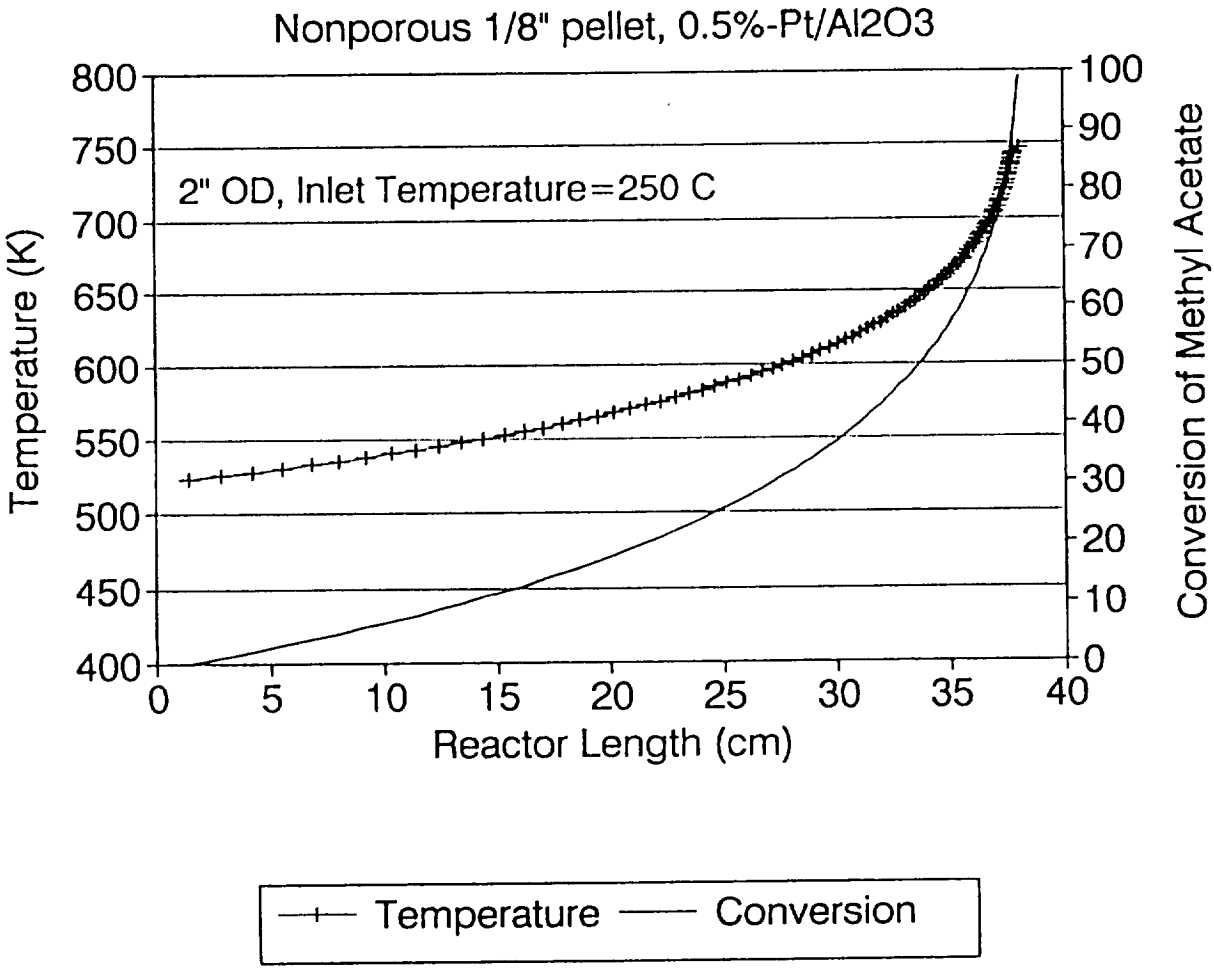

Figure II-31. Model Prediction for an Adiabatic Reactor with Inlet Temperature=300 °C, MA Concentration=13000 ppm, and Reactor OD=2"

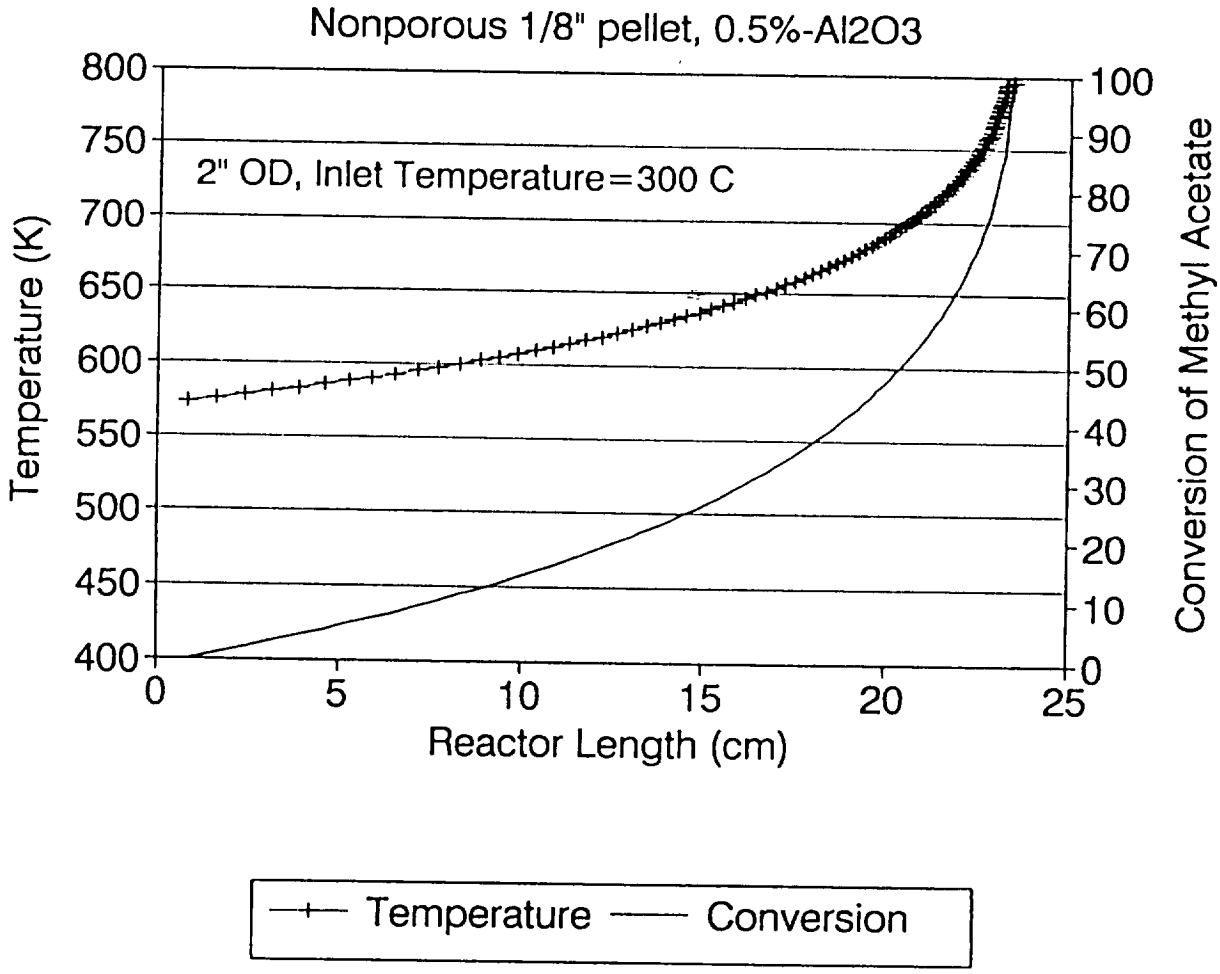

Figure II-32. Model Prediction for an Adiabatic Reactor with Inlet Temperature=250 °C, MA Concentration=13000 ppm, and Reactor OD=4"

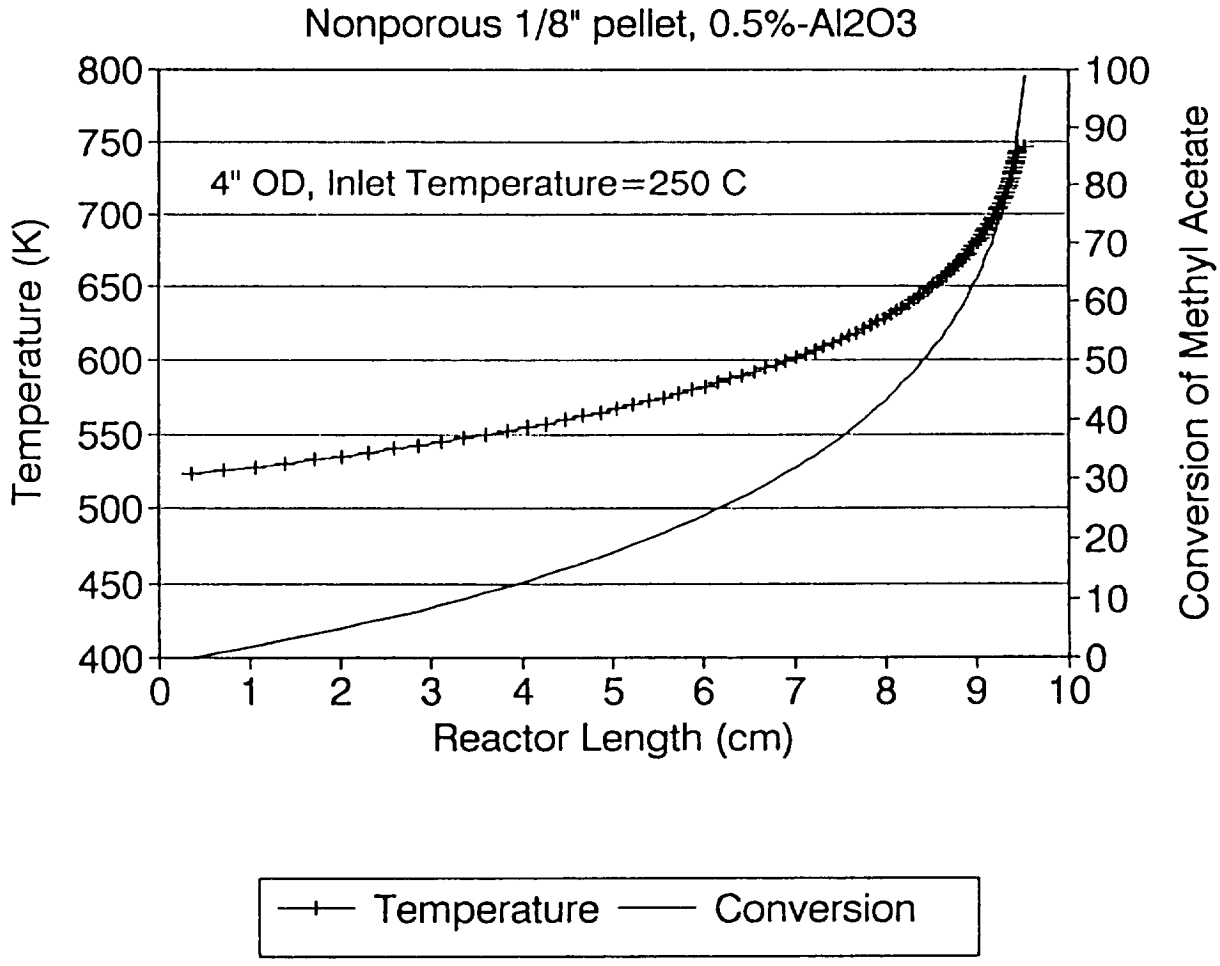

Figure II-33. Model Prediction for an Adiabatic Reactor with Inlet Temperature=300 °C, MA Concentration=13000 ppm, and Reactor OD=4"

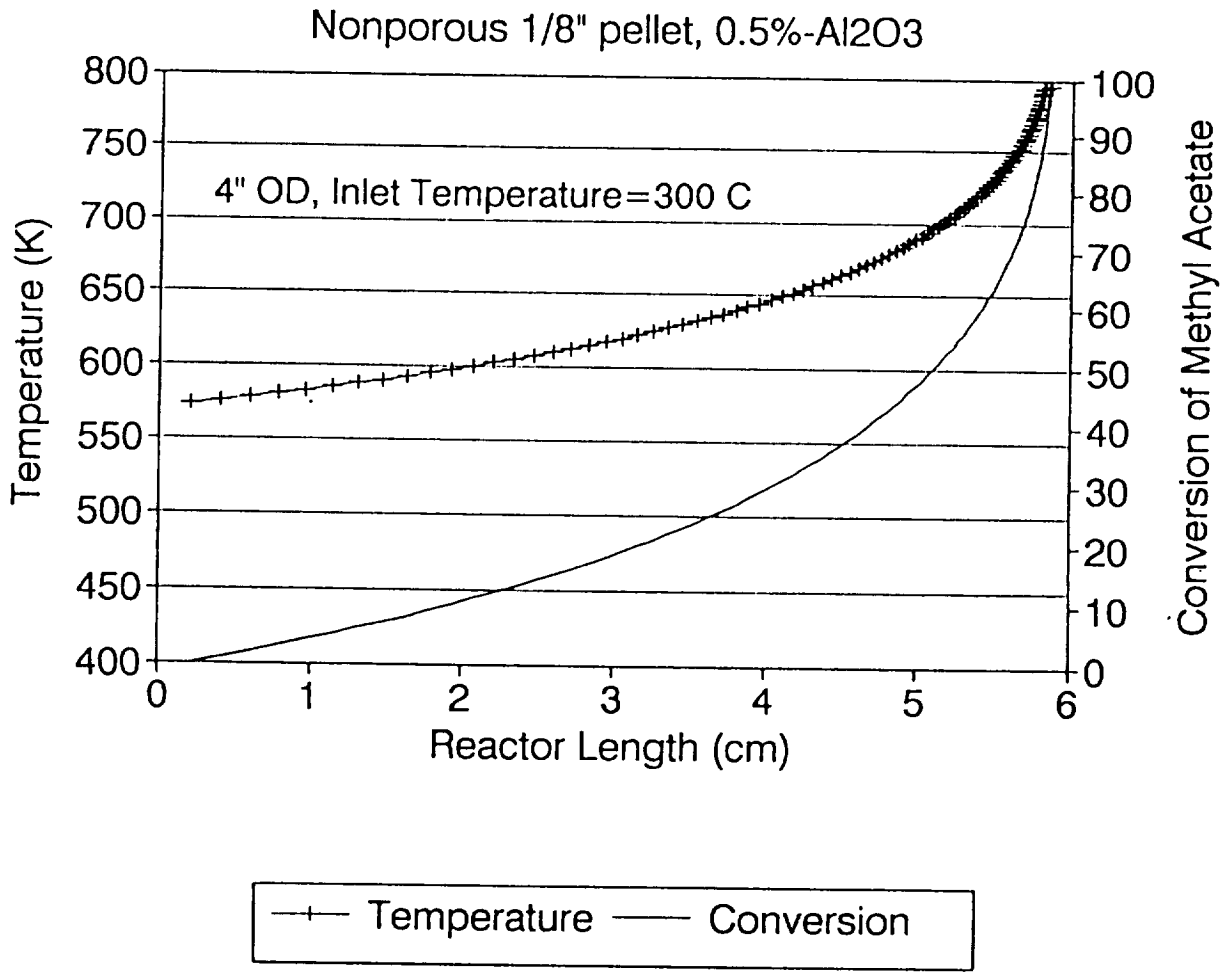

Figure II-34. Model Prediction for an Nonadiabatic Reactor with Inlet Temperature=250 °C, MA Concentration=13000 ppm, and Reactor OD=2"

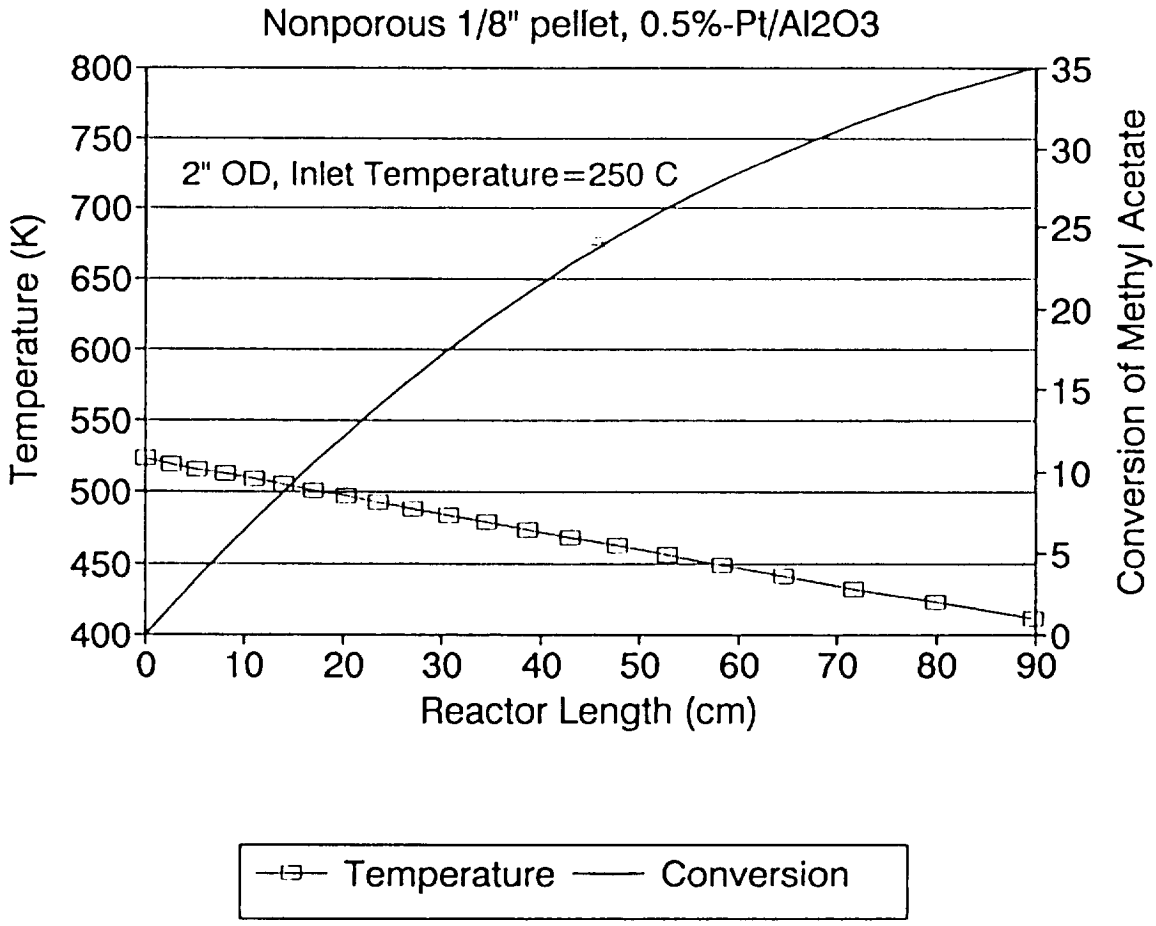

Figure II-35. Model Prediction for a Nonadiabatic Reactor with Inlet Temperature=300 °C, MA Concentration=13000 ppm, and Reactor OD=2"

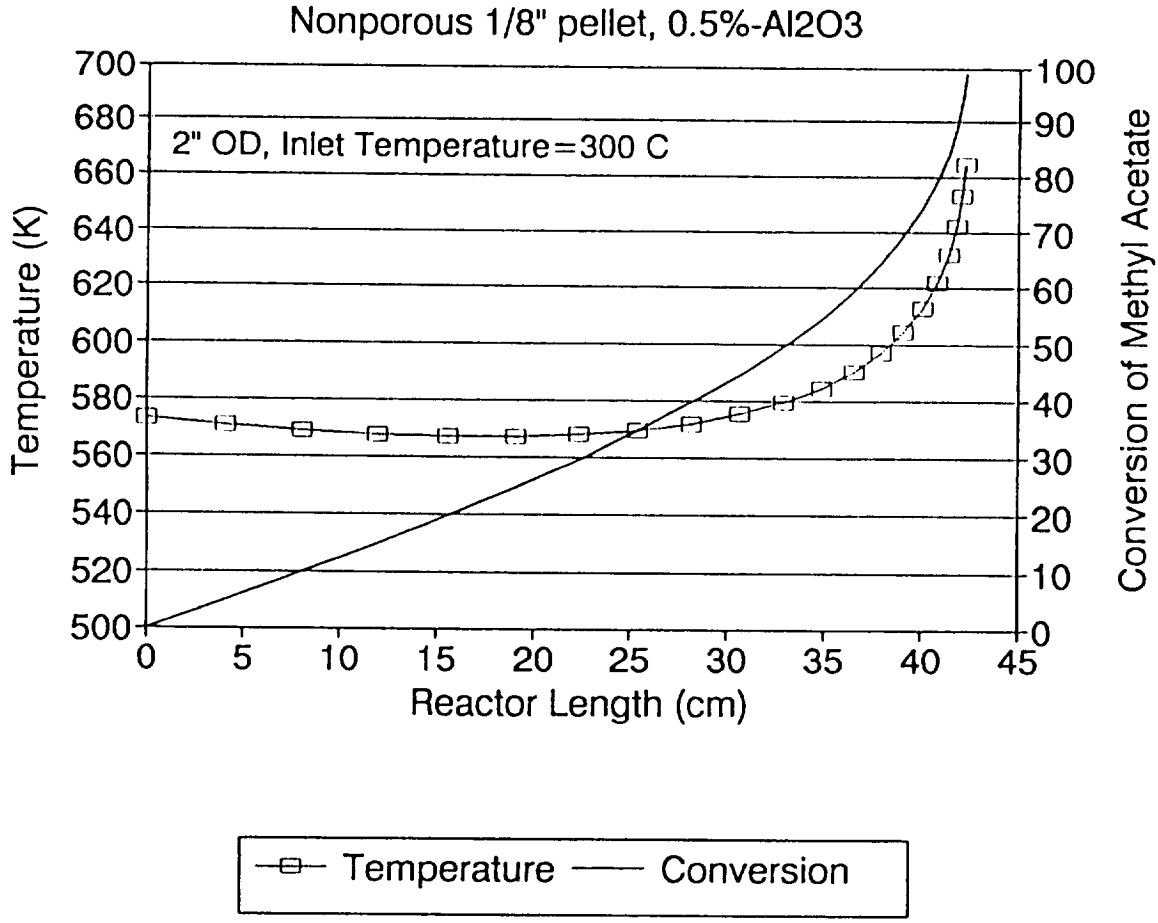

Figure II-36. Model Prediction for a Nonadiabatic Reactor with Inlet Temperature=250 °C, MA Concentration=13000 ppm, and Reactor OD=4"

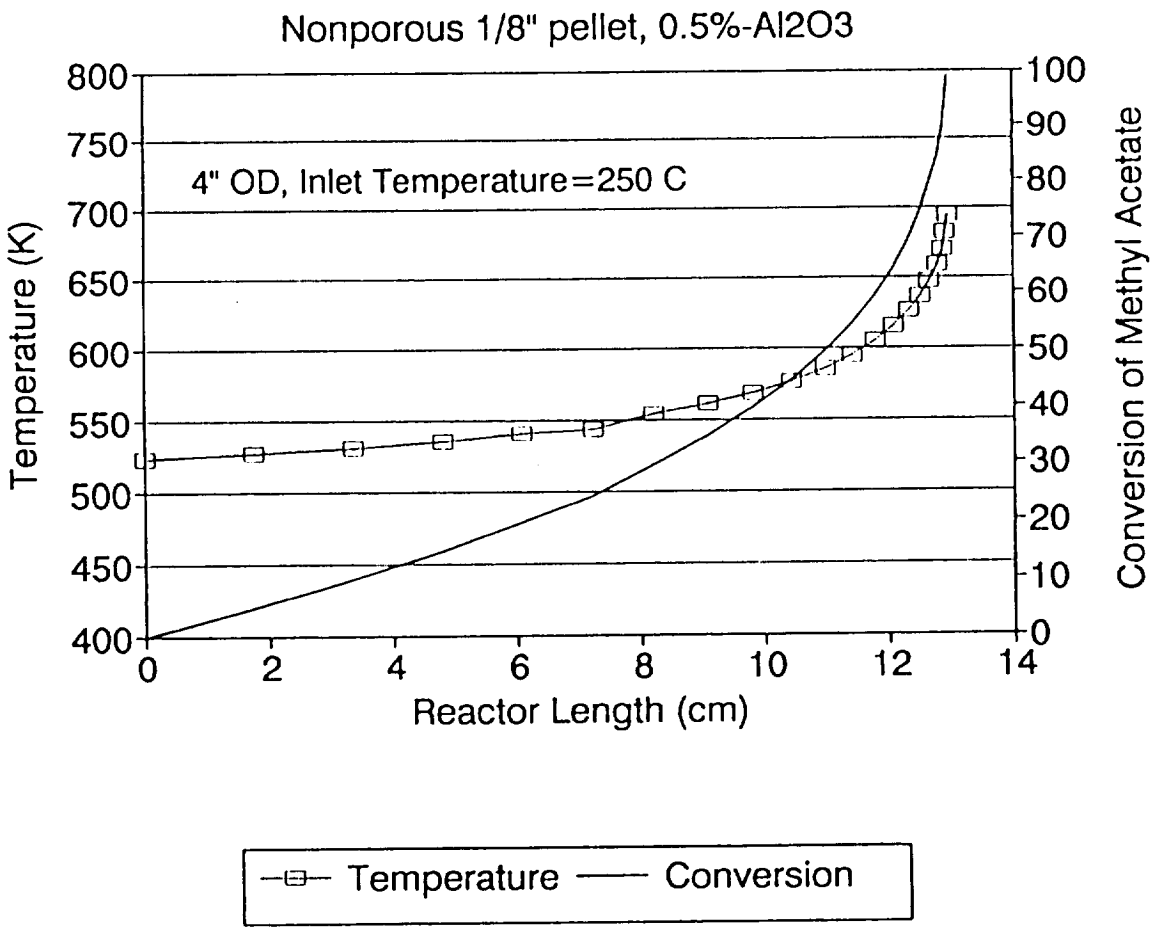

Figure II-37. Model Prediction for a Nonadiabatic Reactor with Inlet Temperature=300 °C, MA Concentration=13000 ppm, and Reactor OD=4"

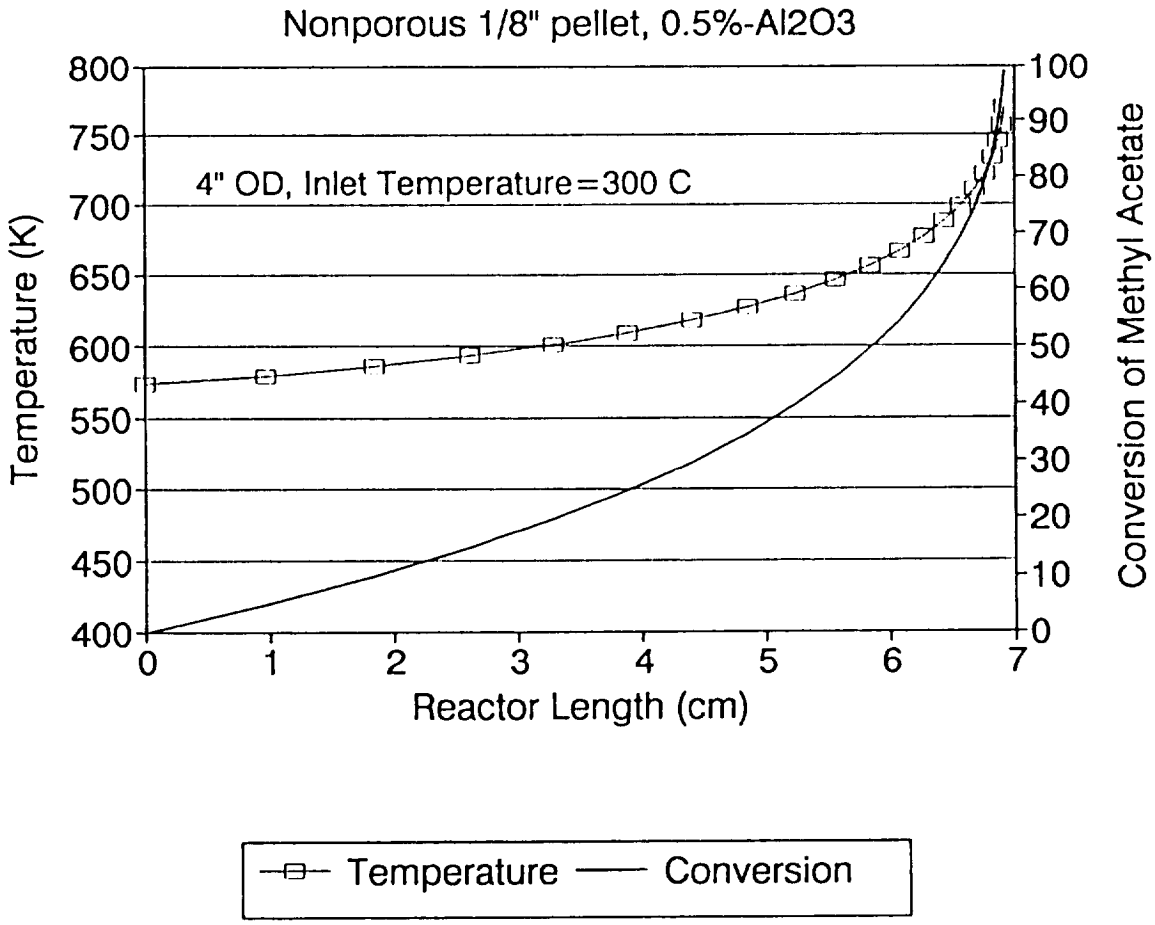

II.10 REFERENCES FOR SECTION II

Becker, E. R., and Pereira, C.J., Catalyst and Reactor Design for Emission Control. AIChE Advanced Seminar Series, (1989).

Bird, R. B., Stewart, W. E., and Lighfoot, E. N., Transport Phenomena. New York: John Wiley & Sons, Inc. (1971).

Elikan, L., "An Approach to Water Management for Long Duration Manned Space Flights," Aerospace Life Support volume of Chemical Engineering Progress Symposium Series Number 63, Volume 62, American Institute of Chemical Engineers, New York, NY (1966).

Froment, G. F., and Bischoff, K. B., Chemical Reactor Analysis and Design. New York: John Wiley & Sons, Inc. (1979).

Henninger, D., "Controlled Ecological Life Support Systems (CELSS) Research and Technology Development at the Johnson Space Center," CELSS Conference of 1993, Alexandria, Virginia, March 1-3, (1993).

Kesselring, J. P., "Catalytic Combustion", Advanced Combustion Method. London: Acdemic Press, 237-275, (1986).

Lange, K. E., "Summarized Work on the Analysis of a Proposed Metabolic Simulator," NASA/JSC Document. (1991).

Lange, K. E., "Requirements for the Test Bed Metabolic Simulator," Report to NASA-JSC, (1992).

Li, Jeffery S., "The Kinetic Study of Methyl Acetate Oxidation Over Platnium Alumina Catalyst," Masters Thesis, Lamar University, Beaumont, Texas, 1993.

Mears, D. E., "Test for Transport Limitations in Experimental Catalytic Reactors", Industrial and Engineering Chemistry Process Design and Development. 10, 541-548, (1971).

Ross, P. T., "Taguchi Techniques for Quality Engineering", McGraw Hill, (1988).

Schwartzkopf, S. H., "Design of a Controlled Ecological Life Support System," BioScience Vol 42, No. 7, 526, (1992).

Spivey, J. J., "Complete Catalytic Oxidation of Volatile Organics", Industrial Engineering Chemical Research, 26, 2165-2180, (1987).

II.11 BIOGRAPHICAL MATERIALS FOR SECTION II

Altman, P. L. and D. S. Dittmer, eds., "Respiration and Circulation," Federation of American Societies for Experimental Biology, Bethesda, Maryland, 1971.

Anderson, B., Experimental Methods in Catalytic Research. New York: Academic Press,(1968).

Aris, R., The Mathematical Theory of Diffusion and Reaction in Permeable Catalysts. Oxford: Charendon Press, (1975).

Bischoff, K. B., "Effectiveness Factors for General Reaction Forms" AIChE Journal, 11, 351-365, (1965).

Butt, J. B., "Transport Resistance in Fine Particles", Advances in Chemistry, 109, 209-213, (1972).

Denn, M. M., Process Fluid Mechanics. London: Prentice-Hall International, Inc. (1980).

Dwidevi, P. N., and Upadhyay, S. N., "Processes Development for Catalysis", Industrial and Engineering Chemistry. Process Research and Development, 16,157-165, (1977).

Farrauto, R. J., Heck, R. M., and Speronello, B. K., "Environmental Catalysts", Chemical and Engineering, 99, 34-44, (Sep. 1992).

Frossling, N., "The Interparticle Transfer Resistance", Gerlands Beitr. Geophys., 52, 170-176, (1938).

Grunewald, T.C., "Carbon Molecular Sieves as Catalyst and Catalyst Supports", Journal of the American Chemical Society. 113(5), 1636-1640,(1991).

Gunst, R. F., and Mason, R. L., Regression Analysis and Its Application. New York: Marcel Dekker, Inc. (1980).

Hatch, L. F., Matar, S., From Hydrocarbons to Petrochemicals. Houston: Gulf Publishing Company, (1992).

Hughmark, G. A., "Elimination of Mass Transfer Resistance", Industrial and Engineering Chemistry. Fundamentals, 19(2), 198-205, (1980).

Hulburt, H. M., Chemical Reaction Engineering Reviews. Washington,D.C.: American Chemical Society, (1974).

Humphries, W. R., Reuter, J. L., and Schunk, R. G., "Space Station Freedom Environmental Control and Life Support System Design - A Status Report", NASA/JSC Document, (1992).

Irandoust, S., "Scaling Up of a Monolithic Catalyst Reactor with Two-Phase Flow", Industrial & Engineering Chemistry Research. 28(10), 1489-1496, (1989).

Kane, J. T., "NO_x Rules in 1990 Clean Air Act amendments", Iron and steel Engineering. 69(12), 17-22, (1992).

Klinghoffer, A. A., and Rossin, J. A., "Catalytic Oxidation of Chloroacetonitrile over 1% Platinum Alumina Catalyst", Industrial and Engineering Chemistry Research, 31, 481-486,(1992).

Lachman, I. M., "Extruded Monolithic Catalyst Supports", Catalysis Today, 14(2), 317-325, (1992).

Langmuir, I., "The Adsorption of Gases on Plane Surfaces of Glass, Mick and Platinum", Journal. American Chemical Society. 40, 1361-1403, (1918).

Lin, C. H., "Space Station Environmental Control and Life Support System Preliminary Conceptual Design," NASA/JSC Doc. No. CSD-SS-059, (1982).

Link, D. E. Jr., and J. W. Angeli, "A Gaseous Trace Contaminant Control System for the Space Station Freedom Environmental Control and Life Support System," SAE Paper No. 911452, presented at the 21st International Conference on Environmental Systems, San Francisco, (1991).

Marquardt, D. W., "An Algorithm for Least-Squares Estimation of Nonlinear Parameters", Journal. Society of Industrial and Applied Mathmatics, 11(2), 431-441, (1963).

Maurel, J.-L., and J.-L. Vernet, "Catalyse. - Etude de la Combustion Catalytique du Formlate et de l'Acetate de Methyle," C. R. Seances Acad. Sci. Ser. 2, 294(1) 25-28 (1982).

Maxted, E. B., "The Deactivation of Catalyst", Advances in Catalysis, 3, 129-139,(1951).

Motiuk, I. L., "The 1990 Clean Air Act Amendments", Seton Hall Law Review, (1991).

Ogg, R. A., "The Transport Resistance in Fine Particle", Journal of Chemical Physics, 15, 337-345, (1947).

Olson, J. H., "Approaches for Numerical Analysis", Industrial and Engineering Chemistry. Fundamentals. 7, 185-189, (1968).

Ross,P.J. "Taguchi Techniques for Quality Engineering," McGraw Hill, (1988)

Roy, R. "A Primes on the Taguchi Method," Van Nostrand Reinhold, (1990)

Schmitt, J. L., "Carbon Molecular Sieves as Selective Catalyst Support",Carbon. 29(6), 743-751, (1991).

Sheintuch, M. , and Brandon, S., "Deterministic Approaches to Problems of Diffusion, Reaction and Adsorption in a Fractal Porous Catalyst", Chemical Engineering Science, 44(1), 69-81, (1989).

Satterfield, C. N., Mass Transfer in Heterogeneous Catalysis, Robert E. Kriegger Publishing Co,(1970).

Smith, J. M., Chemical Engineering Kinetics. New York: McGraw-Hill Book Company, (1981).

Spurlock, J. M. and Spurlock, P. A., "Technology Assessment of the Existing Physical-Chemical Life Support Technology Base," an interim report by S & A Automated System, Inc. prepared under JPL Contract 959091 for Jet Propulsion Laboratory, Pasadena, CA, Mach (1992).

Taguchi, "System of Experimental Design," UNIPUB/Kraus International Publications, (1987).

Tichenor, B. A., "Destruction of Volatile Organic Compounds via Catalytic Incineration", Environmental Progress, 6(3), 172-176, (1987).

Weekman, V. W., "Laboratory Reactors and Their Limitations", AICHE Journal, 20, 833-836, (1974).

Wheeler A., Catalysis. New York: Reinhold Publishing Corporation (1955).

Wick, W. E., and Hugo, P., "The Fundamental of Catalysis", Physical Chemistry. 28(26), 135-145, (1955).

Wheeler, A., Catalysis. New York: Reinhold (1955).

III. HEATING, VENTILATION & AIR CONDITIONING ANALYSIS OF A VARIABLE PRESSURE GROWTH CHAMBER

III.1 INTRODUCTION

The Regenerative Life Support System (RLSS) Test Bed project at the NASA Johnson Space Center (JSC), Houston, TX involves higher plant growth in a closed, controlled environment in conjunction with a physicochemically-based life support system to create an integrated biological/physicochemical RLSS. Additionally, a human metabolic simulator will be integrated into the RLSS and will supply variable metabolic loads to the system to simulate the presence of humans. The integrated RLSS will be fully automated to grow crops from seed to harvest without the need for human intervention.

One of the test bed's two growth chambers, the Variable Pressure Growth Chamber (VPGC), is designed to be operated both at ambient atmospheric pressure and at reduced pressure to more closely duplicate the environment of a Lunar or Martian habitat. The design of the VPGC was required to accommodate a closed, controlled environment which could provide a range of conditions acceptable for plant growth, as well as the capability for measuring selected parameters of interest.

The objective of this task was to perform a heating, ventilation and air conditioning (HVAC) analysis of the air-flow patterns, coil locations and flow directions within the chamber, and to use the results of this analysis to provide JSC with recommendations for design modification to the existing chamber, which has been experiencing operational problems.

The air distribution in the plant growth area will affect the micro-environment of the crop growth process. Under the reduced pressure, because of the reduction in the air density, the volume flow rate will change, and this will affect the operation of the facility.

As a result of this analysis, **a re-selection of the blower** in the VPGC is **necessary**, and a **re-design of the air distribution system** would provide the VPGC a more evenly distributed air flow pattern, resulting in greater uniformity in the plant growth area.

III.2 ANALYSIS OF THE EFFECTS OF REDUCED PRESSURE ON SUBSYSTEM PERFORMANCE

Table III-1 shows the air parameter requirements, operating range, and the selected environment for an experiment conducted at JSC under ambient pressure and temperature conditions.

III.2.1 Heat Load

Contributions to the heat load are derived from the fluorescent lamp, reheat coil, blower, plant transpiration process, air leakage, the human body and the environment of the VPGC (building heat load). Since little is known about the influence of reduced pressure on system heat load and the plant transpiration process, it will be assumed preliminarily that the ambient and reduced-pressure heat loads are the same, i.e., that the pressure reduction within the chamber is not enough to significantly alter the convective heat transfer mechanism. Estimates of these heat loads were developed for the analysis, and these are shown in Table III-2.

III.2.2 Air Flow Rate

For ideal conditions within the VPGC, the air flow rate is determined by the heat load, moisture content, air density, heat capacity, and the temperature difference between the supply and return air. From the heat equilibrium equation, for a proper thermal balance the required velocity of air flowing through the chamber is:

$$V = \frac{Q}{\rho \cdot C_p \cdot \Delta t}$$

where V = air flow rate, m^3/s
Q = heat load, kw
ρ = air density, kg/m^3
C_p = air heat capacity, kJ/kg C
Δt = temperature difference, C

If the heat and humidity loads, as well as the temperature difference of the air, are equivalent for ambient and reduced-pressure operation, the volume flow rate of air is then inversely proportional to its density, i.e.,

$$\frac{V_r}{V_a} = \frac{\rho_a}{\rho_r}$$

The subscripts a and r are used here to represent air parameters under ambient and reduced pressure, respectively. At the reduced pressure condition, e.g., for a lunar colony operation, air pressure is 70 kpa, and air density is 0.804 kg/m^3. Therefore, the volume flow rate of air in the VPGC should be increased by 45%, all other things being equal, for equivalency with ambient-pressure operation.

III.2.3 System Friction Loss

When an airstream flows through the system components such as ducting, fittings, filters, heat exchangers, the reheat coil, etc., an inevitable friction loss is incurred. This head loss is proportional to the air density and the square of the air velocity:

$$H = (f \cdot \frac{l}{d} + \Psi) \frac{\rho \cdot v^2}{2}$$

where H = head loss, Pa
f = Moody friction factor
l = duct length, m
d = duct diameter, mm
ψ = fitting resistance coefficient
v = air velocity, m/s

Assuming the fitting resistance coefficient remains constant for operation under the reduced-pressure condition, the VPGC head loss would increase 45% compared with the ambient-pressure operating condition.

III.2.4 Heat Exchanger

The selection of heat exchanger size depends on the cooling load, overall heat-transfer coefficient, and the temperature difference between the air and the coolant. If the cooling load is unchanged at reduced pressure, the capacity of the heat exchanger used in the Ambient Pressure Growth

Chamber (APGC) is abundant for VPGC testing, because of the increase of air velocity under the reduced-pressure condition.

III.2.5 Blower

The blower size is selected according to the air volume flow rate, head loss, shaft power requirement and the efficiency of the blower. Usually, the data listed in the blower specification supplied by the manufacturer is for standard air conditions (STP). Consequently, the VPGC system air flow rate and head loss must be modified to the manufacturer's standard working conditions for blower sizing.

The shaft power requirement of the blower, under the reduced-pressure condition, is:

$$N_r = V_r \cdot H_r = [(\frac{\rho_a}{\rho_r}) \cdot V_a] \cdot [(\frac{\rho_a}{\rho_r}) \cdot H_a] = (\frac{\rho_a}{\rho_r})^2 \cdot N_a$$

This means that at reduced pressure the shaft power requirement of the blower increases by 110%, i.e., it is greater than twice that at ambient pressure.

With the present configuration, the capacity of the VPGC blower is less than that of the APGC (Table III-3). For proper operation of the VPGC, hardware modifications to the blower, heat exchanger, and reheat coil would therefore be required.

III.2.6 Air Distribution in the Plant Growth Area

For the reduced-pressure condition, the air volume flow rate will increase with a decrease in air density. When this happens, air velocity will increase and system head-loss and blower energy consumption will also rise. The capacity of the cooling heat exchanger is more than adequate compared to the ambient-pressure condition.

Figure III-1-a depicts air flow distribution in the plant-growth area at the present time. Under the present VPGC configuration, the conditioned air passes through a louver, flowing into the plant growth area then up to the lamp bank from the side filter before returning to the AC column. The air flow centerlines incline upward, and a stagnation region will develop in the tail area. In this case, the velocity distribution of air in the growing area is nonuniform. The air velocity near the louver is always greater than that near the edge of the furthermost plant tray from the louver. The effect of this unevenness becomes even more serious under the reduced-pressure operating condition because of the increase of the air velocity in the system.

III.3 CONCLUSIONS AND RECOMMENDATIONS

From this investigation, it is concluded that, for reduced-pressure operation, the air flow rate in the VPGC should be increased by 45% to provide airflow conditions equivalent to ambient-pressure operation. This will cause an increase in the system friction loss by 45%, and since the shaft horsepower of the blower is the product of head loss and volumetric flow rate, the shaft horsepower requirement of the blower will increase by 110%. Hence, it is recommended that a more powerful blower be installed in the VPGC to accommodate the lower density of the air.

To alleviate the problems of nonuniform flow and uneven velocity distribution, it is recommended that the inlet and outlet fittings of the VPGC be reconfigured. The air supply fitting from the side wall to the plant growth tray should be modified, i.e., a number of small openings should be drilled in the tray, thus using holes in the tray to supply air flow instead of the louver. Also, the outlet

from the side of the lamp bank should be moved to the bottom of the lamp bank. And finally, instead of using the panel behind the louver, an air stability chamber should be installed under the tray.

Figure III-1-b shows the new concept containing the air conditioning column with an attached zone. The conditioned air flows upward through the tray openings into the plant growth area, after which it cools the lamp bank before returning to the air chamber below. The resulting vertical air flow pattern in the growth area should provide a uniform air supply to the plants. Since the air supply fitting is integral to the openings in the tray, the panel can be removed and the growth area will be increased by about 25%. This would compensate for the possible reduction of plant growth area caused by the reconfiguration. Table III-4 provides a comparison of existing conditions and conditions under the recommended modification.

III.4 TABLES FOR SECTION III

Table III-1
Air Parameters for the JSC Variable Pressure Growth Chamber (VPGC)

Parameter	General Requirement	Selected Operating Range	Experiment for Lettuce
Air Temp. ^{0}C		16 - 35	23
Relative Humidity %		60 - 95	72
Air Velocity m/s	0.1 - 1.0	0.1 - 1.0	.13 - 1.32
Pressure kpa	70 - 101	70 - 101	101.325

Table III-2
Heat Loads of the VPGC

Sensible	Lamp	6.4 kw
	Reheat Coil	16 kw
	Blower	149.6 kw
	Human Body	0.115 kw/person
Latent	Plant Transparation	3.16 kw
	Human Body	0.050 kw/person
	Leakage, etc.	small

Table III-3
Subsystem Construction and Performance Characteristics

Parts	Type & Model	APGC		VPGC	
		US unit	SI unit	US unit	SI unit
Blower	Centrifugal	2400 cfm	1.133 m^3/s	1350 scfm	0.637 m^3/s
HX (cooling)	Fin-tube HX	77,000 Btu/hr	22.567 kw	32,500 Btu/hr	110 kw
Reheat coil			18 kw		16 kw

Table III-4
VPGC Parameter Comparison

Parameter	Existing Panel	Panel Removed
Air Flow Rate m^3/s	0.412	0.412
Try Area m^2	1.3125	1.6406
Opening/Tray area	39.2 %	25.1 %
Velocity at the opening m/s	0.8	1.0
Velocity in the growing area m/s	0.314	0.251

Air Distribution

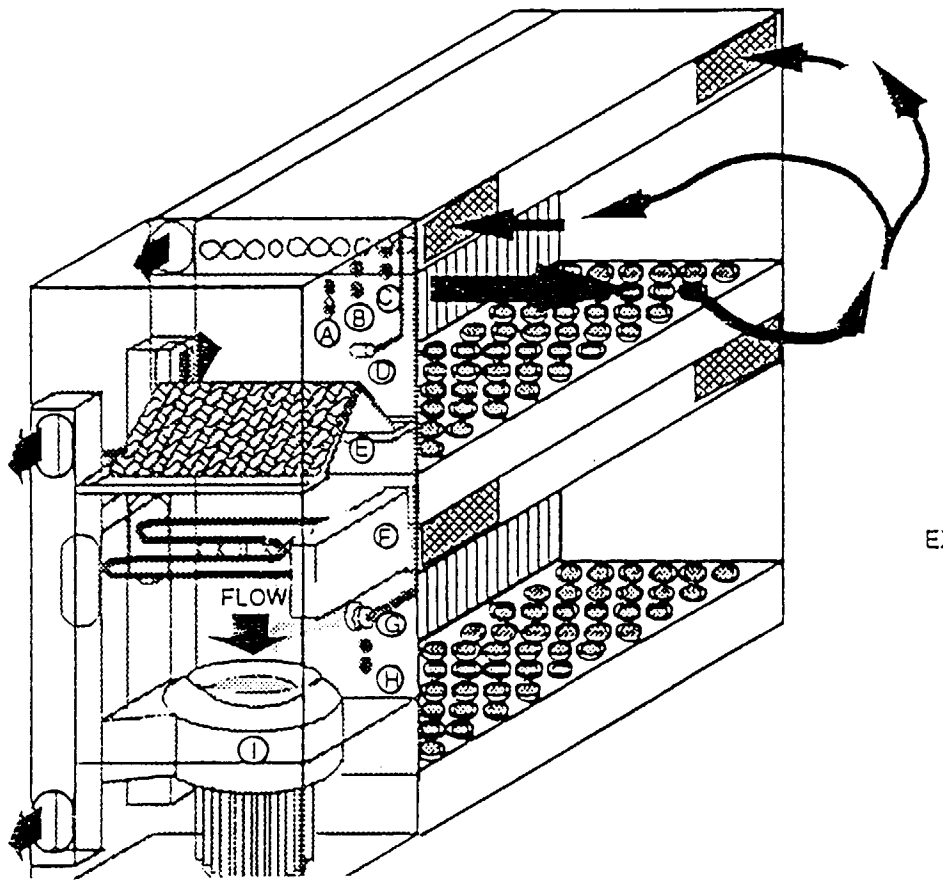

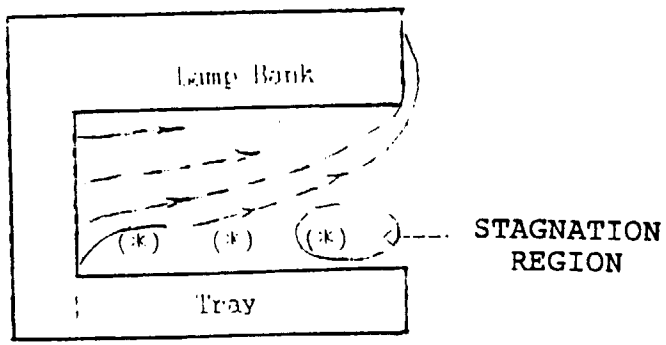

(a) Existing Flow Pattern

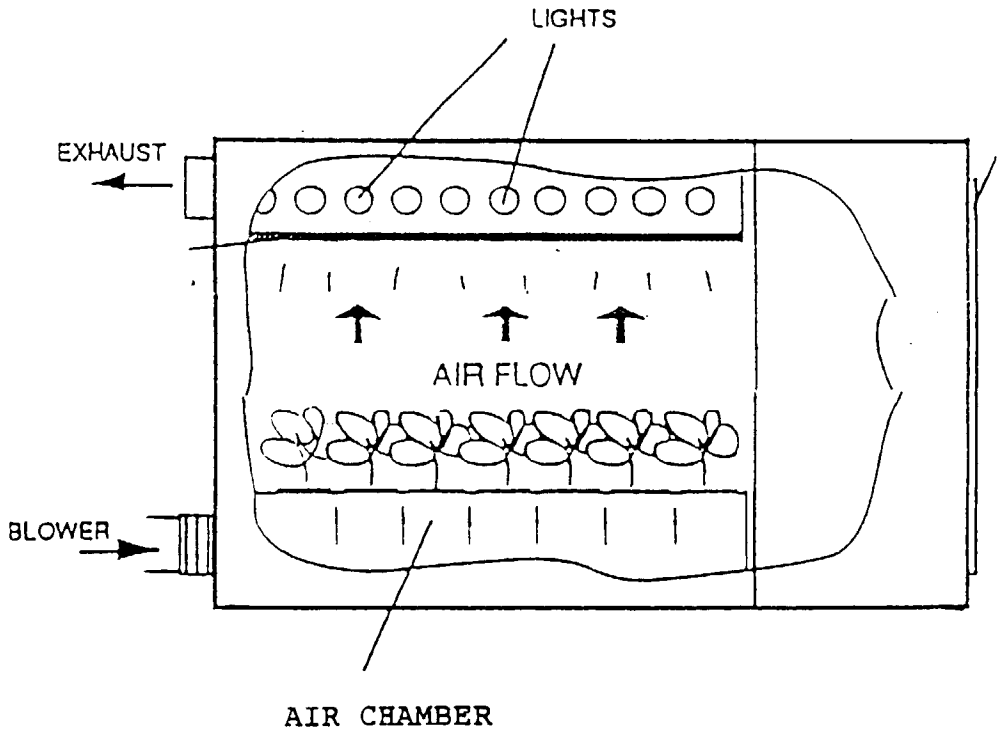

(b) Recommended Reconfiguration

Figure III-1. Comparison of Existing and Recommended Air Flow Distribution Patterns

III.6 BIOGRAPHICAL MATERIALS SECTION III

ASHRAE Handbook, Fundamental, 1993

Barta, Edeen, and Eckhardt, "Regenerative Life Support Systems Test Bed Performance: Lettuce Crop Characterization," SAE paper # 921391, 1992.

Edeen and Henninger, "Regenerative Life Support System (RLSS) Test Bed Performance: Characterization of Plant Performance in a Controlled Atmosphere," SAE paper # 911426, 1991.

Henninger, Tri, Barta, and Stahl, "Johnson Space Center's Regenerative Life Support System Test Bed," Feb., 1992.

McFadden and Miller, "Computer Modeling of the Variable Pressure Growth Chamber Using the CASE/A Simulation Package," SAE paper # 921354, 1992.

McQuiston and Parker, "Heating, Ventilating, and Air Conditioning Analysis and Design," 1982.

Redberg and Norback, "Air Distribution and Draft," ASHVE Trans. 55, 1949

Tri, Brown, Ewert, Foerg, and McKinley, "Regenerative Life Support System (RLSS) Test Bed Development at NASA-Johnson Space Center," SAE paper # 911425, 1991.

IV. RESOURCE RECOVERY ANALYSIS FOR CLOSED LIFE SUPPORT SYSTEMS

IV.1 INTRODUCTION

Current spacecraft life support systems, e.g., that of the Space Shuttle, rely on open-loop technologies. These are simple and sufficiently reliable for human space-flight missions of relatively short duration, small crew sizes, and limited power availability. Life support technologies for the coming era of exploration, however, must address longer-duration missions and larger crew size. One of the most important challenges associated with long-duration manned space flights concerns the development of closed life support systems, including the technologies of air revitalization, water recovery, waste processing, food production, and food processing [Schwartzkopf, 1992].

IV.2 HUMAN CONSUMABLE REQUIREMENTS

A human being requires substantial amounts of various consumable materials to sustain life. A nominal list of life support consumables for a human being is shown in the Table IV-1 [Spurlock, 1992].

IV.3 AVAILABLE TECHNOLOGIES FOR HUMAN LIFE SUPPORT

If these consumables must all be provided by resupply flights from Earth, a substantial logistics infrastructure is required. The cost of launching the current Space Shuttle to low Earth orbit is estimated at $11,000 per kg. The cost of launching material from Earth to a base on the moon or Mars would be much greater. Consequently, supplying the required consumables from Earth is an extremely expensive undertaking. As a result, the development of technologies which recycle waste materials and regenerate consumables is both logistically and economically essential. Technologies available to provide these basic functions of human life support can be divided into two families: physicochemical and bioregenerative.

IV.4 HYBRID SYSTEM

Although it is conceptually possible to design a life support system based exclusively on either type of technology, analysis indicates that the best design combines both families. By carefully selecting and combining technologies with offsetting advantages and disadvantages, it is possible to develop a hybrid design which can offer significant improvement over a purely physicochemical or purely bioregenerative system. One method of combining these technologies is through the development of a controlled ecological life support system (CELSS). Which combines biological functions such as photosynthesis for CO_2 removal and food and oxygen production, with physicochemical functions such as gas separation and the condensation and collection of water vapor on a cooling coil.

An elemental analysis of plant and human tissue is provided in Table IV-2. A closer examination of this table finds the elements, C, H, O, and N are the major elements and must be considered in the resource recovery.

By careful evaluation and selection of physicochemical and bioregenerative subsystem components, it is possible to use this approach to design a life support system that incorporates the benefits of stabilizing internal ecological control mechanisms while simultaneously maintaining the timeliness and cost-effectiveness of the reductionist approach [Henninger, 1993].

IV.5 BIOREGENERATIVE SYSTEMS

Bioregenerative technologies for waste processing include bacterial reactors and combination higher plant-bacterial systems. Bacterial reactors, both aerobic and anaerobic, have an extensive history of application in domestic sewage treatment plants. Aerobic systems typically require higher energy inputs to maintain oxygenation (e.g., aerating pumps and mixers). Anaerobic systems require little energy, but they have slow process rates, and the anaerobic bacteria are more susceptible to changes in environmental conditions [Wolverton et al., 1983]. Combining higher plants with anaerobic bacterial systems provides several distinct advantages. Most significant is the capability for increasing the removal of NH_3^- and NO_3^- nitrogen over that obtained with bacterial systems without plants [Wolverton et al., 1983]. However, such systems are less efficient in removing carbonaceous compounds than are plant-free bacterial systems.

IV.6 CONCLUSIONS AND RECOMMENDATIONS

It can be concluded from this investigation that the advantages of a hybrid bioregenerative/physicochemical CELSS do in fact merit further consideration. Furthermore, since NASA is currently pursuing the physicochemical approach as well as the aerobic bioregenerative technology, the area of concentration most logical for the Lamar Universiy Research Team is that of anaerobic bioremediation for waste processing. Consequently, it is recommended that further work be undertaken to develop and test a prototype bioreactor for that purpose.

IV.7 TABLES FOR SECTION IV

Table IV-1
Nominal Consumables Requirements for Humans

Consumable	Mass(kg/year)
Food(dry mass)	219
Oxygen	329
Drinking water	657
Sanitary water	840
Domestic water	6132

Table IV-2
Elemental Content of Plant and Human Tissue

Element	Zea Maize	Man	Sucrose	Fat	Protein
O	44.33	14.62	51.42	11.33	24
C	43.57	55.99	42.10	76.54	52
H	6.24	7.46	6.48	12.13	7
N	1.46	9.33			16
Si	1.17	0.005			
K	0.92	1.09			
Ca	0.23	4.67			
P	0.20	3.11			
Mg	0.18	0.16			
S	0.17	0.78			
Cl	0.14	0.47			
Al	0.11	-			
Fe	0.08	0.012			
Mn	0.04	-			
Na	-	0.47			
Zn	-	0.01			
Rb	-	0.005			

IV.8 REFERENCES FOR SECTION IV

Henniger, Donald, "Controlled Ecological Life Support Systems Research and Technology Development at Johnson Space Center," CELSS Conference of 1993, Alexandria, VA, March 1-3, 1993.

Schwartzkopf, S.H., "Design of a Controlled Ecological Life Support System," Bioscience, Vol. 42, No. 7, p. 526 (1992).

Spurlock, J.M., "Technology Assesment of the Existing Physical-Chemical Life Support Technology Base," Interim Report, JPL Contract 959091, March 1992.

V. DATA ACQUISITION SOFTWARE DEVELOPMENT FOR AUTOMATION OF ENVIRONMENTAL GROWTH CHAMBER

V.1 INTRODUCTION

The objective of this task was to write a LabView-based data acquisition software to automate the monitoring and control of the environmental growth chambers (EGCs) at JSC. Prior to the development of the software, the EGCs had been monitored and controlled manually. The task requirements called for the simultaneous on-screen display of up to six instrument panels, one per chamber. Each instrument panel was to monitor a temperature reading, a CO_2 level reading, and a light intensity reading. In addition, each panel must issue two binary control signals to nutrient supply and CO_2 batch sampling relay valves. The software was to run a MacIntosh Quadra 950 connected to a Hewlett-Packard 3852A multichannel data acquisition front end. The task was initially estimated by a contractor to consume 0.3 man-year. Assuming that the present cost of one man year, including benefits and overhead cost, is $60,000, the above estimate translates to $20,000 in labor. The Lamar team completed the task at a fraction of this estimate.

V.2 HARDWARE CONFIGURATION

Figure V-1 shows the hardware setup. The HP 3852A is equipped with two (2) HP 4408A 20 channel multiplexers, a 16 channel general purpose switch board, and a voltmeter board. Sensor readings and control signals are multiplexed to and from the Quadra 950 via the use of slot address and channel ID on the HP 3852. Each panel requires three (3) multiplexer channels and one or two output channels, depending on whether or not a CO_2 batch sampling valve is used.

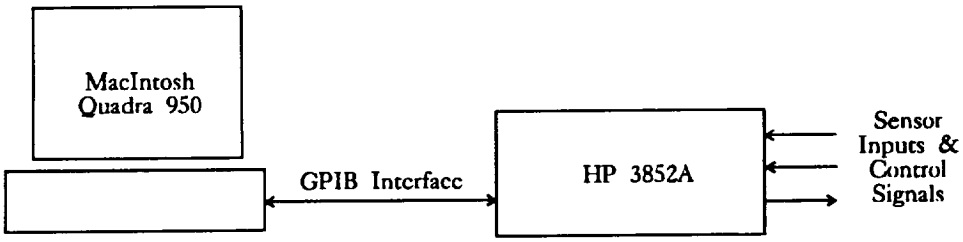

Figure V-1. Data Acquisition Hardware Setup

V.3 SOFTWARE DESIGN

The software was designed to display an unlimited number of panels simultaneously; the maximum practical number of panels running at the same time is limited only by input/output channel capacity and CPU processing speed. The current hardware configuration can support at most 6 panels due to limitation in the number of output channels. In the minimized view, the panels display current data values and control signals. When maximized, each panel also displays bar charts and running averages of past data values, as well as control strategy selections and sensor calibration parameters. Sensor readings and valve status are written to an ASCII file for off-line analysis. Appendix A provides a full description of panel layout and operations.

V.4 CONCLUSION

The required software was developed and checked out satisfactorily in the Mechanical Engineering Computer Facility at Lamar University on JSC hardware. The hardware and installed software were then returned to JSC with a User's Guide (included in this report as Appendix A), also developed as a part of this task.

VI. STATISTICAL ANALYSIS AND DESIGN OF EXPERIMENTS

VI.1 INTRODUCTION

A primary task in the JSC plant growth area is to design a test program for investigating environmental parameters that affect plant yield and the optimal levels of these parameters for maximum growth. Since there are numerous environmental parameters and resources constraints (such as time, funding, and available facilities), the use of a full factorial experiment would not be feasible. For a cost-effective and efficient program, it is necessary to minimize the number of experiments and the amount of test data taken in these experiments. The use of minimal sets of test data is not a problem in itself; problems arise only when experimenters fail to correctly consider what should constitute a valid experiment from a risk standpoint. Hence the task is to design an effective experimental program for investigating the effects of environmental parameters on plant growth, and to determine the optimal environmental parameter levels for maximum yield of each candidate crop.

VI.2 DESIGN OF EXPERIMENTS

The present design for plant growth experiments at NASA-JSC is based on Dr. Tze-San Lee's proposal "A Study of System Performance of the Variable Pressure Growth Chamber at NASA-JSC: Taguchi's Approach." This design considers three two-level factors: substrate, pressure, and physicochemical (Table VI-1). An orthogonal array L4 is used for the experiment design (Table VI-2).

After meetings with JSC personnel and a review of the literature [Glover, 1991], [Sirko, 1991], [Strowp, 1992], [Kozo, 1992], a new, improved design for these experiments has been developed. The candidate crops for these experiments are: soy and, peanuts, wheat, rice, potatoes, carrots, chard, cabbage, lettuce, tomato, mushroom, sugar beet, mustard greens, and collard greens. The recommended design includes four two-level factors and one four-level factor. The four two-level factors are: partial pressure of CO_2, air temperature, irradiance level, and relative humidity. The four-level factor is growth media. The recommended L8 orthogonal array for this application is shown in Table VI-3. The wisdom of this choice can be evaluated only after JSC has completed the growth cycle which implements the recommended area. At this writing this data was not available.

Following the application of the Taguchi technique to the plant growth process, it was requested by JSC that the statistical analytical analysis be redirected to focus on the catalytic reactor test program. Consequently, an experiment design for the testing of the subscale catalytic reactor was developed. This design consists of five three-level factors and interactions between three of the five factors (Section II, Table II-9). The analysis is described in more detail in Section II of this report.

VI.3 STATISTICAL ANALYSIS

The results of plant growth from established trial conditions shown in Table IV-3 are required for statistical analysis. A statistical analysis of the results will identify environmental parameters that are significant for plant growth and determine their optimal levels for maximum yield. The design experiment for testing of the subscale catalytic reactor was carried out and the results are shown in Section II, Table II-9. The statistical analyses are shown in Section II, Table II-10 and Table II-11.

VI.4 CONCLUSION

A test program using Taguchi's orthogonal array L8 is developed to identify environmental parameters significant for plant growth. The test program considers four two-level environmental parameters and one four-level environmental parameter. The test program provides a viable cost-effective design for experiments.

Additionally, an experimental design using an orthogonal array L27 was developed for testing the subscale catalytic reactor. This design was tested and the results analyzed. The experimental design is considered to be accurate and cost-effective.

VI.5 TABLES FOR SECTION VI

Table VI-1
Design Factors and Their Levels

Columns	Factors	Level 1	Level 2
1	Substrate	Solid	Hydroponic
2	Pressure	14.7 psi	10.2 psi
3	Physicochemical		

Table VI-2
Orthogonal Array Used for a Typical Experiment

Trial / Column	1	2	3
Trial 1	1	1	1
Trial 2	1	2	2
Trial 3	2	1	2
Trial 4	2	2	1

Table VI-3
Orthogonal Array L8 Used for Plant Growth

Factor / Col. / No.	A 1 2 3	B 4	C 5	D 6	E 7
1	1	1	1	1	1
2	1	2	2	2	2
3	2	1	1	2	2
4	2	2	2	1	1
5	3	1	2	1	2
6	3	2	1	2	1
7	4	1	2	2	1
8	4	2	1	1	2

FACTOR
A: GROWTH MEDIA
B: PARTIAL PRESSURE OF CO_2
C: AIR TEMPERATURE
D: IRRADIANCE LEVEL
E: RELATIVE HUMIDITY

VI.6 REFERENCES FOR SECTION VI

Glover, G., "Optimization of Crop Growing Area in a Controlled Environmental Life Support System," 21st International Conference on Environmental Systems, July 1991.

Kozo, Sato, "A Trade Study Method for Determining the Design Parameters of CELSS Subsystems," 22nd International Conference on Environmental Systems, July 1992.

Sirko, Robert, "Plant Growth Modeling and the Design of Experiments in the Development of Bioregenerative Life Support Systems," 21st International Conference on Environmental Systems, July 1991.

Stroup, T., "Crop Interactions in Polyculture ant Their Implications for the CELSS Design," 22nd International Conference on Environmental Systems, July 1992.

VII. GENERAL CONCLUSIONS AND RECOMMENDATIONS

The results achieved by the Lamar Engineering Team in this program, in both the hardware and software development tasks and in the analysis tasks, should be helpful to JSC designers in advancing the state of technology readiness of required CELSS systems for future missions.

The kinetic data obtained in the subscale catalytic reactor hardware development task, and the analytical model developed for characterization of reactor performance, will assist JSC in the design and development of a full-scale reactor for its planned test bed activity. Results from the Taguchi experimental design method, which was applied to the reactor test program, helped to streamline the test effort by pinpointing those performance parameters having the most significant effect on the reaction, thereby eliminating many test hours to explore the effects of less important parameters.

The HVAC analysis of the VPGC resulted in recommendations for obtaining more uniform flow within the chamber, and for providing reduced-pressure air-flow conditions which would have the same effect on plant growth as those conditions existing during ambient-pressure operation.

A brief analysis of resource recovery for long-duration CELSS operations indicates that a hybrid physicochemical/bioregerative system for recycling waste materials and recycling precious consumables may be optimal for advanced-technology systems. It is also recommended that Lamar be permitted to further explore the concept of anaerobic bioremediation, an area in which it has particular expertise. In fact, subsequent to the initiation of this grant effort, a separate project was initiated to construct and test this type of bioreactor. This project is currently in progress at Lamar and will be completed by January 1995.

The data acquisition software development task for automation of the monitoring and control of operations for the JSC environmental growth chambers resulted in the development of both an installed set of working software and a user's guide to assist operators in the use of this equipment.

And finally, the statistical analysis and "design-of-experiments" task, focusing initially on the plant growth process, then shifting to the catalytic reactor test operation, produced results which were both useful in the near-term to reduce catalytic reactor testing, and for the long-term in outlining some "design-of-experiments" techniques for plant growth experimentation. If implemented by JSC, these techniques and recommendations could result in many hours of reduced time for plant growth experimentation.

Taken all together, it is felt that the Lamar Engineering Team has made significant contributions to the solution of NASA's CELSS problems, and we remain prepared to continue working with NASA and JSC in the future in these and other areas.

VIII. APPENDIX A

PLANT GROWTH CHAMBER DATA ACQUISITION SOFTWARE USER'S GUIDE

Vinh D. Nguyen and Andrew Li

Department of Mechanical Engineering, Lamar University, P.O. Box 10028, Beaumont, TX 77710

INTRODUCTION

This manual explains how to configure and use the data acquisition software developed at Lamar University for data monitoring and control of the plant growth chambers at the Johnson Space Center (JSC). At present, the software is configured to take readings of temperature, CO_2 concentration, and light intensity in each chamber. (The CO_2 and light intensity readings make use of a generic quadratic calibration function and therefore can be easily modified to read other kinds of data.) In addition, the on/off setting of a CO_2 sampling valve, a CO_2 supply valve, and a nutrient supply valve for each chamber can be controlled from the instrument panel. Readings and valve status are written to ASCII data files. In addition, current readings, running averages, and daily averages are displayed on the instrument panel. The software was developed on a Macintosh Quadra 950 computer with the HP 3852A data acquisition unit acting as the front-end interface to the sensors. The software can be found under the LABVIEW \ CHAMBERS subdirectory.

CONFIGURATION GUIDE

Each plant growth chamber must be assigned a separate instrument panel. Each panel requires three input channels on the HP 44708A multiplexer (20 channels per board) and three output channels on the HP 44725A general purpose switch (16 channels per board). The multiplexer routes voltage readings to the HP 44701A voltmeter. At the time of this writing, the HP 3852A has:

- 2 multiplexers (total 40 channels)
- 1 general purpose switch board (total 16 channels)
- 1 voltmeter board

At the time of this writing, 6 instrument panels have been preconfigured for the user. This number is dictated by the number of available channels on the HP 44725A board. The number of panels running simultaneously is limited only by the number of available input

and output channels and the required sampling rate. It takes about 1 sec for and instrument panel to obtain its readings. Thus, the minimum sampling rate for 6 simultaneous panels is roughly 6 sec.

Input Channel Configuration

The input channel configuration is user-selectable. To configure the input channels, the user must specify the voltmeter slot number, multiplexer slot number, and the channel selection. In the default configuration, the voltmeter is in slot 7 the multiplexer used (only one multiplexer is needed for 6 simultaneous panels) is in slot 0. The input channel selections are tabulated below:

Table 1. Default Input Channel Selections

Instrument Panel #	1	2	3	4	5	6
Temperature Channel	00	03	06	09	12	15
CO_2 Channel	01	04	07	10	13	16
Light Intensity Channel	02	05	08	11	14	17

Temperature readings are assumed to be taken with a type T thermocouple. This can be changed easily to any other type supported by the HP 3852A. CO_2 and light intensity readings use a generic quadratic calibration function and therefore can be reconfigured for other kinds of data. The calibration function used is shown below:

$$R = a + bx + cx^2$$

where R is the reading in engineering unit,
x is the sensor voltage,
and a, b, c are the user-supplied calibration parameters.

For instructions on thermocouple installation, refer to *pp.* 4-19 of *HP 44708 Relay Multiplexers* in Plug-in Accessories Configuration and Programming Manual. For instructions on installation of other sensors, refer to *pp.* 4-15 in same section.

Output Channel Configuration

The output channels are not user-selectable. The output channel settings are tabulated below:

Table 2. Output Channel Settings

Instrument Panel #	1	2	3	4	5	6
CO_2 Supply Valve	00	03	06	09	12	14
Nutrient Supply Valve	01	04	07	10	13	15
CO_2 Sampling Valve	02	05	08	11	N/A	N/A

The CO_2 sampling valve output channel is used to turn on a CO_2 batch analyzer prior to the reading. Instrument panels 5 and 6 do not have a CO_2 sampling valve channel assignment. At the moment only four chambers at JSC use batch analyzers. Additional chambers are expected to use on-line analyzers.

For instructions on using the general purpose switches please refer to Chapter 2 of *HP44725A General Purpose Switch* in Plug-in Accessories Configuration and Programming Manual.

Supply Valve Control Strategies

Four control strategies are implemented for the supply valves. They are described below.

Preset Frequency. This control strategy turns the valve on an off at specified intervals. The user needs to specify an on duration, and off duration, and a delay start time. The cycle will start after the delay start time has elapsed counting from the moment the cycles are activated. The valve is turned on at the start of the cycle. To reset the cycle parameters or to phase shift the cycles, the user needs to deactivate the cycles, reset the appropriate parameters, and reactivate the cycles. The preset frequency control strategy is overridden when other control strategies are selected. In this case, the cycles continue in the background.

Bang-Bang. This is a closed-loop control strategy aimed at maintaining the monitored variable within a specified band. The user specifies the upper and lower limits of the dead

band. When the monitored variable exceeds the upper limit, the valve is turned off. When the monitored variable drops below the lower limit, the valve is turned on. The user should take care not to specify to narrow a dead band to prevent excessive fluctuations.

Constant On. This control strategy always turns the valve on.

Constant Off. This control strategy always turns the valve off. Note that this can also be accomplished by deactivating the preset frequency cycles. There is a subtle difference, however. Using the constant off strategy to override the preset frequency preserves the current phase setting of the cycles. Deactivating the cycles will cause the current phase setting to be lost.

The control strategy availability is tabulated in Table 3 for the CO_2 supply valve and the nutrient supply valve.

Table 3. Control Strategy Availability

Control Strategy	CO Supply Valve	Nutrient Supply Valve
Preset Frequency	Yes	Yes
Bang-Bang	Yes	No
Constant On	Yes	Yes
Constant Off	Yes	Yes

CO_2 Sampling Valve Control Strategy

The user must specify a time interval for which the CO_2 sampling valve must be turned on prior to the reading. This control strategy is necessary only for chambers using a CO_2 batch analyzer.

OPERATIONS GUIDE

The six preconfigured panels are labeled Chamber 1 - 6 in anticipation that they will be assigned to the correspondingly numbered chambers. Only the panels assigned to a chamber in used need to be activated.

Minimized View

Each panel appears initially minimized, showing, in addition to the current data readings, the control strategy selection boxes, the valve status indicators, and a power switch. A label appears on each panel indicating the chamber assignment. The following paragraphs discuss the operation of these subVIs.

Control Strategy Selection Boxes. There are two control strategy selection boxes, one for the CO_2 supply valve and one for the nutrient supply valve. The currently selected control strategy is displayed in the window. By clicking on the right or left arrow, the user can cycle through a list of available control strategies. The control strategies are described in the preceding section.

Valve State Indicators . Two round status indicators appear to the right of the control strategy selection boxes. The following color scheme is used to indicate valve status:

Table 4. Color Scheme for Valve Status Indicators

Valve Status	ON	OFF
Color	Green	Gray

Power Switch . The power switch provides a safe way to power down a panel. Always use the power switch to turn off a panel to ensure that buffered data is written to the data file. Stopping a panel with the LabView stop button does not guarantee that buffered data is saved. To take a single reading, start the panel with the power switch in the OFF position. The panel will turn itself off after the first reading. For continuous operation, start the panel with the power switch in the ON position.

Maximized View

The panel can be maximized by clicking on the maximize box in the upper right corner of the panel. The minimized view now occupies the upper left corner of the maximized panel. The following subVIs are shown in the maximized view:

Data File. This subVI displays the name of the current data file. Data files are named as "Chamb*n.v*", where *n* denotes the chamber number and *v* denotes the version number. The user can specify the maximum size for the data file. When the data file exceeds this maximum size, the current file is automatically closed and a new file opened with the same name and an incremented version number. Thus, each panel is associated with a series of data files, each of which is a different version of the same file name. The current file size is also displayed.

Sampling Rate. The sampling rate is specified as the elapsed time between two readings. Keep in mind that each panel takes about 1 sec to take a reading. Hence, running 6 panels side-by-side will put the minimum sampling time at about 6 sec. If the specified sampling interval is less than the minimum sampling time, the actual sampling intervals may become erratic.

Strip Charts. Three strip charts are used to display the recent histories of temperature, CO_2, and light intensity readings. In addition, a running average and a daily average are displayed at the bottom of each strip chart. The running average is reset when the panel is powered up. The daily average is reset at precisely midnight everyday.

Calibration Parameters. Calibration parameters are shown for the CO_2 and light intensity readings. The user can click on these parameters and change their values at any time. The new values are instantaneously reflected in the display data.

Valve Control Parameters. The valve control parameters are described in the preceding section. An activate button is shown near the control parameter windows for the supply valves. The user needs to press on these buttons to activate the preset frequency cycles. Press on the button again to deactivate the cycles.

Channel Selections. The channel selection parameters include the chassis slot numbers for the voltmeter and the multiplexer boards and the input channel assignments on each

multiplexer board. The output channel assignments are fixed. Refer to the preceding section for listings of the default channel assignments.

Data Files

Data is written to data files in ASCII format. Each chamber is assigned a series of files where each file has the same name and a different version number. Data files are named as "Chamb*n.v*" where *n* denotes the panel number and *v* denotes the version number. Each data record contains 6 data fields described below:

Time Stamp. The time stamp is recorded in the format "YYYYMMDDhhmmss".

Temperature. Temperature data is recorded as a real value.

CO_2 Level. CO_2 concentration level is recorded as a real value.

Light Intensity. Light intensity is recorded as a real value.

CO_2 Supply Valve Status. CO_2 supply valve status is recorded as a single digit, 1 for ON, 0 for OFF.

Nutrient Supply Valve Status. Nutrient supply valve status is recorded as a single digit, 1 for ON, 0 for OFF.

PLANT GROWTH CHAMBER DATA ACQUISITION SOFTWARE

PROGRAMMER'S GUIDE

Andrew Li and Vinh D. Nguyen

Deparment of Mechanical Engineering, Lamar University, P.O. Box 10028, Beaumont, TX 77710

INTRODUCTION

The six basic application VIs are located in the folder Chambers, which is in the folder LabView. They are named Chamber 1 though Chamber 6 . In addition, sub VIs Data Acq., Switch and Write are also important components. In Chambers there is another folder named Globals, in which all the global variables are placed. Data files written by sub VI Write for each application are placed in folder Data files.

The basic application VI Chamber 1 through Chamber 6

Because they have the same structure, we use Chamber 1 as the example. The fundamental structure of Chamber 1 is a sequence which includes five cases.

. 0 Checks the Test Time Recorder. Set it to current time if it is zero.

. 1 Turns the CO2 sampling valve on a certain time before a testing is made (available for only Chamber 1 and Chamber 2).

. 2 Check if it is time to read data and write them into files. When it is true, the following nine sequences are carried out.

0) Assembles the instruction for 3852A for the temperature testing. The instruction is composed of several sections by using Concatenate String function.

1) Gives instruction to 3852A and get data from it, through sub VI Data Acq. The average data is calculated in this step, and the real time and the average data are converted into string stored in local variables.

2) Same as "1)" but for the data of CO2 level.

3) Same as "1)" but for the data of light intensity.

4) After reading and writing data, resets the frequency recorder.

5) Date is obtained from system clock and is converted into the format "YYMMDD".

6) Time is obtained from system clock and is converted into the format "HHmmSS".

7) The function of this step is writing average value in to data file. At first it makes a judgment if current time is at 00:00:00 of this day. If it is, jump into the sequence of writing.

Step 0, write Daily Average into file,

Step 1, calculate temperature Running Average,

Step 2, calculate CO2 level Running Average,

Step 3, calculate light intensity Running Average,

Step 4, write Running Average into file,

Step 5. clear all global variables for Daily Average.

8) The status of two supply valves are converted into string to be written into data file.

9) Write the date, time, real time data and status of two supply valves into file.

. 3 This is for the control of CO2 supply valve. It is composed of two case structures. The first one contains four cases, from 0 to 3, corresponding to the four control strategies, Bang-Bang, Preset Frequency, Constant On, and Constant Off. Case "0" is Bang-bang control while case "1" represents Preset Frequency stile, "2" and "3" are Constant On and Constant Off respectively. In Bang-bang, real time data will be compared to upper limit and lower limit separately. Once it is higher than upper limit, turn the valve off, or if it is lower than the lower limit, turn the valve on. In Preset Frequency, it is divided into two main cases by the Activate Timer. When Activate Timer is off, it turns both supply valves off and checks when the Timer is changed to on. When it is on, the timing sequence is counted. To form the timing sequence, the first is to see if it is in on status or off status. Then compare the time it has lasted from last change of valve status with On or Off duration. When time is up, change the status of valve from on to off or off to on. The operation of change the status of valve is done through sub VI Switch.

.4 It is for the control of nutrient supply valve. There is no Bang-Bang strategy. Everything else is same as those described in ".3".

.5) Displays the current status of the two supply valves.

Sub VI Data Acq.

Data Acq. is designed as a sub VI to communicate with 3852A Data Acquisition/Control Unit, with which the sensors are connected. Data Acq. gives instruction to and takes data from 3852A. The instruction is composed in the upper level VI, which is Chamber 1 here, and is shown on the panel of Data Acq. The address of 3852A for LabView is 9.

Sub VI Switch

Switch is used to turn the valves on and off in control. It give instruction to 3852A, and 44725A 16 Channel General Purpose Switch Card on 3852A performs this control action.

Sub VI Write

Write is an important sub VI that performs the file management. When a data string is ready to be written to a file, Write is called by Chamber 1, and the name of the file is given by the caller. The first thing to do is to check the current version number of this file. Then open the file and write. If the file in the version is not existed, Write will create that file, and then write. The global Version is used to record the current version of data files.

The global variables

av Temp — Records the average temperature in one day.

av CO2 — Records the average CO2 level in one day.

av Light — Records the average of light intensity in one day.

AVR Temp — Records the average since beginning of temperature.

AVR CO2 — Records the average since beginning of CO2 level.

AVR Light — Records the average since beginning of light intensity.

Day Time T — Records the number of data obtained in one day for temperature.

Day Time CO2 — Records the number of data obtained in one day for CO2 level.

Day Time L — Records the number of data obtained in one day for light intensity.

All Time T — Records the number of data obtained since the beginning for temperature.

All Time CO2 — Records the number of data obtained in one day for CO2 level.

All Time L — Records the number of data obtained in one day for light intensity.

Time Rec. — Records the time at which the last data was obtained.

Version — Records the current version of files.

CO2 Time Records the time when the status of CO2 valve is changed.

Nutr Time Records the time when the status of nutrient valve is changed.

CO2 State Records the current status of CO2 valve.

Nutr State Records the current status of nutrient valve.

Test Frq Rc Records the time since last data reading.

CO2 Level Records the CO2 level data obtained in last reading. This is used for CO2 valve bang-bang control.

Bang Records the status of the outputs for the two valves in Bang-Bang control.

Delay Time Records the time when the Activate Timer of CO2 control is set to "On" while the delay time is used.

Delay T N. Same as Delay Time, for nutrient.

Timer Sign It is used to distinguish the "On" and "Of" status of Activate Timer button of CO2 Control and changes its value according to if the delay time is counted up to zero.

T Sign N. Same as Timer Sign, fort nutrient.